November 2023

TRANSCRIPTIONAL REGULATION OF BONE FORMATION, MECHANOSENSING, AND EVOLUTION

Emily R. Tetrault
University of Massachusetts Amherst

TRANSCRIPTIONAL REGULATION OF BONE FORMATION, MECHANOSENSING, AND EVOLUTION

A Dissertation Presented

by

Emily R. Tetrault

Submitted to the Graduate School of the University of Massachusetts Amherst in partial fulfillment of the requirements for the degree of

Doctor of Philosophy

September 2023

Molecular and Cellular Biology

TRANSCRIPTIONAL REGULATION OF BONE FORMATION, MECHANOSENSING, AND EVOLUTION.

A Dissertation Presented

by

Emily R. Tetrault

Approved as to style and content by:

_____
R. Craig Albertson, Chair

_____
Courtney Babbitt

_____
Helene Cousin

_____
Rolf Karlstrom

_____
Meg Stratton
Graduate Program Director
Molecular and Cellular Biology

ACKNOWLEDGMENTS

I would like to first thank my advisor, R. Craig Albertson, for his years of time and dedication to seeing me succeed, his patience, and creating a space where I could thrive and take the time I needed to work through my projects and personal struggles. Thank you for being an amazing mentor, but also a friend when I needed it. A big thank you to all my committee members for their guidance, suggestions, and lending their expertise throughout all stages of my project. A tremendous thank you to Benjamin Aaronson for his four years of work as my undergrad, without whom I would not have generated nearly as much data as I did. Thank you for years of help and friendship.

Thank you to my parents, my biggest fans and supporters from day one. I appreciate you both for always listening to me rant about my struggles and achievements, even if you didn't have any idea what I was talking about. I appreciate you more than words can describe, and I love you. A huge thanks to my daughters who have dealt with me being in school for the entirety of their lives and busy so often. Thank you for your patience and always being a light in my life. I hope you are all proud.

ABSTRACT

TRANSCRIPTIONAL REGULATION OF BONE FORMATION, MECHANOSENSING, AND EVOLUTION

SEPTEMBER 2023

EMILY TETRAULT, B.A., MOUNT HOLYOKE COLLEGE

Ph.D., UNIVERSITY OF MASSACHUSETTS AMHERST

Directed by: Professor R. Craig Albertson

Given that bone remodeling is a dynamic process, the output of which is dependent upon time, levels of mechanical input, and the ability of bones to respond to that mechanical stimulus, I assessed regulation of gene expression in the craniofacial region to determine how a response happens during mechanosensing and bone remodeling. To do this, I used African cichlids as a model, as they known for their rapid speciation rates, high phenotypic variation within and between species, and ability to remodel their bones in response to mechanical loading. In chapter 2, I combined RNA-seq and ATAC-seq datasets to determine with high confidence genes are responsible for plasticity and shape differences in cichlid species with different feeding morphologies. In particular, I found genes that were both differentially expressed and differentially accessible to transcriptional machinery that were implicated in cell cycle progression. In chapter 3, using qPCR, I was able to determine that time is a critical factor in assessing plasticity and the response of certain species to mechanical input. This was paired with 2D morphometrics for shape analysis over time to show that species that do not fall on the extreme end of phenotypic variation are more genetically plastic, and gives insights into the underpinnings of evolution in cichlid jaw morphology. Results from both

chapters 2 and 3 suggested that certain environments facilitate larger changes in gene expression than others. In chapter 4, using molecular techniques such as qPCR coupled with enzymatic staining, I found that when mechanosensitive structures in the cell are ablated, gene expression regulation collapses over time, and specific sites of bone remodeling activity are less predictive. Taken together, this body of work supports previous research in the field and gives insight into the regulation of gene expression during bone remodeling, plasticity, and evolution.

TABLE OF CONTENTS

List of Tables

List of Figures

CHAPTER I

GENERAL INTRODUCTION

The road from genotype to phenotype is not simple nor linear. It would be convenient for many aspects of biology if things encoded in the genome directly resulted in a particular observable characteristic. However, both internal and external environmental interactions can modify a genomically-encoded phenotype (Figure 1). During development, molecules interact within and between neighboring cells. Cell-cell communication gives rise to tissues, structures, and organs. These interactions are not explicitly encoded in the genome, however, modifications to any one of these levels of organization can cause changes to a trait ranging from no change to extreme change (Figure 1). For example, molecular interactions such as the addition of methyl groups to a DNA strand cause decreased gene transcription (reviewed in Doerfler, 1983.). Cell-cell spatial interactions and tissue form can generate stress that feeds back to alter proliferation rates (Nelson et al., 2005). External environmental inputs such as nutrition and temperature also modify phenotypes (Figure 1). For example, early temperature changes in zebrafish larval development alters the general body size and number of multiple fin rays (Sfakianakis & Leris, 2011). Ewes that graze on *Veratrum californicum* ingest the teratogen cyclopamine, a potent inhibitor of the sonic hedgehog pathway. Lambs born to ewes that have ingested cyclopamine present with a range of potentially fatal birth defects, including cyclopia, holoprosencephaly, and mandibular and maxillary deformations or dysplasia (Welch et al., 2009). For the purpose of this dissertation, the phenotype is the craniofacial skeleton.

The craniofacial skeleton is formed and patterned by a sequential series of early cell movements and specific gene expression location and timing. Maintaining the skeleton requires mature bone to be replaced with new bone over time. This is done via activation of bone resorbing cells, the osteoclasts, that carve out mature or fractured bone which is followed by deposition of bone by osteoblasts (Al-Bari & Al Mamun, 2020). This bone turnover is known as bone remodeling, which is important during fracture repair, exercise, and general skeletal maintenance. Under normal conditions, the rate/amount of bone resorption and bone deposition should be in equilibrium. Too much resorption leads to bone diseases like osteoporosis, which is characterized by low bone mass and mineral density (Elson et al., 2022). Conversely, overly dense bones form when bone deposition is higher than rates of bone resorption (Nakahama, 2010). Bone remodeling can be induced via changes in mechanical loading. Increases in mechanical loading stimulates bone deposition, while extended periods of rest causes high rates of resorption (Zhang et al., 2008).

Bone remodeling requires a bit of phenotypic plasticity, which is the idea that a single genotype can give rise to multiple phenotypes. This is so because levels of gene expression, epigenetics, and environmental cues can change and fine-tune a phenotype. For example, the genetic background of mice affects tibia area and bone formation in response to loading (Akhter et al., 1998). Mechanosensing is a form of plasticity that is important for bone remodeling.

African cichlids from the African Rift Valley lakes are a great model for phenotypic plasticity, specifically in the craniofacial region, owing to their rapid speciation and vast variation in size and shape. It is estimated that around 1000 species

have arisen in the past 1-2 million years (Seehausen, 2006). While variety in cichlids is abundant, much of the variation is localized to the upper and lower jaws, the shape and size of which are adapted to the foraging style a particular species uses and falls along the benthic-pelagic axis. Benthic foraging cichlids tend to have deep heads, a rounded craniofacial profile, small eyes, and robust jaws that are adapted for the biting/twisting motions of rocky habitats. Conversely, pelagic fish have shallower head depths, gradually sloped craniofacial profiles, large eyes, and gracile upturned jaws adapted for the speed of rapid gaping required for suction feeding (Cooper et al., 2010; Parsons et al., 2016).

Benthic/pelagic bone shape traits can be induced using laboratory feeding methods imposing different functional demands on the cichlid jaw that mimic benthic or pelagic foraging in the lake (Huysseune, 1995; Gunter et al., 2013; Parsons et al., 2016). Results from these types of plasticity experiments show that the direction of craniofacial bone shape and size, globally and locally, are what would be expected given the nature of the foraging environment. For example, certain cichlid species fed on a pelagic diet had more of a straight craniofacial profile (Parsons et al., 2014), with faster bone growth in specific bones important for a fast jaw rotation (Navon et al., 2020), rather than bones associated with a strong rotation. The same species fed a benthic diet presented with a comparatively more rounded craniofacial profile (Parsons et al. 2014), and faster bone growth in bones related to a stronger jaw rotation (Navon et al., 2020). However, plastic responses manifest at different times depending on the specific area of the head being assessed. This is also reflected in the transcriptional response induced by alternate foraging regimes, in that there are differences in gene expression as early as 5 weeks and as late as 18 months after the onset of treatment (Gunter et al., 2013; Parsons et al., 2016;

Navon et al., 2020). Interestingly, the cichlid craniofacial region has many homologous structures in humans, making it a great model for human variation and disease in this area.

Studying aspects of craniofacial shape in response to mutations, varying mechanical inputs, and time can be fruitful in the field of evolution, medicine, and development. However, every phenotype has a genetic component. All levels of organization—and modification—have a transcriptional output, and levels of gene expression is what regulates organismal complexity. Looking into the regulation of gene expression under varying conditions will be informative as to why a phenotype or response presents as it does. For example, assessing the transcriptional response under different mechanical load in different species of cichlid can give insight into the molecular regulation of plasticity and whether/how different species' responses have evolved. As time has been shown to play a critical role in the plastic transcriptional response, assessing the regulation of gene expression along a series of time would lend insight into how/how quickly a plastic response presents. In addition, because mechanosensing is intimately linked to the primary cilium, determining the effect of ablated/mutated cilia could be crucial in establishing how stable bone-related gene networks are.

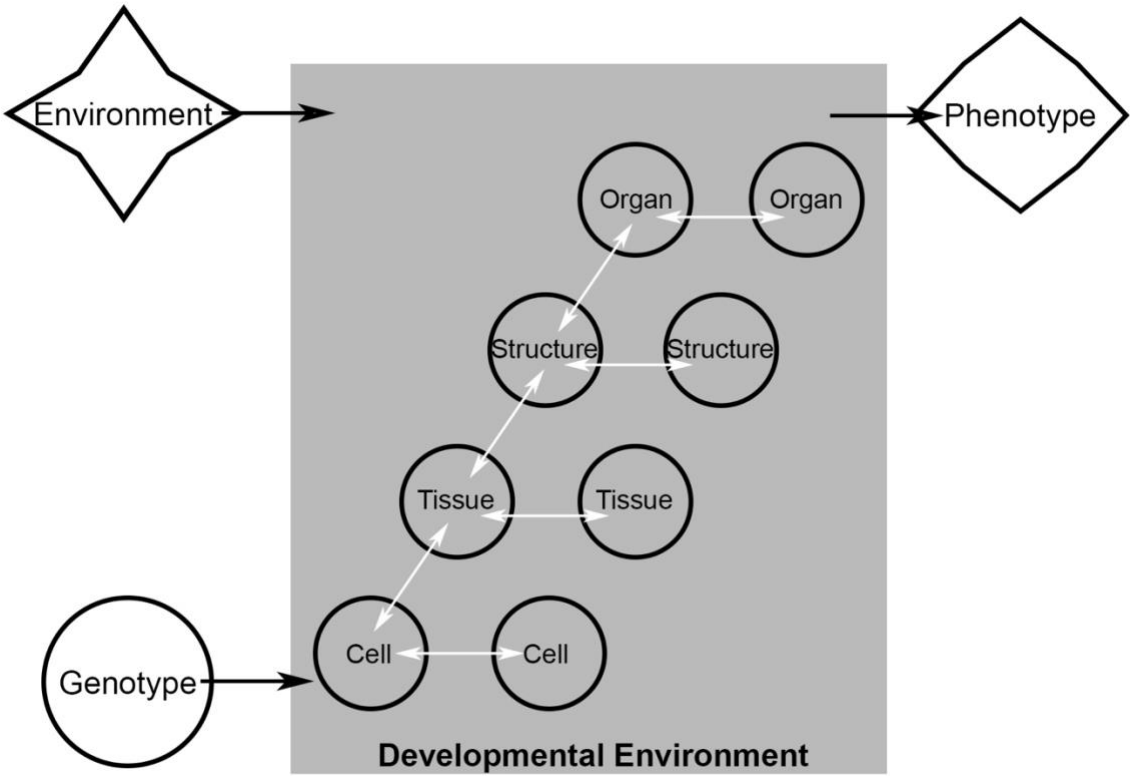

Figure 1: Genotype-phenotype map. A genotype does not inherently encode a phenotype, as epigenetics, such as interactions between cells and tissues or epigenetic modifications to the genome, and external environmental stimuli, can modify the phenotype. Figure modified from Jamniczky et al. (2010), *Bioessays*, *32*(7), 553-558.

CHAPTER II

THE TRANSCRIPTIONAL STATE AND CHROMATIN LANDSCAPE OF CICHLID JAW SHAPE VARIATION ACROSS SPECIES AND ENVIRONMENTS

Tetrault, E.R., Swenson, J., Aaronson, B., Marcho, C., & Albertson, R.C. (2023). *Molecular Ecology*, *32*(14), 3922-3941.

Introduction

A major ongoing challenge in biological research is to understand the origin and maintenance of biodiversity, with broad implications in conservation, ecology and evolutionary biology. Traditionally, these endeavors have involved characterizing the forces and mechanisms operating above the organismal level (e.g. selection, environmental change (Burns et al., 2009; Callaghan et al., 2004; Schluter, 2000; Siepielski et al., 2017)) or within the organism (e.g. genetic and developmental mechanisms (Hohenlohe, 2014; Kawajiri et al., 2014; Margres et al., 2015)). Understanding the intersection of extrinsic and intrinsic forces (Laitinen & Nikoloski, 2019; Levis et al., 2020; Mccairns & Bernatchez, 2012; van Heerwaarden & Sgrò, 2017) holds significant potential to advance the field.

African cichlids are a hyperdiverse group of fishes that have long been used as an evolutionary model (Kocher, 2004; Seehausen, 2006) and have been especially useful in revealing both the genetic and environmental factors that contribute to biodiversity (Ding et al., 2015; Genner et al., 2004; Malinsky et al., 2018; McKaye et al., 1984; Sturmbauer & Meyer, 1992). In Africa, approximately 2000 cichlid species have arisen over the past ~20 million years, which is unparalleled compared with the speciation rates of other vertebrates (Seehausen, 2006). Moreover, cichlid diversity is pronounced across several

phenotypic axes, including coloration (Maan et al., 2006; Salzburger, 2009; Seehausen et al., 1999), activity levels (Lloyd et al., 2021), as well as reproductive and foraging behaviors (Balshine-Earn & Earn, 1998; Genner et al., 1999; López-Fernández et al., 2014). Variation in feeding architecture, which relates to the foraging niche exploited by each species/population, is another critical axis of cichlid diversity (e.g. Cooper et al., 2010). Cichlid craniofacial variation is largely continuous, but there are also examples of extreme or discontinuous variants (reviewed by Powder & Albertson, 2016). In general terms, cichlids partition their foraging niche along a benthic–pelagic ecomorphological axis, with concomitant shifts in foraging anatomy (Conith & Albertson, 2021; Cooper et al., 2010; Young et al., 2009). For instance, species inclined towards a benthic mode of feeding tend to have steeply descending facial profiles, small eyes positioned towards the top of their heads, and short, robust oral jaws with closely spaced, multicuspid teeth optimal for biting and scraping (e.g. Figure 2a,b). On the opposite end of this spectrum, pelagic feeders tend to possess longer, streamlined heads, large eyes and long, up-turned oral jaws with large, widely spaced teeth optimal for suction/ram feeding (e.g. Figure 2c,d; Albertson et al., 2003; Cooper et al., 2010).

Significant efforts over the past 20 years have focused on characterizing the genetic basis of cichlid craniofacial variation (e.g. Albertson et al., 2005; DeLorenzo et al., 2022; Hu & Albertson, 2017; Powder et al., 2014; Roberts et al., 2011; Singh et al., 2017). In addition, cichlids have long been a model of phenotypic plasticity (Huysseune, 1995; Machado-Schiaffino et al., 2014; Meuthen et al., 2018; Meyer, 1987; Navon et al., 2020; Schneider et al., 2014; Wimberger, 1991), which is defined as the ability of a single genotype to produce a range of phenotypes in response to

environmental inputs. Plasticity is critical for organismal survival in an era of rapid environmental change (Gugger et al., 2015; Karasz et al., 2022; Morgan et al., 2022; Sih et al., 2011; Willis et al., 2008). It can also influence the direction and/or speed of future evolutionary change by exposing new phenotypic and genetic variants to natural selection (Campbell et al., 2021; Landy et al., 2020; Ledón-Rettig et al., 2010; Mcguigan et al., 2011). In spite of its importance across a range of biological disciplines, there are many outstanding questions about plasticity, including its genetic basis and evolutionary potential (Gibert, 2017). Plasticity is well-documented in cichlids across a range of morphological traits including full body, craniofacial, oral jaw and pharyngeal jaw shapes (Gunter et al., 2013; Huysseune,1995 ; Muschick et al., 2011; Navon et al., 2020; Parsons et al., 2014). A notable theme that has come from these data is that closely related species can differ in either their magnitude or direction of the plastic response to the same stimulus (Navon et al., 2020; Parsons et al., 2014), suggesting that plasticity itself is an evolvable trait. If true, then plasticity must also have an explicit genetic basis (Diouf et al., 2020; Küttner et al., 2014; Lafuente et al., 2018); however, understanding plasticity at this level has proven challenging (Gibert, 2017).

Previous efforts in our laboratory have sought to describe the genetic basis of plasticity and have described roles for Wnt (Parsons et al., 2014) and Hh (Hu & Albertson, 2017; Navon et al., 2020) signalling, respectively. In addition, genetic mappings studies within different foraging environments led to the discovery of *ciliary rootlet coiled-coil 2* (*crocc2*) as a regulator of functionally relevant cichlid jaw shape (Gilbert et al., 2021). *Crocc2* encodes a protein that is a major structural component of the primary cilium's rootlet (Yang et al., 2002). Primary cilia are important

mechanosensors that help cells sense and respond to environmental stimuli, but roles of the rootlet in mechanosensing are less clear (Styczynska-Soczka & Jarman, 2015). Notably, this gene was only implicated in regulating cichlid jaw shape in the mechanically demanding benthic/biting environment (Gilbert et al., 2021; Parsons et al., 2016), and functional analyses in zebrafish showed that mutations in *crocc2* led to degeneration of cilia, decreased mechanosensing abilities, dysmorphic bone shapes and misregulation of gene networks in bone tissue (Gilbert et al., 2021). Together, this incipient literature has implicated a small handful of genes that contribute to mechanosensitive signal transduction pathways (e.g. Hh) and structural components of the cell (e.g. rootlets) in the evolution and plasticity of cichlid bone shape.

Beyond inquiries into plasticity *stricto sensu*, we have shown that the environment can significantly influence the genotype–phenotype map in cichlids. Specifically, when reared in alternate foraging environments, loci that underlie variation in various feeding-related traits map to largely distinct regions of the genome (Parsons et al., 2016; Zogbaum et al., 2021). Notably, this genetic modularity was observed regardless of whether or not the traits themselves were plastic (Parsons et al., 2016). Such cryptic genetic variation has long been recognized as an important factor regulating evolutionary potential, developmental outcomes and the penetrance of disease (Gibson & Dworkin, 2004); however, the genes that underlie cryptic genetic effects on phenotype remain poorly understood, especially in vertebrate systems.

Here, we seek to advance an understanding of the genetic and epigenetic control of adaptive variation in the cichlid feeding apparatus. We utilize two complementary methods of assessing transcriptional output: RNA-seq to analyze gene expression and

ATAC-seq to assess chromatin accessibility. We focus on an important functional complex—that is, the interopercle- retroarticular (IOP-RA) linkage—which (1) is part of the opercle 4-bar system, (2) helps to drive lower jaw depression, (3) is comprised of hard and soft tissues, (4) varies among Malawi cichlids in a manner that predicts foraging mode/habitat, and (5) has been shown to be plastic in previous research (Figure 2; Hu & Albertson, 2014, 2017; Navon et al., 2021). Environmental input is explicitly incorporated into our experimental design, as we force animals to collect prey in a manner that mimics alternate benthic-pelagic modes of feeding. Our goals are to identify genes that are both differentially expressed (DE) and differentially accessible (DA) between species and environments. In doing so, we will characterize the molecular/cellular basis through which species-specific jaw shapes arise over development, as well as the roles played by the foraging environment in shaping the feeding apparatus.

Materials and Methods

Fish husbandry

Wild-caught cichlids were purchased from the aquarium trade, and housed and bred in 40-gallon glass aquaria at ~28°C on a 14-h light/10-h dark cycle. Each aquarium was part of a recirculating system, with automated daily water changes and chemical dosing to ensure consistent water quality (pH ~8.5 and 350 μS). Cichlid husbandry follows protocols approved by the institutional animal care and use committee at the University of Massachusetts.

Experimental design

To determine how alternative feeding regimes affected gene expression and the cis-regulatory system, we used a benthic diet or pelagic diet to impose a power or speed demands, respectively, on the oral jaw apparatus. This experimental design was used in two cichlid species, *Tropheops* sp. '*red cheek*' (TRC) and *Maylandia zebra* (MZ) (Figure 2a–d). Animals used in this study were juvenile stage and 2–3 generations removed from wild-caught. We chose this life history stage to mitigate the confounding effects of dominance, as cichlids are territorial and aggressive toward conspecifics. It is also the period of development when all bony elements have formed but animals are still actively growing (Fujimura & Okada, 2007, 2008a, 2008b). Diet treatments ran for 17 days for RNA-seq and 28 days for ATAC-seq (Figure 2e). The combination of approaches allowed us to examine both differential expression and differential chromatin accessibility between species and environments. That the experiments were performed at two different time points following the onset of foraging challenges, allowed us to identify loci with effects over extended periods of time.

RNA-seq

We terminated the diet treatment at 17 days and each individual was sacrificed. The interopercle, interopercle-mandibular ligament and retroarticular (i.e. IOP-RA complex, Figure 2) were dissected from the left side of each fish for RNA-seq and qPCR. It is to be noted that this complex is a mix of tissue types (e.g. bone, ligament and epithelial tissue). For RNA-seq, six animals were randomly selected from each treatment and species, and dissected tissues were stored in Trizol (Invitrogen) at −80°C, homogenized using a Next Advance Bullet Blender and five UFO beads each, and

processed using the phenol–chloroform method of RNA extraction, but did not undergo cDNA conversion. We standardized each sample to 500 ng total RNA in 50 μL and produced libraries using the TruSeq Stranded mRNA Library Prep Kit (Illumina). Any remaining RNA not used for RNA-seq was stored at −80°C. Libraries were sequenced at the University of Massachusetts Medical School Deep Sequencing Core with a HiSeq 4000 with 50 × 50 paired end reads.

Raw reads from RNA-Seq were assessed using FastQC (Andrews, 2010), and ends were trimmed accordingly using cutadapt (Martin, 2011). Cleaned reads were mapped against the *Maylandia zebra* genome version UMD2a (Yates et al., 2020) with Bowtie2 (Langmead & Salzberg, 2012) and a matrix of read counts was generated from the alignments with HT-Seq count (Anders et al., 2015). Nucleotide diversity in Lake Malawi cichlids can be higher within than between species (Malinsky et al., 2018); therefore, it is not a surprise that MZ and TRC individuals in our study showed similar alignment rates to the MZ genome (Table S1). As such, there does not appear to be any analytical bias stemming from mapping reads from both species to one genome.

We used edgeR v3.30.3 (Chen et al., 2014; Robinson et al., 2010) to identify differentially expressed genes between treatments, as well as those that showed an additive effect between species and environment. Results were groundtruthed by visually comparing normalized counts (counts-per-million; cpm) among treatments. We used FDR (Benjamini–Hochberg method) to determine significance (threshold of .05) for DEGs in pairwise comparisons, as well as our additive model, which took the form $E(y) = \beta 0 + \beta spxsp + \beta envxenv$ where E(y) is the expected number of read counts (applied to each gene). This model allowed us to detect DEGs that showed an effect across both

species and environment. Heatmaps were made using Euclidean distance with the heatmap.2 function in the gplots v3.1.1 package (Warnes et al., 2015). Gene ontology (GO) terms were as- signed using the annotated Maylandia zebra genome (ensembl.org) via biomaRt v2.44.4 (Durinck et al., 2005, 2009) in the biomartr package v0.9.2 (Drost & Paszkowski, 2017), and enrichment analysis was conducted via topGO v2.40.0 (Alexa & Rahnenfuhrer, 2009) in the R environment v4.0.5 (R Core Team, 2021) using the weight01 algorithm and Fisher's exact test with a significance threshold of .05.

Tissues from individuals not used for RNA-seq, were stored in Trizol at −80°C, and homogenized as previously described. We followed the phenol–chloroform RNA extraction method and converted RNA to cDNA using a High-Capacity cDNA reverse transcription kit (Applied Biosystems) for gene expression validation purposes. These samples were standardized to an RNA concentration of 70 ng/μL.

qPCR was used to measure expression of genes found to be differentially expressed and differentially accessible from the RNA-seq and ATAC-seq datasets using the comparative CT method. qPCR primer sequences are listed in the Table S2.

ATAC-seq

We designed an ATAC-seq protocol optimized for bony/ligamentous fish tissues (adapted from Buenrostro et al., 2013; Corces et al., 2017). The diet treatment was terminated after 28 days (Figure 2e), and similar to the RNA-seq experiment, each animal had the IOP-RA complex from the left side of the face removed after being euthanized. Briefly, each sample was placed in 3% collagenase II in 5% FBS/DMEM for cell collection for 2 h. To ensure we collected cells of the appropriate size, we filtered the cells through a 70μm strainer. Cell quality and count was confirmed by inverted light

microscopy. We collected up to 500,000 cells for each sample. Cells were then lysed to isolate nuclei and underwent a transposition reaction to cut chromatin, and the resulting DNA fragments were purified using a Qiagen MinElute Cleanup Kit. We constructed libraries from the transposed DNA and performed double-sided bead purification to remove large (>1000 bp) and small (e.g. primer dimer) DNA fragments. The detailed protocol can be found on github at http://github.com/tetra22e/Genomics2022. Libraries were sequenced in the same manner as RNA-seq libraries.

Raw reads were again aligned against the Maylandia zebra genome using bowtie2 v2.4.1, and data were converted to appropriate formats for downstream analyses using samtools v1.9 (Li et al., 2009) and bedops v2.4.14 (Neph et al., 2012), with parallelization enabled by gnu parallel (Tange, 2018). Peaks were called for each individual sample using Genrich (https://github.com/jsh58/Genrich), and flags were set to filter mitochondrial reads and PCR duplicates before peak calling.

Differential accessibility was assessed using DiffBind v3.0.15 (Stark & Brown, 2011). Significance was determined using FDR (Benjamini–Hochberg method, threshold of 0.05). Peaks that were differentially accessible between any two treatments were annotated by intersecting the genomic coordinates of the peaks with the *Maylandia zebra* gtf file using bedtools v2.29.2 (Quinlan & Hall, 2010), with the requirement that 30% of the peak must overlap with the annotated feature.

Results and Discussion

Extensive species differences in gene expression

The cichlid genome has over 25,000 protein-coding genes (Conte et al., 2019). Of these, 17,525 were expressed in focal tissues, and 5318 were differentially expressed

(DE) between our two species, across both foraging conditions, with 2667 upregulated in MZ (relative to TRC—red in Figure 3a) and 2651 upregulated in TRC (relative to MZ—blue in Figure 3a; Table 1). Cluster analysis using the top 500 most differentially expressed genes (DEGs) illustrates a clear separation of species (Figure 3b), but differences between foraging environments are less apparent. While MZ shows some separation by environment, this pattern is not as apparent among TRC.

Gene ontology (GO) analyses were performed on DEGs to determine what biological processes were enriched (Figure 3c). Whereas processes related to cell cycle regulation were among the most enriched in genes upregulated in MZ, a diversity of other processes were enriched in upregulated genes in TRC. These data suggest that there may be divergent modes of bone growth operating in these species at the time when tissues were collected.

Differential gene expression is rare between foraging environments

Craniofacial plasticity is well-documented in cichlids (Meyer, 1987; Navon et al., 2020; Schartau et al., 2009; van Snick Gray & Stauffer, 2004; Wimberger, 1991), and skeletal plasticity has been associated with changes in gene expression (Navon et al., 2020). However, most work on the transcriptional basis of craniofacial plasticity in cichlids has focused on the lower pharyngeal jaw (Gunter et al., 2013; Schneider et al., 2014). Our work complements this body of literature by focusing on skeletal and soft-tissue elements critical for lower oral jaw depression (i.e. IOP-RA complex, Figure 2). While 38 DEGs were detected between foraging environments in MZ, none were detected for TRC (Table 1, Figure 4a,b), suggesting that MZ is more plastic than TRC, and/or plasticity arises earlier in MZ compared to TRC. Of the DEGs within MZ, 25 were

upregulated in the pelagic environment, whereas 13 were upregulated in the benthic environment (Table 1, Figure 4b). Assuming upregulated genes have a positive effect on bone deposition rates, these data are consistent with previous data showing greater rates of bone deposition in MZ exposed to a pelagic environment (Navon et al., 2020).

Within MZ, genes upregulated in the pelagic environment (relative to the benthic environment) seemed to be largely associated with proliferation, which was reflected by the GO analysis (Figure 4c). For example, *ccna2* is a cyclin that activates *cdk2* and promotes cell cycle progression through both G1/S and G2/M phases (Pagano et al., 1992), and *cks1b* slows the progression of G1/S and can block entry to M phase (Westbrook et al., 2007). In addition, *cdc20* regulates metaphase–anaphase transition during mitosis via activation of APC, which targets proteins for degradation (Visintin et al., 1997; Yu, 2002). Finally, *cdca5*, which encodes Sororin, plays an important role in cell proliferation (Fu et al., 2020), and more specifically in the binding of Cohesin to chromatin during cell division (Rankin et al., 2005; Schmitz et al., 2007). Each of these genes was upregulated in our study in pelagic foraging MZ compared with benthic foraging conspecifics. Given the well-studied roles for cell proliferation in bone formation, shape and growth (Capecchi et al., 2018; Du et al., 2021; Gao et al., 2020; Le Pabic et al., 2022; Shekhar et al., 2019), the data presented here suggest that this mechanism is important in mediating skeletal plasticity in this species.

For MZ in the benthic environment, the only GO term enriched for upregulated genes (relative to pelagic) was stress response. In addition, a diversity of other processes are implicated by specific upregulated genes, including skeletal muscle changes in response to stimuli (e.g. *arrdc3b*, Gordon et al., 2019; *myoglobin*, Beyer & Fattore,

1984), and osteoblast proliferation via regulation of *cyclins* (e.g. *per2*, Fu et al., 2005). Our previous work suggested that benthic foraging might be a nonpreferred environment for MZ, at least in terms of environmentally stimulated bone growth (Navon et al., 2020). Here, this assertion is supported by the observation that genes upregulated in the pelagic environment all seemed to contribute to the same biological process—that is, cell proliferation—with known roles in bone formation/growth (Capecchi et al., 2018; Du et al., 2021; Gao et al., 2020; Shekhar et al., 2019). Alternatively, genes upregulated in the benthic environment were involved in a diversity of processes, including stress response.

Craniofacial plasticity has been noted in both MZ and TRC (Navon et al., 2020; Parsons et al., 2014), and so the lack of more extensive DEGs between foraging treatments, especially in TRC, was somewhat surprising. However, we note that plasticity in these species was (a) subtle, and (b) described weeks or months following the onset of foraging trails (Navon et al., 2020; Parsons et al., 2014). For instance, while rates of bone matrix deposition were significantly different within both MZ and TRC (Navon et al., 2020), there is a fair amount of overlap between treatments, particularly in TRC (Figure 4b). In fact, a closer look at the data by Navon et al. (2020) clearly shows that MZ is more plastic than TRC, and that plasticity in MZ is driven by the pelagic foraging environment (blue, Figure 5a). Timing is also a potentially con- founding factor in the study of plasticity. Previous studies have used time points measured in months (Schneider et al., 2014) or years (Gunter et al., 2013) to examine DEGs between foraging environments in the cichlid lower pharyngeal jaw, and so it is possible that we did not allow enough time for a plastic response to manifest. Alternatively, mechanical load has been shown to induce gene expression changes in bone cells in a matter of hours (Govey

et al., 2015; Kelly et al., 2016; Mantila Roosa et al., 2011; Raab-Cullen et al., 1994). It is therefore also possible that a more robust plastic response in gene expression might occur earlier than the time point sampled here. Finally, FDR is a stringent metric, and it is possible that biologically relevant changes in expression have occurred but are not detected by standard pipelines. In this regard, examining genes with high fold changes, but FDR-values >0.05, might prove fruitful. For example, a transcript that was upregulated in benthic TRC (log2FC = 5.44, p = .015, FDR = 1.0) corresponds to *receptor transporting protein 3* (*rtp3*), which has been linked to human femoral cortical thickness and buckling ratio, as well as hip fractures (Zhao et al., 2010), and another upregulated benthic gene (log2FC = 4.83, p = .015, FDR = 1.0), *poly(ADP-ribose) polymerase 14* (*parp14*), has been shown to regulate cell cycle progression via Cyclin D1 (O'Connor et al., 2021). Thus, viable candidates for craniofacial bone plasticity may be found just under the threshold set by RNA-seq protocols.

We stress that a relatively low number of DEGs within species does not preclude more general roles for the environment in determining species-specific bone shapes. For example, bone matrix deposition data (Figure 5) suggest that pelagic foraging is leading to a greater difference between species than benthic foraging. As a next step, we therefore assessed the effect of foraging environments on DE between species.

<u>The pelagic environment drives species-specific differences in gene expression and reveals signature of genetic assimilation</u>

We have shown previously that foraging conditions can have a marked impact on the genotype–phenotype map. Specifically, quantitative trait loci (QTL) for the same trait map to distinct regions of the genome when animals are reared under alternate benthic/pelagic foraging conditions (Parsons et al., 2016; Zogbaum et al., 2021). We

therefore examined expression differences between species within each environment and documented a striking imbalance in DEGs. Specifically, when only considering animals exposed to pelagic conditions, we found 3761 DEGs between species, whereas only 984 DEGs were detected between species when only comparing animals reared under benthic conditions (Table 1, Figure 6a– c). Additionally, when comparing environment-specific DEGs to the total dataset (i.e. combining both environments), we found that 2609 genes from pelagic animals were represented in the global comparison, whereas only 155 genes from benthic animals overlapped between datasets (Table 1, Figure 6c). These data underscore the importance of environmental context in determining the genetic basis of species-specific bone shapes (Parsons et al., 2016; Zogbaum et al., 2021). More specifically, they suggest that the pelagic foraging environment is driving species differences in gene expression within the IOP-RA functional complex.

This trend is drawn out when comparing genes from an additive model (S + E), whereby DEGs were detected at the level of both species and foraging environment (Figure 7a). When illustrated as a heatmap, these data support the assertion that species differences in gene expression are driven by the pelagic environment, and reveal patterns consistent with either genetic accommodation or assimilation. Genetic assimilation is a mechanism by which plasticity is lost over evolutionary time as genetic variation that facilitated plasticity in an ancestral population becomes fixed as descendent populations adapt to a specific environment (reviewed by Pigliucci et al., 2006). If we assume that plasticity is ancestral, evidence for genetic assimilation is apparent in several gene clusters (denoted by pink dots, Figure 7a), whereby TRC expression levels are indistinguishable between foraging environments and match those of benthic MZ.

Consistent with previous data, many of the DEGs identified by this model contribute to cell cycle regulation—for example, *cdc20*, *cdca5*, *cdca8*, *ccne2*, *ccnb1*, *ccnb2*, *ccnf*. A list of all the DEGs in this model can be found on github at http://github.com/tetra22e/Genomics2022.

Alternative to genetic assimilation is genetic accommodation, or an increase in genetic plasticity over evolutionary time. We cannot rule this out, as it is possible that plasticity has been enhanced beyond the ancestral condition in MZ. Regardless, the main conclusion to be drawn from these data is that the evolution of plasticity in this system may be traced to divergent patterns of gene expression associated with cell cycle regulation.

We next performed GO analyses for DEGs between species in each foraging environment. When considering animals reared in the pelagic foraging environment, GO analysis revealed a diversity of biological processes; however, those associated with cell division were among the most enriched in MZ, whereas translation and cell differentiation were among the most enriched processes in TRC (Figure 6d). For animals reared in the benthic environment, comparatively fewer biological processes were enriched in general, consistent with fewer DEGs being identified. Similar to pelagic fishes, this analysis found enrichment of cell cycle genes in MZ, and cell differentiation in TRC (Figure 6e).

Unsurprisingly, enriched GO terms for the additive model are similar to those for MZ in the pelagic environment, and include cell cycle, cell division and chromosome segregation (Figure 7b). In addition, this analysis found enrichment of cytoskeleton organization, which is critical to many cellular functions relevant to bone formation and

plasticity, including mechanotransduction (Gunst & Zhang, 2008), and primary cilia formation (Mirvis et al., 2018), which we and others have found to be necessary for load-induced bone formation (Chen et al., 2016; Gilbert et al., 2021; Moore et al., 2019).

Species-specific differences in chromatin accessibility are influenced by foraging conditions

Areas of the genome that contain open chromatin are more accessible to transcriptional machinery and therefore able to increase gene expression, whereas closed chromatin sites are less accessible for transcription. The differences in accessibility (e.g. between species or environments) are considered differentially accessible (DA), and may be due to either genetic (e.g. deletion of a TF binding site) or epigenetic (e.g. methylation changes) processes. When comparing species across both environments, we identified 10,770 areas of accessible chromatin, and of these 297 were DA. Note that many genes contain more than one accessible chromatin peak (e.g. Figure 8b,d). The number of DA genes was considerably less than the number DE of genes, which may reflect differences in the timing and/or nature of each experiment. In addition, we did not observe a marked bias in one environment versus the other in terms of the number of differentially accessible genes (DAGs) between species, with 114 DAGs identified when animals were forced to feed pelagically and 157 DAGs when animals foraged using a benthic mode (Table 1). These data suggest that the number of DAGs between species is not being driven by one environment at the time when tissues were collected.

The overlap between RNA-seq and ATAC-seq datasets implicates loci acting over extended periods of time (i.e. at both 17- and 28-day time points) following the onset of foraging trials (Figure 8a, Table S3). In all, we identified 15 genes in the interspecies

comparisons that were both DE and DA in fishes reared in the pelagic foraging environment, and 11 from the benthic environment. We also identified 13 genes that were DE and DA in both environmental conditions, which suggest that their expression is robust to differences in the environment. The direction of DE and DA across all genes was generally consistent (Table S3). In particular, out of 39 genes, the polarity of DE and DA was similar in 34. Differences in the other five could be due to DA being associated with the binding of a repressive transcription factor. Alternatively, given that RNA-seq and ATAC-seq experiments were performed at different time points, it is also possible that expression of these factors may oscillate over time.

Determining whether or not these factors are DA due to genetic or epigenetic factors would be a fruitful line of future study. Resequencing a panel of cichlids around DA peaks would allow us to assess whether any indels or SNPs might underlie differences noted here. In addition, the co-occurrence of DA peaks and CpG islands would suggest that differential DNA methylation might be driving differences in expression. For example, the DA peak associated with KIAA0586 expression is in intron 7– 8 (Table S3), which is large and contains several predicted CpG islands, although none overlap with the DA peak (Figure 8c).

Candidate genes in craniofacial divergence among cichlid species

A few of the genes identified as both DE and DA have been implicated in craniofacial development, including *KIAA0586* (also known as *talpid3*), which is essential for primary cilia formation and Hedgehog (Hh) signalling (Schock et al., 2016), and *etv4* (Ahi et al., 2016; Rodriguez et al., 2020). *KIAA0586* is notable given previous work from our laboratory that has demonstrated important roles for the primary cilium-

Hedgehog molecular mechanism in cichlid and zebrafish craniofacial development (Gilbert et al., 2021; Hu & Albertson, 2014; Navon et al., 2020; Zogbaum et al., 2021). While *KIAA0586* is well-studied in the context of early craniofacial patterning events (reviewed by, Schock et al., 2016), roles at latter stages, including bone growth and mechanosensing, have not been explored. Taken together, multiple independent experiments in the cichlid system support the thesis that the primary cilium-Hedgehog 'signal transduction machinery' is an important and evolvable mechanism for shaping the craniofacial skeleton.

Etv4, a member of the ETS family of transcription factors, is a particularly interesting candidate as it connects environmental stress and craniofacial morphogenesis. This gene encodes the main co-factor of Hypoxia-inducible factor (Hif; Wollenick et al., 2012), a 'master switch' for hypoxia-induced transcription in fishes (Nikinmaa & Rees, 2005). Hypoxia-inducible factor can also act through Ahr signalling, another regulator of environmental stress, including oxygen levels (Schulte, 2007). Notably, Ahr signalling was recently implicated in benthic–pelagic divergence of Arctic charr, with greater relative expression of *ahr2b* observed in benthic versus pelagic morphs (Ahi et al., 2015). While neither *ahr2b* nor *hif* were DE in our dataset, a number of their transcriptional targets were (Figure 9). The link to hypoxia is of note since benthic habitats are characterized by relatively low oxygen levels (Nikinmaa & Rees, 2005), and many fish assemblages partition their habitat along the benthic–pelagic eco-morphological axis (reviewed in Cooper et al., 2010). Within Lake Malawi, for example, cichlid communities are structured by depth (Parnell & Streelman, 2011), and oxygen levels show a steady decrease with depth (Martin et al., 1998). Thus, oxygen may represent an

important factor in the ecological segregation of cichlid species (Martin et al., 1998). Etv4 can also act through oestrogen signalling (i.e. oestrogen receptor alpha, ER) to promote the expression of skeletogenic factors such as *bmp2*, *ptch1/2*, *rankl*, and *rara* (Ahi et al., 2016; Rodriguez et al., 2020), and experimental reduction in oestrogen levels in zebrafish leads to the development of shortened, benthic-like crania (Cohen et al., 2014). Thus, etv4 appears to have pleiotropic effects on hypoxia adaptation and craniofacial geometry.

Figure 9 supports much of the above discussion. Here, we examined *etv4* expression within the context of various downstream effectors, including those acting through Hif, Ahr and/or oestrogen signalling (Figure 9a). The cluster analysis did not return wide-spread structuring by signalling, which may point to their interdependence or to Etv4 acting through multiple pathways to influence the development of species-specific bone shapes. Similar to studies by Ahi et al. (2014, 2015), who showed greater expression of *ahr2b* and *ets2* (another ETS transcription factor) in benthic Arctic charr species, etv4 was expressed at a higher level in our benthic species, TRC (Figure 9b). We also note that *bmp2b* expression was the most similar to *etv4*, which aligns with previous work demonstrating roles for Bmp levels in craniofacial development of an extreme benthic cichlid species, *Labeotropheus fuelleborni* (Albertson et al., 2005).

The gene, *Wiskott–Aldrich syndrome* (*was*), is another interesting candidate in light of recent work. This gene is a member of the Was/Wasl protein family that signals through the actin cytoskeleton to regulate numerous cell behaviours (Snapper & Rosen, 1999). Until recently, no roles for Was/Wasl signalling had been reported in craniofacial or bone biology, but in 2021, Hawkins and colleagues demonstrated that it regulates

patterning of the appendicular skeleton in both zebrafish and mouse models (Hawkins et al., 2021). Other genes in this dataset are largely new to the field of craniofacial biology, but implicate biological processes important in bone patterning, formation, growth and homeostasis, including chromatin remodelling (e.g. *actr6* (Yoshida et al., 2010)), cell signalling (e.g. *asb5* (Yoshioka et al., 2006)) and cell growth (e.g. *impdh1* (Chang et al., 2015)). In all, this dataset provides a robust foundation for future inquiry.

Validation of select candidate genes by qPCR

We validated a subset of genes from this analysis with qPCR, focusing on those that overlapped in the RNA-seq/ATAC-seq datasets (Figure S1a–e). Trend across transcript counts (i.e. counts per million, cpm) and qPCR expression were generally equivalent, but we note that qPCR picked up significant differences in gene expression that did not meet the threshold for RNA-seq significance. For example, *actr6*, which plays important roles in heterochromatin formation in yeast, *Drosophila* and vertebrates (Ohfuchi et al., 2006), was DE between benthic and pelagic TRC according to qPCR, but not RNA-seq (Figure S1a). In addition, *gnmt*, a methyltransferase involved in the methionine pathway, which has been linked to bone density (Ables et al., 2012; Vijayan et al., 2014; Wang et al., 2011), exhibits an expression pattern that is similar to the RNA-seq data, but it is also plasticity expressed among *Maylandia* reared in different environments (Figure S1d). We also validated the expression of *cdc20*, a gene that is involved in cell cycle regulation (Visintin et al., 1997; Yu, 2002), and was significantly DE between benthic and pelagic MZ. Expression of this gene via qPCR did not quite reach significance at the .05 alpha level, but exhibited a lot of variation across samples, and showed a similar pattern to the RNA-seq data ($p = .17$, Figure S1e).

Conclusions

A number of general themes emerge from these data. First, they provide further support for the hypothesis that foraging environment influences the genotype–phenotype map for craniofacial skeletal traits (Navon et al., 2021; Parsons et al., 2016; Zogbaum et al., 2021). More specifically, our data suggest that pelagic foraging is an especially potent driver of species- and environment-specific differential gene expression. This may seem counterintuitive as diets that involve large/hard prey items are generally considered to be more mechanically demanding com- pared to small/soft food (Gunter et al., 2013; Hulsey et al., 2020; Muschick et al., 2011). However, Navon et al. (2020) showed that in MZ, bone matrix was deposited at a fast rate under pelagic foraging conditions, and speculated that suction feeding imposes high mechanical load on the feeding apparatus as animals repeatedly open and protrude their jaws. Our data support this assertion, and thus we consider the foraging treatments utilized here to challenge the feeding apparatus in two distinct ways (compared to a 'standard' flaked food diet); our benthic treatment was designed to impose high amplitude but low frequency loading on the feeding apparatus as animals scraped food from rocks, whereas our pelagic treatment translated to higher frequency but lower amplitude loading as animals repeatedly protruded their jaws to gather small food items.

These results are relevant to the broader context of fish adaptive radiations, which are characterized by repeated, almost stereotypical, divergence along a benthic–pelagic ecomorphological axis (Cooper et al., 2010; Doenz et al., 2019; Harrod et al., 2010; Maldonado et al., 2009; McGee et al., 2013; Wilson et al., 2013). Whereas benthic species typically evolve relatively short jaws, deep bodies and smaller dorsally displaced

eyes to locate and consume large, tough and/or harder prey items, pelagic species possess longer jaws, fusiform bodies and large eyes to foraging on small and/or elusive prey. In terms of the opercle 4-bar linkage system, this translates to shorter IOPs and longer RAs as seen in TRC, versus longer IOPs and shorter RAs as seen in MZ (Figure 2; Hu & Albertson, 2014; Westneat, 1990). These parallel anatomical changes are observed across distantly related fish lineages, as well as at widely different timescales. For instance, signatures of benthic–pelagic divergence have been documented between species in deep time (e.g. Cretaceous-Palaeogene boundary; Ribeiro et al., 2018), and as a plastic response within species (e.g. Day & McPhail, 1996). Thus, a major contributor to fish biodiversity, in both freshwater and marine habitats, appears to be selection acting along (i.e. parallel to) the benthic-pelagic ecomorphological axis.

Insofar as connecting phenotypic plasticity to morphological evolution, our data also detected evidence for genetic assimilation. In particular, when considering loci that were DE between species + environments, patterns in benthic MZ resembled those across TRC. *Tropheops* species, including sp. '*red cheek'*, are generally found in a benthic environment (Ribbink et al., 1983), and may have lost a degree of plasticity as they evolved to specialize on benthic food items. MZ on the contrary are true generalists in the sense that they routinely forage from both the benthic and pelagic zones (Ribbink et al., 1983). While plasticity has been noted in TRC (Navon et al., 2020; Parsons et al., 2014), our data suggest that MZ is more plastic in that they mount a more pronounced transcriptional response, at least at the time point analyzed in this study.

Cell cycle regulation consistently appeared in GO analyses, describing species differences, as well as plasticity within MZ. This implicates cell proliferation as an

important biological mechanism of species- and environment-specific bone growth in cichlids. This observation is notable as our previous work has implicated Hedgehog signalling in the evolution and plasticity of the cichlid jaw, including the IOP-RA complex (Hu & Albertson, 2014; Navon et al., 2020; Parsons et al., 2016). While canonical members of the Hedgehog signalling pathway were not significantly DE or DA in this dataset (although KIAA0586 regulates the signal, Schock et al., 2016), cell proliferation is well-known to be regulated by this pathway (St-Jacques et al., 1999; Sun & Deng, 2007; Tiet et al., 2006; Zaman et al., 2019), providing a potential cellular mechanism through which variation in Hedgehog signalling leads to differences in bone shape among and within cichlid species.

Finally, with these large overlapping genome-wide datasets, we were able to narrow thousands of DEGs to a few dozen that were both DE and DA. Given that each experiment was conducted at a different time point, this reduced dataset points to loci whose expression is important for species divergence over extended periods of growth. Among these were genes that were both sensitive and robust to the environment. Notably, nearly all of these genes are new to the field of bone biology, and while some encode known effectors of well-studied signalling pathways (e.g. EST, interleukin/Wnt, Talpid/Hh) and cell behaviours (e.g. Casp6/apoptosis, Impdh1b/cell cycle), others implicate largely novel mechanisms (e.g. Gnmt/methionine cycle). Thus, this work establishes a robust foundation for future studies into how genotype and the environment combine to influence bone formation, remodeling, and evolution.

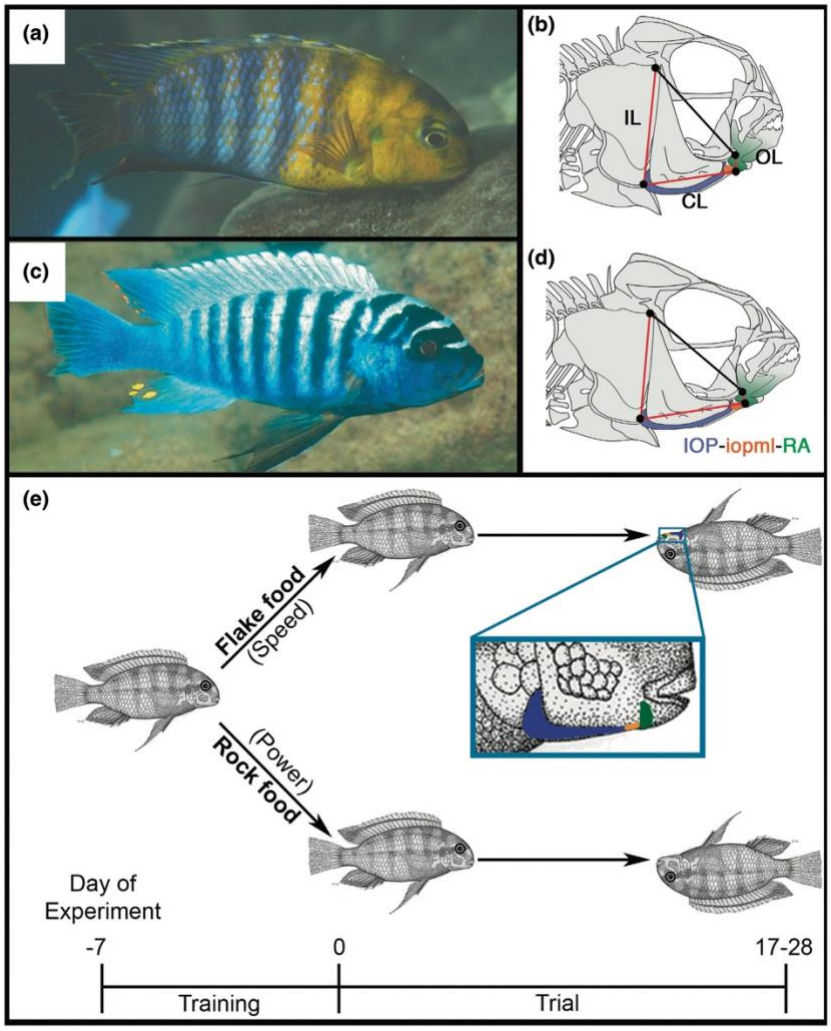

Figure 2: African cichlids from Lake Malawi display differences in foraging anatomy. (a) *Tropheops* sp. 'red cheek' (TRC) has a more downturned oral jaw apparatus, and a steeply sloping craniofacial profile, adapted for benthic foraging via scraping/biting/nipping. (b) A schematic of the opercle 4-bar linkage chain, which is critical for lower jaw depression, is shown for TRC. (c) *Maylandia zebra* (MZ) is characterized by a more upturned oral jaw, better suited for pelagic feeding via fast jaw rotation. (d) A schematic of the opercle 4-bar linkage chain is shown for MZ. Relative to TRC, MZ possesses a longer coupler link (CL) and shorter output link (OL). (a, c) Images courtesy of Ad Koning at Cichlid Press. (b, d) Red bars indicate movable linkages—input link (IL), CL, and OL—while the black bar represents the fixed link. Blue depicts the interopercle (IOP) bone, and green shows the retroarticular process (RA) of the lower jaw, while orange is the interopercle- mandibular (ioml) ligament that connects the two bones. Throughout the text, we refer to this as the IOP-RA functional complex. (e) Experimental schematic in which we fed cichlids either flake or rock food for 17 days (RNA-seq) or 28 days (ATAC-seq), with a 1-week training period. Inset shows an external view of the IOP-RA complex dissected for all experiments.

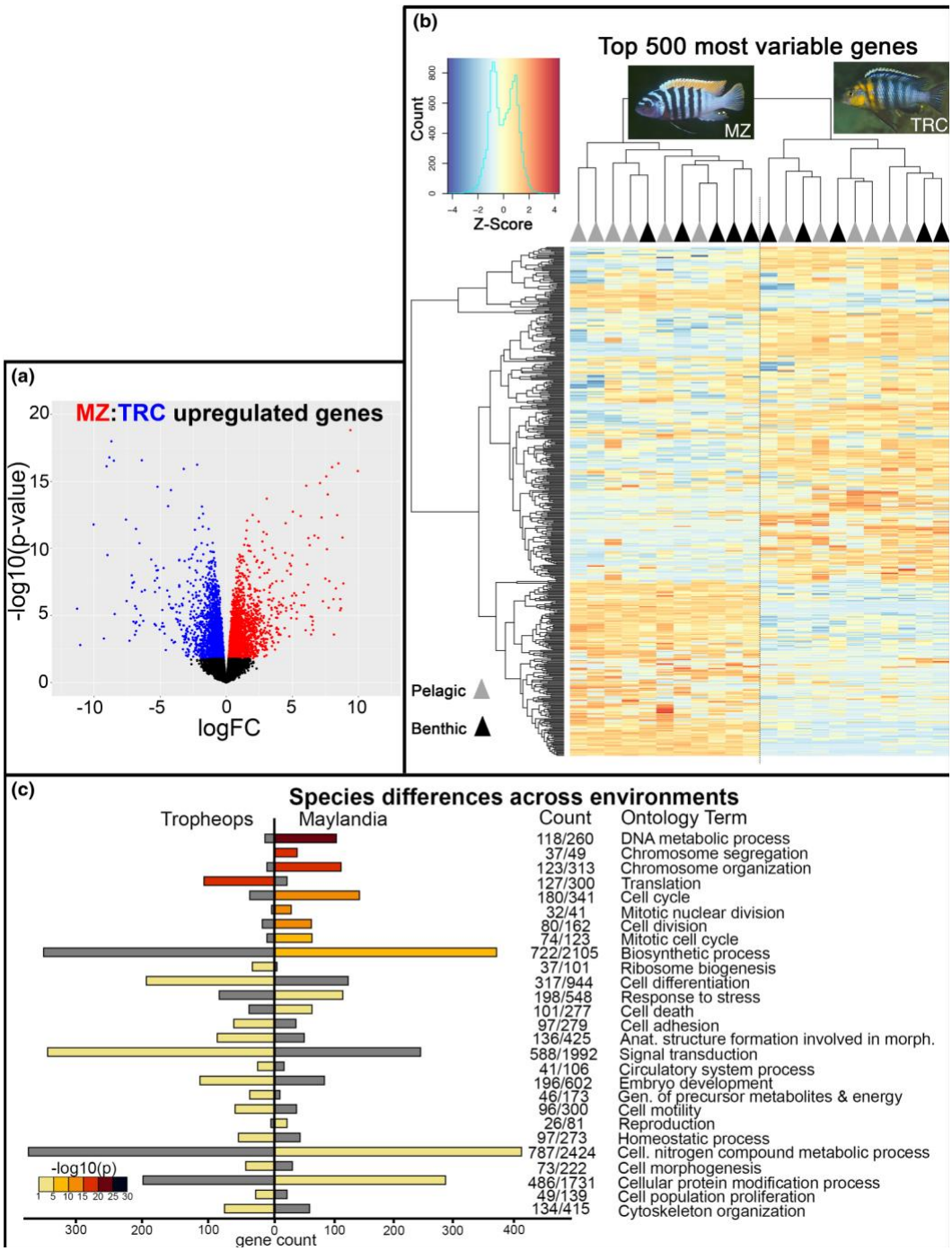

Figure 3: Differential expression between species is more robust than between foraging environments. (a) Volcano plot of the pairwise comparison between MZ and TRC across environments, showing a large number of DEGs (*n* = 5318) with roughly equal numbers of significantly upregulated genes between species (*n* = 2667 MZ; *n* = 2651 TRC). Given the nature of the comparison, genes considered upregulated in MZ are downregulated in TRC, and vice versa. Red indicates upregulated genes for MZ, blue depicts genes upregulated in TRC, while black represents genes that do not meet the significance threshold of <0.05 FDR. (b) Heatmap of the top 500 most variable genes in

the RNA-seq dataset is shown. Individuals from the pelagic foraging treatment are labelled with grey triangles, while benthic individuals are labelled with black triangles. Species cluster together, but there is less obvious structuring by foraging environment, although MZ segregate by environment more so than TRC. Photographs courtesy of Ad Koning at Cichlid Press. (c) Enriched GO terms associated with genes upregulated in the MZ:TRC comparison across environments. Colors are representative of the −log10(*p* value). Grey bars indicate no significance. Gene counts are given as a total for both species along with the corresponding GO term.

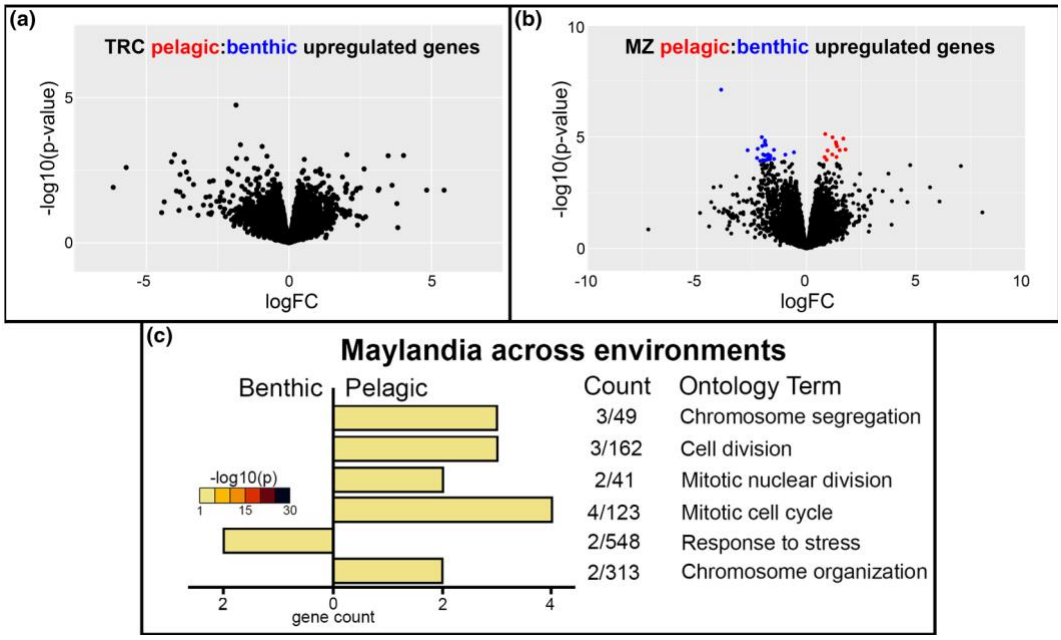

Figure 4: Little differential expression is detected between foraging environments. (a) Within TRC, the volcano plot shows no DEGs between environments. (b) Within MZ, a small number of DEGs (*n* = 38) were detected between environments, with more upregulated in the pelagic (*n* = 25; blue) versus the benthic (*n* = 13; red) environment. Black dots represent genes that are not significantly DE at FDR < 0.05 (c) Within MZ, more GO terms were returned for upregulated genes in animals exposed to pelagic versus benthic environments. Cell cycle regulation features prominently in the pelagic environment.

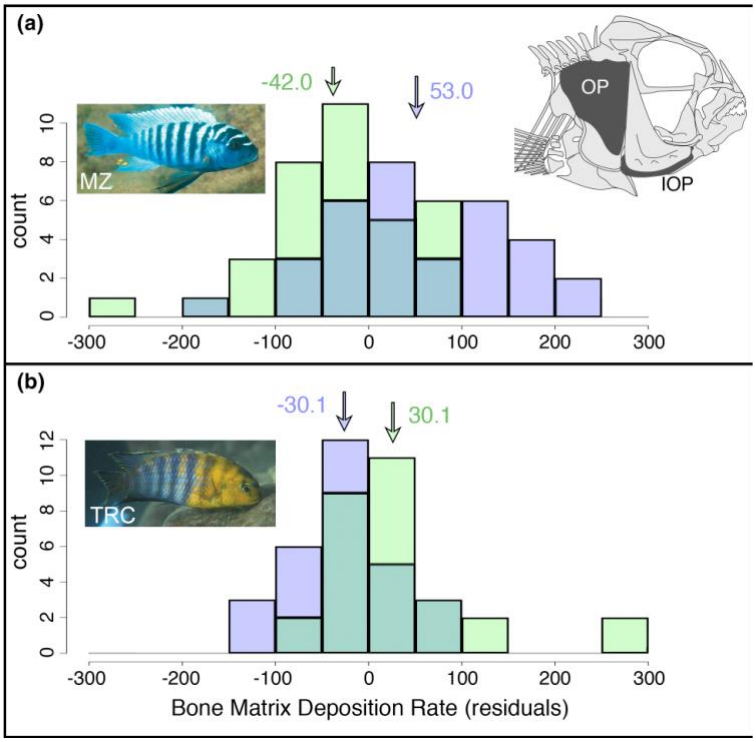

Figure 5: Bone matrix deposition rates from three areas along the opercle (OP)-interopercle (IOP) series are plotted as histograms in MZ (a) and TRC (b). Green indicates values from animals reared in the benthic environment, and blue are values from benthic fishes. Note the relatively broader distribution in MZ (a) compared to TRC (b). Mean values for pelagic- versus benthic-reared animals are plotted above each histogram. Note that while in TRC mean benthic/pelagic values are equally displaced from '0', the pelagic mean in MZ is further from '0' than the benthic mean, suggesting that the pelagic foraging environment is driving plasticity in this species. Data presented here are from Navon et al. (2020).

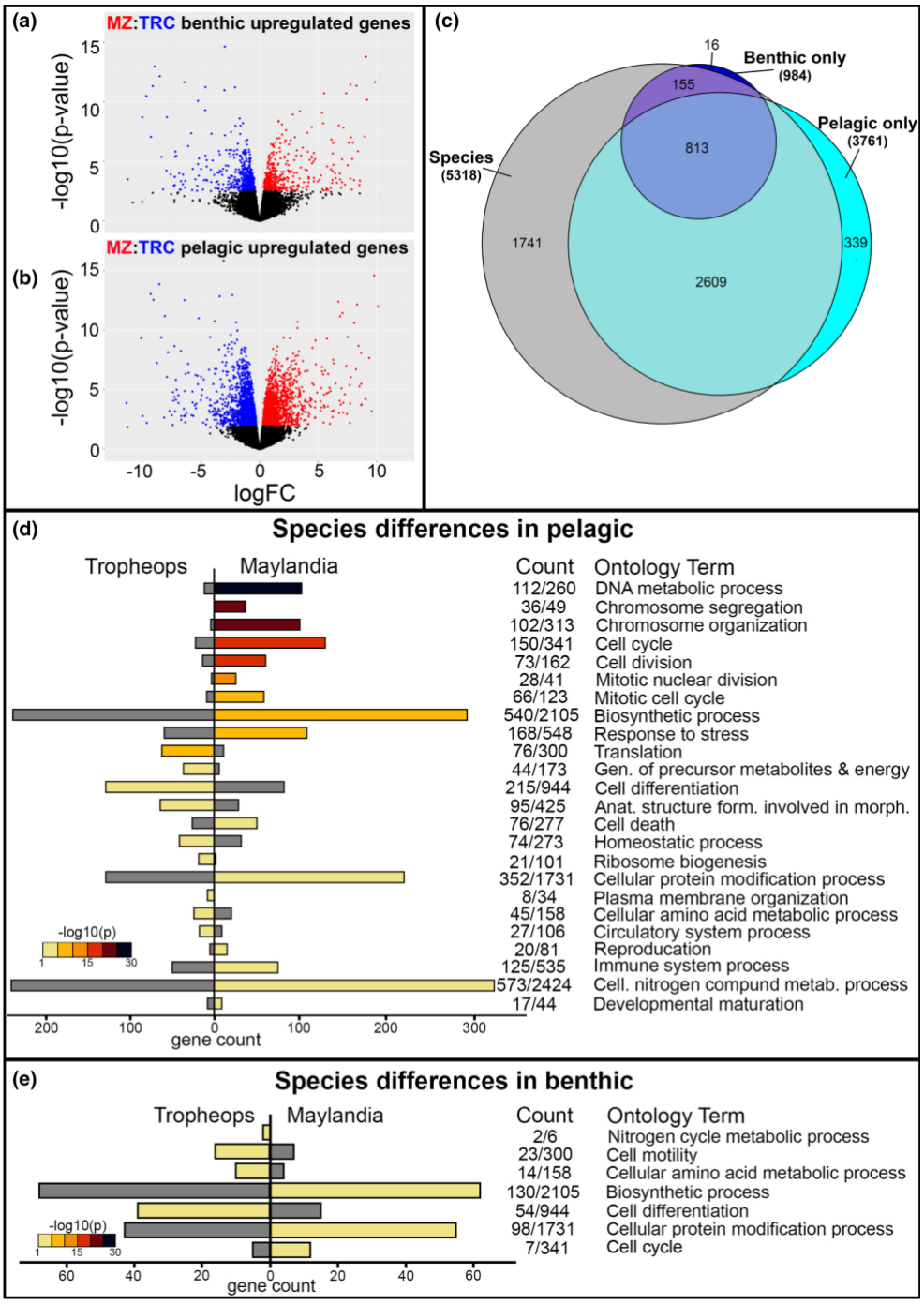

Figure 6: The pelagic environment drives differences in expression between species and implicates cell cycle regulation as a mode of increased bone deposition. (a) Volcano plot depicting DE between species in the benthic environment (*n* = 984 total; *n* = 549 MZ in red; *n* = 435 TRC in blue). (b) Nearly four times the number of DEGs are detected in the pelagic environment (*n* = 3761 total; *n* = 1927 MZ in red; *n* = 1834 TRC in blue). (c) The venn diagram shows that not only are there more DEGs in the pelagic versus benthic environment, but that most (813/984 = 83%) of the DEGs detected in the benthic environment are also DE in the pelagic environment. Alternatively, only 22%

(813/3761) DEGs detected in the pelagic environment are also DE in benthic fish. (d, e) Enriched GO terms are shown for MZ versus TRC in the pelagic (d) and benthic (e) environments. Colours are representative of the −log10(*p*-value). Grey bars indicate no significance. Gene counts are given as a total for both species along with the corresponding GO term. Many terms enriched for in MZ in both environments are associated with cell cycle (e.g. cell cycle and cell division).

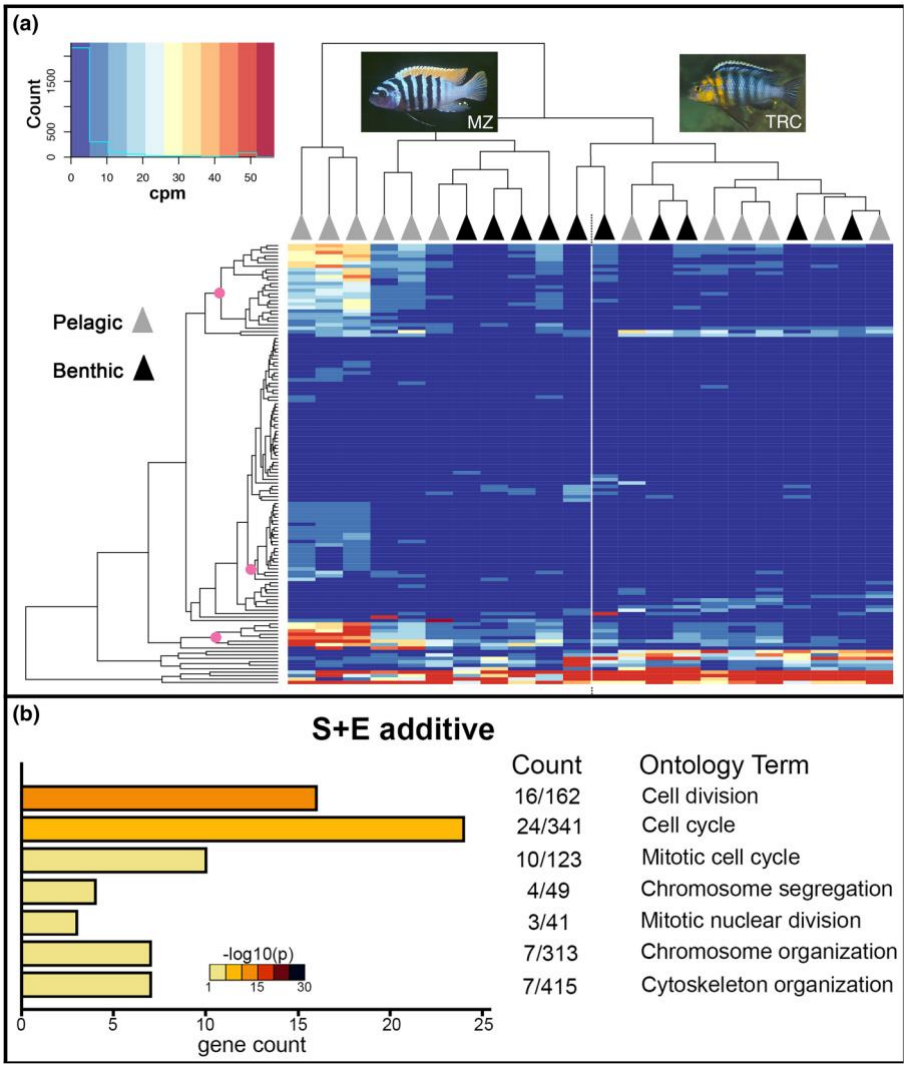

Figure 7: Differential expression across species plus environment reveals signatures of genetic assimilation and further supports a role for the cell cycle in promoting species differences. (a) We constructed an additive model to identify genes that were differentially expressed between species and environment (S + E), which identified 128 DEGs. With the exception of a single MZ individual, species clustered together. Clustering by environment was observed in MZ but not TRC. Assuming that plasticity represents the ancestral condition, this analysis also provides evidence for genetic assimilation, whereby pelagic MZ exhibited relatively high gene expression compared to benthic MZ, which generally resemble TRC in terms of expression. Pink dots on the cladogram to the left of the heatmap denote gene clusters that exemplify this pattern. We note that three pelagic MZ exhibited especially robust expression levels. (b) Enriched GO terms associated with genes in the S + E model. Colours are representative of the −log10(*p*-value). Grey bars indicate no significance. The nature of the additive model precludes us from having an up- versus down-regulated analysis of genes, because it takes into account both species and environment at the same time. These GO terms are similar to previous analyses in returning processes involved in cell cycle regulation.

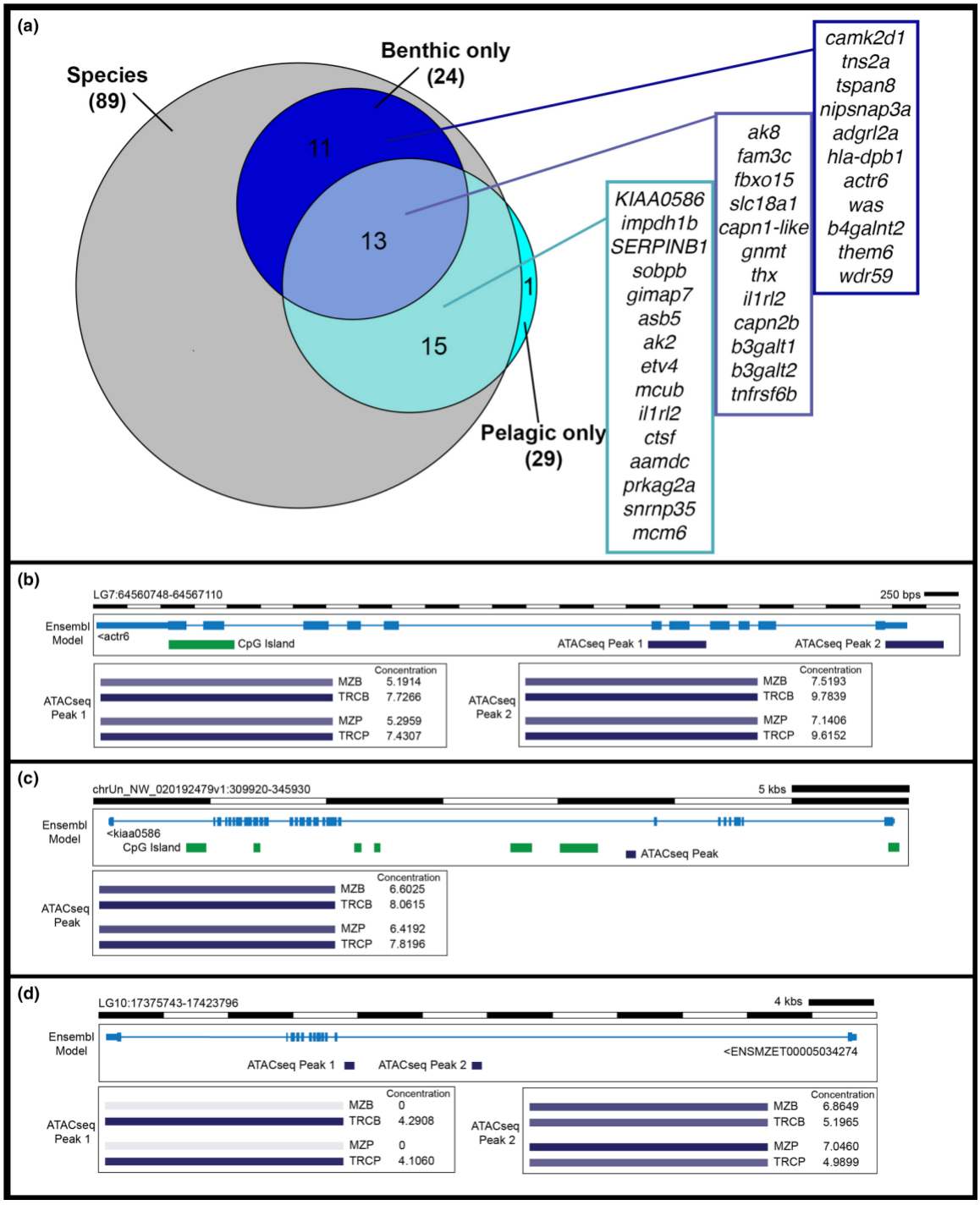

Figure 8: Overlap of RNA-seq and ATAC-seq datasets narrows the list of candidate genes. (a) In total, 89 genes were identified that were both differentially expressed (DE) at 17 days and differentially accessible (DA) between species. Of these, 15 overlapped with genes identified in the pelagic dataset (light blue), 11 overlapped with genes from the benthic dataset (dark blue), and 13 were identified in both foraging environments.

These overlapping datasets identified a relatively small subset of genes where expression differences may be due
to differences in the cis-regulatory region. Boxes to the right of the venn diagram display the specific genes from each area of overlap. (b–d) Diagrams of genes are shown (each panel has its own scale bar), as well as the location of ATAC-seq peaks based on DA analyses, and CpG islands (from the UCSC genome browser CpG island track based on at least 50% GC content, >200 bp, and >0.6 ratio of observed number of CG dinucleotides). Shown are representative data from the benthic dataset (b, actr6 on LG7), the pelagic dataset (c, kiaa0586 on an unlinked contig), and a gene that was significantly DE and DA in both environments (d, capn1-like on LG10). Beneath each gene model, ATAC-seq peaks are colored based on concentrations, with lighter colors indicating lower concentrations and darker colors indicating higher concentrations.

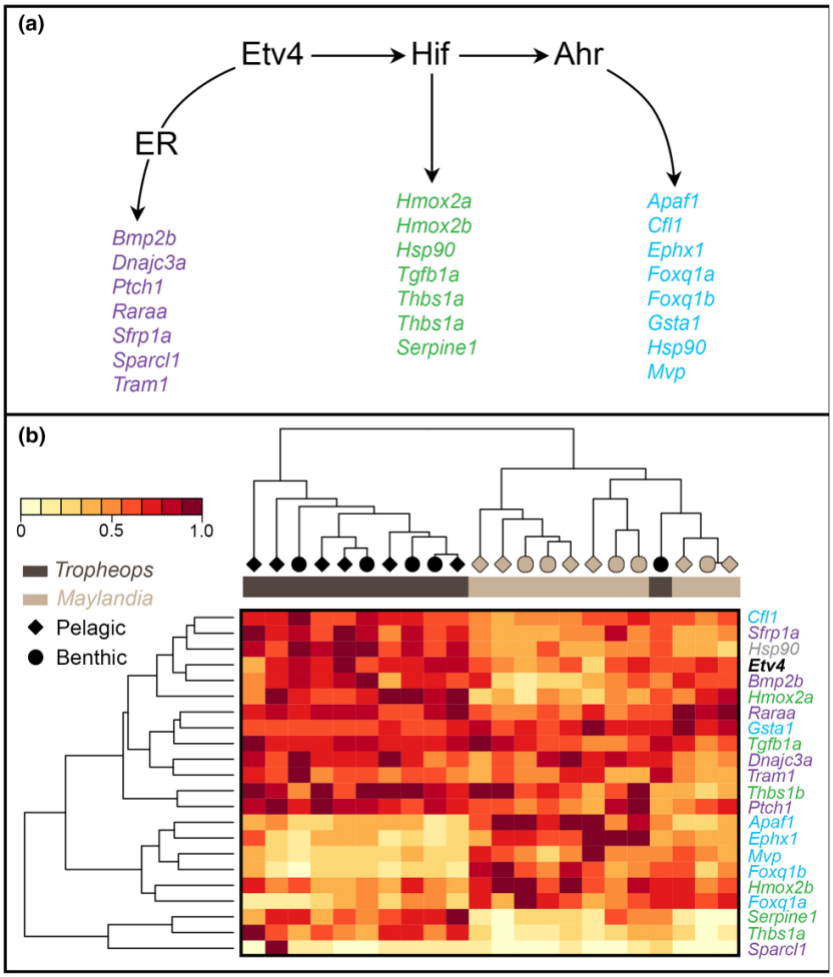

Figure 9: Roles for Etv4 and associated pathways in species-specific bone growth. (a) Etv4 connects environmental stress response, including hypoxia, through Hif and Ahr signalling, and craniofacial development through ER signalling. Lists of genes that were DE between MZ and TRC are colour-coded based on the pathway they associated with. Note that Hsp90 participates on more than one pathway, suggesting that these pathways may be interdependent. (b) A heatmap of these factors is shown. Because of differences in overall expression levels between genes, cpms were scaled as a percentage to the highest value. MZ are labelled with light grey and TRC as dark grey. Symbols indicate the foraging environment that the individual was exposed to.

Table 1: Number of genes that are DE or DA from RNA-seq and ATAC-seq datasets, respectively.

RNA-seq (DE)	MZ:TRC	MZB:TRCB	MZP:TRCP	MZB:MZP	TRCB:TRCP	S+ E
Total	5318	984	3761	38	0	128
MZ	2667	549	1927	n/a	n/a	n/a
TRC	2651	435	1834	n/a	n/a	n/a
Benthic	n/a	n/a	n/a	13	0	27
Pelagic	n/a	n/a	n/a	25	0	101

ATAC-seq (DA)	MZ:TRC	MZB:TRCB	MZP:TRCP	MZB:MZP	TRCB:TRCP
Total	297	157	114	0	0
MZ	202	118	60	n/a	n/a
TRC	95	39	54	n/a	n/a
Benthic	n/a	n/a	n/a	0	0
Pelagic	n/a	n/a	n/a	0	0

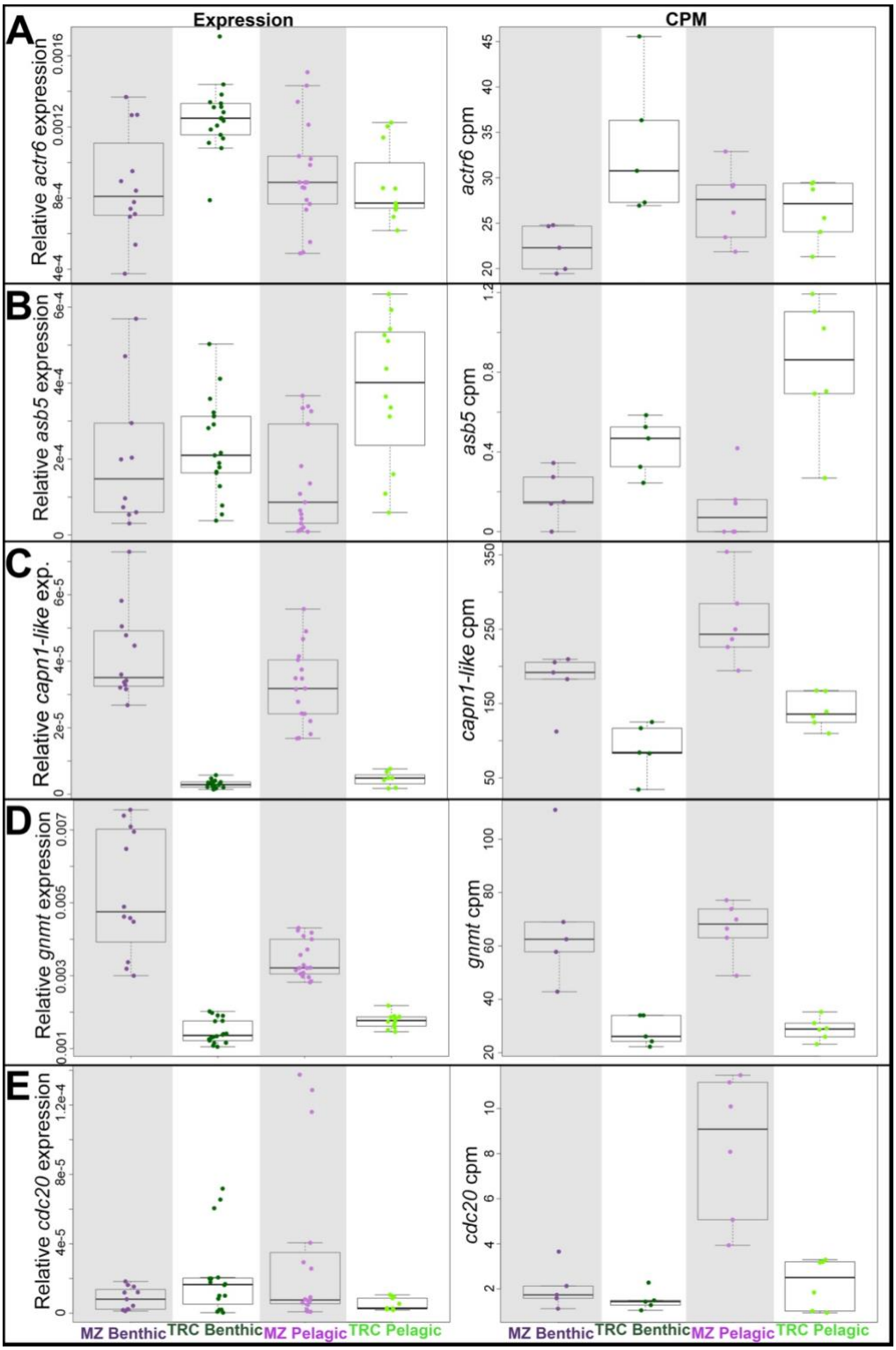

Figure S1: qPCR validation of a subset of genes from the overlap of the RNA-seq and ATAC-seq datasets. In general, the trends of gene expression matched the trends of cpm from RNA-seq libraries. For all panels, gene expression via qPCR is on the left, and the corresponding cpm is on the right. (A) Actr6 is from the benthic overlapping dataset and therefore is expected to be significantly different between species exposed to benthic

foraging: Expression MZB:TRCB p=9.39e-4; Expression TRCB:TRCP p=0.00154; cpm MZB:TRCB p=0.00805; cpm TRCB:TRCP p=0.11. Note that qPCR suggests that this gene is also plastically expressed within TRC. (B) Asb5 is from the pelagic overlapping dataset and expected to be significantly different between species exposed to pelagic foraging: Expression TRCB:TRCP p=0.0592; Expression MZP:TRCP p= 9.19e-4; cpm TRCB:TRCP p=0.0353; cpm MZP:TRCP p=1.48e-4. Based on qPCR, expression of this gene is also distinct between environments in TRC. (C) Capn1-like was identified in both pelagic and benthic datasets and expected to be DE between species in both environments. Expression MZB:TRCB p=1e-8; Expression MZP:TRCP p=2e-7; cpm MZB:TRCB p=0.0105; cpm MZP:TRCP p= 4.72e-4. (D) Gnmt was also from this "robust" dataset: Expression MZB:TRCB p=1e-8; Expression MZP:TRCP p=7.7e-6; cpm MZB:TRCB p=9.12e-4; cpm MZP:TRCP p= 7.52e-4. (E) We also examined cdc20 which was not found in the DE:DA overlapping dataset, but was a gene found to be plastic in MZ. It is also involved in cell-cycle regulation, which was implicated many times in this study. The trend is similar between expression and cpm dataset, however only the cpm data reached significance between pelagic and benthic MZ: Expression MZP:MZB p=0.17; cpm MZP:MZB 1.48e-4.

Table S1: Alignment data across all individuals. All reads were aligned to the MZ genome.

Species	Individual	Treatment	Reads	Align Rate(%)
Maylandia	MZ1r	Benthic	39429421	83.45
Maylandia	MZ2r	Benthic	36709816	82.81
Maylandia	MZ3r	Benthic	21312522	83.5
Maylandia	MZ5r	Benthic	27753598	82.49
Maylandia	MZ6r	Benthic	27510625	84.21
Maylandia	MZ8r	Pelagic	44701983	81.67
Maylandia	MZ9r	Pelagic	27678241	83.52
Maylandia	MZ10r	Pelagic	27593463	83.85
Maylandia	MZ11r	Pelagic	25069226	85.38
Maylandia	MZ13r	Pelagic	25925780	84.09
Tropheops	TRC1r	Benthic	36882758	83.65
Tropheops	TRC2r	Benthic	48038591	83.82
Tropheops	TRC3r	Benthic	40974594	84.44
Tropheops	TRC5r	Benthic	31433515	83.9
Tropheops	TRC6r	Benthic	30233914	83.06
Tropheops	TRC11r	Pelagic	33655345	82.92
Tropheops	TRC12r	Pelagic	37770476	83.73
Tropheops	TRC13r	Pelagic	28706744	83.31
Tropheops	TRC14r	Pelagic	31868378	83.3
Tropheops	TRC15r	Pelagic	36830798	83
Tropheops	TRC16r	Pelagic	34917788	85.78

Table S2: Cichlid qRT-PCR primer sequences for expression validation.

Gene	Sequence (5'-3')
actr6 For	GCAAATCCCGTCTGTTACGC
actr6 Rev	CATAGTCCTCCCGCATCACC
asb5 For	CAGTGTGATGGTACCCGTCC
asb5 Rev	CACAAAACGAGCAGCTCAGAAA
capn1 For	ATGTTTAGGGTTGGGACTCCAG
capn1 Rev	GGTGACAACCAACTGATCCCT
gnmt For	GTGTCGGACCAGTGTTTTGC
gnmt Rev	AGCCCAAAGAGATGAACGCA
cdc20 For	GGCTCCTGTATCAGTTCGCT
cdc20 Rev	AGGCGAATGGTCTCATCTGC
actb2 For	GTATGTGCAAGGCCGGATT
actb2 Rev	TTCTGACCCATACCCACCAT

Table S3: Differential expression and differentially accessibility overlapping genes, the environmental condition in which they are upregulated, and where differential accessibility peaks occur. Colors correspond to Figure 8 in the main text.

Ensembl_id	Gene_name	Environment	DE	DE_FDR	DA	DA_FDR	DA_in
ENSMZEG00005001000	**asb5**	**Pelagic**	**TRC**	**0.01156174**	**TRC**	**9.83E-09**	**5' flanking--intron 1**
ENSMZEG00005024961	gimap7	Pelagic	TRC	0.01080607	TRC	0.033698174	intron 1
ENSMZEG00005005887	ctsf	Pelagic	TRC	4.14E-05	TRC	0.003640002	5' flanking--exon 1
ENSMZEG00005018947	snrnp35	Pelagic	TRC	0.01523367	TRC	0.00763847	intron 3--exon 4
ENSMZEG00005024667	aamdc	Pelagic	TRC	0.00742822	TRC	0.010974519	intron 1
ENSMZEG00005020024	prkag2a	Pelagic	TRC	0.01155025	TRC	0.003061195	intron 3--exon 4
ENSMZEG00005018223	sobpb	Pelagic	TRC	0.00957963	TRC	0.029994701	exon 7--UTR
ENSMZEG00005007459	etv4	Pelagic	TRC	0.02918761	TRC	0.016803017	intron 4
ENSMZEG00005019100	il1rl2	Pelagic	TRC	0.05489003	TRC	0.001717386	intron 6
ENSMZEG00005027541	**KIAA0586**	**Pelagic**	**TRC**	**0.00199194**	**TRC**	**0.043908005**	**intron 7**
ENSMZEG00005005561	impdh1b	Pelagic	MZ	0.00383998	MZ	0.024572016	intron 1
ENSMZEG00005016815	SERPINB1	Pelagic	MZ	0.00445556	TRC	1.87E-09	intron 5
ENSMZEG00005019577	mcub	Pelagic	MZ	0.04672242	MZ	2.03E-08	5' flanking--exon 1
ENSMZEG00005026160	mcm6	Pelagic	MZ	0.02718694	MZ	0.046314643	5' flanking--exon 1
ENSMZEG00005026032	ak2	Pelagic	MZ	0.02069088	MZ	6.38E-04	5' flanking--intron1
ENSMZEG00005002411	**actr6**	**Benthic**	**TRC**	**0.00936915**	**TRC**	**1.40E-09**	**intron 4--intron6**
					TRC	**9.10E-08**	**5' flanking--exon 1**
ENSMZEG00005006938	nipsnap3a	Benthic	MZ	7.80E-05	MZ	1.18E-04	intron 1
ENSMZEG00005022151	hla-dpa1	Benthic	MZ	0.00935691	MZ	1.34E-04	5' flanking--intron 1
ENSMZEG00005022984	camk2d1	Benthic	MZ	0.00059887	MZ	3.26E-04	5' flanking--intron 1
ENSMZEG00005009504	n-wasp	Benthic	MZ	0.00966982	MZ	4.07E-04	exon 2--intron 3
ENSMZEG00005025763	adgrl2a	Benthic	MZ	0.00855149	MZ	0.024653634	intron 4
ENSMZEG00005018733	b4galnt2	Benthic	MZ	0.00984306	MZ	0.001738169	5' flanking--intron 1
ENSMZEG00005021009	tspan8	Benthic	TRC	0.01409865	MZ	0.009624277	intron 1
ENSMZEG00005023557	them6	Benthic	MZ	0.02186381	MZ	0.035666661	5' flanking--exon 1
ENSMZEG00005028342	wdr59	Benthic	MZ	0.0265954	MZ	0.025420487	5' flanking--intron 1
ENSMZEG00005012056	tns2a	Benthic	TRC	0.00791493	MZ	0.026294009	intron 1
ENSMZEG00005025584	tnfrsf6b	Robust	MZ	6.74E-09	MZ	9.95E-24	5' flanking--exon 1
ENSMZEG00005014061	b3galt2	Robust	MZ	3.99E-08	MZ	1.64E-20	exon 2
ENSMZEG00005021026	thx	Robust	MZ	4.70E-08	MZ	3.85E-19	intron 3
ENSMZEG00005020951	ak8	Robust	TRC	3.23E-07	TRC	4.35E-13	intron 3
ENSMZEG00005016544	b3galt1	Robust	MZ	5.77E-13	MZ	8.38E-13	5' flanking--exon 1
ENSMZEG00005010628	capn2b	Robust	MZ	7.54E-06	TRC	5.67E-12	intron 1--exon 2
ENSMZEG00005024744	**capn1**	**Robust**	**MZ**	**0.00562961**	**TRC**	**2.18E-11**	**intron 4**
					MZ	**3.89E-07**	**intron 4**
ENSMZEG00005025773	il1rl2	Robust	MZ	5.36E-05	MZ	3.56E-10	5' flanking--intron 1
ENSMZEG00005002433	fam3c	Robust	TRC	4.65E-12	TRC	4.37E-10	5' flanking--exon 1
ENSMZEG00005019407	fbxo15	Robust	TRC	1.68E-05	TRC	3.47E-09	5' UTR--exon 1
ENSMZEG00005018769	novel gene	Robust	MZ	2.16E-05	MZ	4.64E-09	intron 5
					MZ	1.97E-06	intron 2
ENSMZEG00005006910	**gnmt**	**Robust**	**MZ**	**1.52E-07**	**MZ**	**8.25E-07**	**exon 3--intron 3**
ENSMZEG00005000687	slc18a1	Robust	TRC	1.04E-05	MZ	9.94E-05	intron 5--intron 6

CHAPTER III

CRANIOFACIAL PLASTICITY VIA ROBUST AND EARLY EXPRESSION OF ENVIRONMENTALLY SENSITIVE GENES

Tetrault, E.R., Aaronson, B., Gilbert, M.C., & Albertson, R.C.

This chapter was submitted to *PNAS* in August 2023.

Introduction

How complex phenotypes arise and are maintained over time remains an important question in evolutionary biology (Komarova 2014; Schwander et al., 2014; Musser & Clarke, 2020). The craniofacial skeleton (e.g., skull, jaws, and other supporting hard- and soft-tissue traits in the head) is an exquisitely complex organ whose final form relies on a balance between genetic and environmental factors (Szabo-Rogers et al., 2010; Roosenboom et al., 2016). Furthermore, due to the explicit connection between craniofacial form, function and ecology, it is one of the most diverse and rapidly evolving traits among vertebrates (Albertson & Kocher, 2006; Navalón et al., 2020; McGirr & Martin, 2021). For example, adaptive radiations, which constitute a major source of biodiversity (Schluter, 2000; Hu et al., 2016 ; Borko et al., 2021), are often driven by divergence in diet, and concomitant changes in foraging-related structures, including the craniofacial skeleton. The proximate mechanisms through which divergence in craniofacial shape occurs remains an open question, but given the complex nature of this structure, both genetic and environmental factors are undoubtedly involved.

The search for sources of craniofacial variation have largely involved genetic, molecular, and cellular mechanisms (Roberts et al., 2011; Pallares et al., 2014; Parsons et al., 2014 (1); Parsons et al., 2014 (2); Ito et al., 2015; Parsons et al., 2015; Percival et al.,

2017), focusing on early developmental processes. However, allometry also figures prominently in craniofacial shape, providing opportunities for natural selection to target various life history stages (Schaefer et al., 2004; Tamagnini et al., 2017; Hallgrímsson et al., 2019; Marugán-Lobón et al., 2021). Allometric changes in the craniofacial skeleton are often associated with dietary niche shifts over ontogeny (Hellig et al., 2010; Chatterji et al., 2022; Patterson et al., 2022), which suggests that phenotypic plasticity may play an important role in influencing the geometry of the skull. Under this scenario distinct mechanical inputs associated with different foraging modes would be interpreted by distinct sets of progenitor cells, resulting in environment-specific remodeling and growth of the feeding apparatus. The genetic mechanisms that enable this capacity are an important and ongoing topic of investigation.

The genetic complexity of bone mechanosensing has long been appreciated. In the mouse tibia model, for example, load-induced bone formation is linked to multiple loci and interactions, each of relatively small effect (Kesavan et al., 2006). Other studies have shown that while load-induced bone formation in the tibia is associated with the regulation of Wnt signaling, the effects are dependent upon the number of loading bouts and the age of the animals (Holguin et al., 2016). Our work in cichlids has also implicated Wnt signaling in craniofacial bone formation and plasticity (Parsons et al., 2014), as well as extensive gene-by-environment effects, whereby genetic mapping of a range of hard- and soft-tissue traits under different foraging conditions, resulted in almost completely non-overlapping genotype-phenotype maps (Parsons et al., 2016; Zogbaum et al., 2021).

Additional efforts in our lab have characterized roles for primary cilia and the Hedgehog pathway in the evolution and development of the cichlid feeding apparatus. In particular, Hh signaling was linked to the size and shape of the interopercle (IOP) bone and the retroarticular process (RA) of the lower jaw (Roberts et al., 2011; Hu & Albertson, 2014). Variation in the relative sizes of these elements can determine whether the feeding apparatus is adapted for a pelagic (i.e suction feeding; speed) or benthic (i.e scraping/biting; power) foraging (Westneat, 1991). Further, Hh levels were shown to be necessary and sufficient to sensitize bone to mechanical load (Navon et al., 2020). Members of the Hh signal transduction pathway localize to the primary cilia, a mechanosensitive organelle (Rohatgi et al., 2007), and we recently implicated the ciliary rootlet in cichlid bone shape and plasticity (Gilbert & Tetrault et al., 2021). Specifically, we showed that allelic variation in *crocc2*, which encodes a major structural component of the primary cilium (Yang et al., 2005), is associated with species that exhibit different bone shapes and environmental sensitivities. In addition, zebrafish *crocc2* mutants were unable to elicit a plastic response, were characterized by dysmorphic bone geometry particularly at sites of high mechanical stress, and exhibited dysregulated bone homeostasis at the transcript and tissue levels (Gilbert & Tetrault et al., 2021).

To complement this gene-by-gene approach we next used multiomics to increase the pace of discovery of environmentally sensitive genes that underlie species-specific differences in jaw shape. Focusing on the IOP-RA functional complex we used overlapping both RNA-seq and ATAC-seq datasets to assess differences in transcription levels and chromatin accessibility between species and environments (Tetrault et al., 2023). The RNA-seq experiment was performed at ~2 weeks, while the ATAC-seq

experiment was carried out at ~4 weeks, allowing us to ~50 identify loci with effects at both time points. This dataset included genes involved in primary cilia formation, chromatin structure, DNA methylation, cell-cycle regulation, and apoptosis (Tetrault et al., 2023). While these data were informative of the genomic regulation of environmentally sensitive genes, they were limited to a relatively narrow window following the onset of foraging challenges. Here we seek to characterize the expression dynamics of these environmentally sensitive genes over time. As a negative control we also used another species to our dataset that is characterized by a feeding apparatus that is robust to foraging mode (Parsons et al., 2014; Navon et al., 2020). Finally, to compare the relative timing of plasticity at the transcript and anatomical levels, the same animals were used for gene expression and shape analysis at 1, 2, 4, and 8 weeks following the onset of the feeding experiment.

Several predictions can be made based on our previous work, as well as the broader literature on bone plasticity/mechanosensing. First, we expect that plasticity in gene expression will be more pronounced and occur earlier in the species known to be plastic at the tissue level. Correspondingly, the canalized species should exhibit little in the way of environmentally sensitive gene expression. Second, we expect that plasticity in gene expression will precede that in anatomy. Next, we expect that the pelagic foraging mode will drive plasticity at both levels (e.g., Tetrault et al., 2023). In terms of when plasticity will manifest, there are multiple possibilities. For instance, since plasticity of gene expression in the cichlid pharyngeal jaw in response to hard vs soft diets was not observed until after 1 month (Schneider et al., 2014), it is possible that the magnitude of plasticity in gene expression will increase over time. Alternatively, in

various mammalian models a transcriptional response to bone loading has been detected in less than a day (Terai et al., 1999; Mantilla Roosa et al., 2011; Holguin et al., 2016), and thus robust plastic gene expression may be observed at the earliest time point. The answer to these questions, in concert with the broader body of research, will advance a better understanding of how genes and the environment interact to determine adaptive variation in jaw shape.

Materials and Methods

Fish Husbandry

Cichlids were purchased and housed at equal density in 40-gallon glass aquaria at ~28°C on a 14 hour light/10 hour dark cycle. Each aquarium had constant water flow and air stones to aerate the water. Cichlid husbandry follows a protocol approved by the institutional animal care and use committee at the University of Massachusetts.

Experimental design

We used three species of African cichlid from Lake Malawi, two generalist species, *Maylandia gallireya* (MG; n=51), a true generalist that forages on many food types, *Tropheops olive* (TO; n=61), a generalist who has a slight benthic preference, and one benthic specialist, *Labeotropheus fuelleborni* (LF; n=42) (Figure 10a). We split each species of cichlid into two separate tanks to isolate each treatment/species combination. Individuals in the pelagic treatment were given ground cichlid flake food to impose a cyclic load on the oral jaw, while animals in the benthic treatment had an equal amount of ground flake food mixed with 1.5% food-grade agar, and pasted over two lava rocks, which imposed a more static load. Groups were given one week to train on their respective diet to ensure they learned how to forage correctly before the start of the

experiment. We sacrificed animals at four time points: 1 week, 2 weeks, 4 weeks, and 8 weeks (Figure 10b; Table S4). This allowed us to track gene expression and bone shape changes over time. The IOP-RA complex on the left side of each animal was stored in Trizol at -80°C for RNA extraction.

RNA extraction and qPCR

RNA-extraction was performed using the phenol-chloroform method with each sample standardized to 70ng/µL RNA. cDNA was prepared using the High Capacity Reverse Transcription Kit (Applied Biosystems). We assessed gene expression dynamics over time in the IOP-RA functional complex using qPCR. Our panel included 11 genes including six environmentally sensitive loci from genome-wide study (i.e., *actr6, asb5, capn1, cdc20, gnmt, kiaa0586*; Tetrault et al., 2023). Five additional genes were added to this panel based on known roles in bone development, mechanical stimulation and remodeling (*sp7, opg, rankl, ptch1, notch1a*). See primer sequences in the supplementary information (Table S5).

Bone staining

After dissection of the left IOP-RA complex, each animal was stored in 4% paraformaldehyde for approximately 1 week at room temperature, washed with RO water, and stepped through an ethanol series until 70% and stored in fresh 70% EtOH until staining. Each specimen was soaked in Alizarin Red (Sigma-Aldrich) bone stain in 70% EtOH for 24-48 hours depending on the size of the animal. Excess stain was removed by further soaking each sample in 70% EtOH for 2-3 days, and stored in fresh 70% EtOH until imaging. We captured images of the right lateral surface of each

specimen using a Leica M165 FC microscope with an attached Leica DFC450 camera (Leica Camera AG, Wetzlar, Germany).

2D morphometrics and linear measures

The global craniofacial landmarking scheme consisted of 11 fixed landmarks. In addition, two curves were drawn with 11 and 5 sliding semilandmarks to outline the eye and the slope of the head, respectively (see Figure 13). To determine whether the geometry of the 4-bar linkage of the cichlid oral jaw changes in response to alternate foraging treatment, we landmarked the joint of each linkage. All images were digitized using StereoMorph (Olsen and Westneat, 2015). We then ran a generalized Procrustes analysis (GPA) on landmark data. From whole shape landmark data, we quantified shape change trajectories between environments (shape ~ species x treatment, ~centroid size), or over time (shape ~ species x time, ~centroid size) using the trajectory.analysis function in the Geomorph v3.0 package (modified from Packard et al., 2023). This function uses ANOVA to evaluate the trajectories, and calculates the differences in trajectory path and magnitude. Landmark data was subjected to 10000 random permutations via a randomized residual permutation procedure. Each trajectory was then superimposed over the morphospace of PC1 and PC2. A test was considered significant if $\boldsymbol{\alpha} \leq 0.05$.

Using ImageJ, we also took linear measures of each linkage of the 4-bar system individually to measure length over time. Each animal was plotted an individual linkage against their head length to get a growth slope by species and treatment. An ANCOVA determined whether slopes were significantly different from each other. Statistically different slopes indicated a plastic response between each treatment, or faster/slower growth between species. A test was considered significant if $\boldsymbol{\alpha} \leq 0.05$.

Results

Gene expression varies by species, time, and environment

We assessed gene expression across 3 species, reared in 2 foraging conditions, and at 4 time points. Several notable trends emerged from these data (Figure 11; Figure S2). First, we found that the overall highest levels of gene expression were observed at week 1 in pelagic *Maylandia* and 2 weeks in benthic *Maylandia*. *Tropheops* exhibited a similar, though less pronounced, pattern whereby expression was higher at 1 and 2 weeks, relative to later time points within this species. Conversely, *Labeotropheus* exhibited overall dampened expression across all markers, and at all timepoints. Notably, these trends were not only observed in genes selected from our genome-wide dataset as being environmentally sensitive (Tetrault et al., 2023), but held across all other bone markers, suggesting that the pattern is not an artifact of choosing a biased set of genes, but rather an intrinsic feature of a large bone network.

In addition to relatively high early gene expression, *Maylandia* exhibited plasticity in expression at both weeks 1 and 2. At week 1, all but two genes were significantly upregulated in the pelagic compared to benthic foraging condition (but even *gnmt* and *opg* were trending higher in the pelagic environment; Figure 11a). These data were consistent with our prediction that pelagic foraging is driving craniofacial plasticity in this cichlid genus (Navon et al., 2020; Tetrault et al., 2023). It is notable, however, that this pattern switches by two weeks. While fewer genes are differentially expressed between environments in *Maylandia* at 2 weeks, those that are are upregulated in animals reared in the benthic environment (Figure 11b). While there was an uptick in expression of some genes in *Tropheops* at week 1, none were differentially expressed between

environments (Figure 11a). By two weeks *Tropheops* exhibited relatively high expression of *kiaa0586* in the pelagic environment, and *opg* in the benthic environment (Figure 11b). Thus, plastic gene expression is more limited and takes longer to manifest in *Tropheops,* which is consistent with previous work showing that anatomical plasticity may be more muted in this genus. In contrast to *Mayandia* and *Tropheops*, gene expression in *Labeotropheus* was neither dynamic nor especially plastic in the first two weeks following the onset of foraging trails (Figure 11a,b). This is consistent with previous research showing that *Labeotropheus* bone formation is canalized with respect to alternate foraging conditions. The one exception was *sp7*, a core osteoblast marker (reviewed in Long, 2012), which was expressed at a significantly higher level in pelagic versus benthic fish at 2 weeks (Figure 11b). Although, given that levels of *sp7* in *Labeotropheus* were low compared to the "spikes" in expression of *sp7* and other genes observed in *Mayandia* and *Tropheops*, it's hard to know the extent to which this difference is biologically relevant.

By 4 weeks we observed relatively lower levels of expression across all species and treatments (Figure 11c), a pattern that seems to persist to 8 weeks (Figure 11d). A handful of genes were differentially expressed between environments in *Tropheops* at 4 weeks and in all three species at 8 weeks; however overall levels were low, which again makes inferences about the biological significance of these differences tenuous. In all, we found that gene expression was highly dependent on genomic background (e.g., species), foraging mode, and time. This assertion is reflected in the dendrograms in figure 11, which do not point to any consistent covariation in expression over time. It is also supported statistically by an ANOVA model (expression ~ species * treatment * time)

that returned significant S:T:T interactions for 9/11 genes (Table 2). The exceptions being *gnmt* and *opg*, although the S:T:T p-value for *opg* was 0.056.

Anatomical plasticity over time

Whereas *Maylandia* and *Tropheops* have both been shown to be plastic in rates of bone matrix deposition in response to the same foraging challenges (Navon et al., 2020), *Maylandia* showed a greater response that was largely driven by the pelagic foraging treatment (Tetrault et al., 2023). *Labeotropheus* was not observed to be plastic in either environment, although it showed a high degree of variation in bone matrix deposition in both environments (Navon et al., 2020). Here we sought to characterize anatomical plasticity over time. Importantly the same fish were used for both anatomical and gene expression analyses.

We first examined growth of the same elements, from the contralateral side of the head, used to obtain expression data. These include the IOP and RA, which represent 2/3 movable links of the opercle 4-bar linkage system, the coupler and output links, respectively (Figure 10a). We also included the 3rd mobile link, depth of the opercle, which constitutes the input link. Growth of each element was assessed by plotting each against head length and then statistically comparing slopes for animals from different foraging environments (Figure 12). No significant differences were detected for the input in any species (Table 3). For both the coupler and output links, *Maylandia* from the pelagic treatment exhibited significantly steeper slopes than those from the benthic treatment (Figure 12a; Table 3), suggesting that pelagic foraging stimulates faster growth of the IOP and RA. This does not appear to be due to an overall difference in growth between treatments, as head length (x-axis) exhibits a similar range across treatments. In

Tropheops, slopes were nearly identical between treatments for both the coupler and output links (Figure 12b; Table 3), indicating similar growth rates; however, we note that benthic foragers exhibited generally longer output links, relative to head length, which suggests a degree of plasticity in this element. *Labeotropheus*, likewise, exhibited nearly identical slopes between foraging treatments for the coupler link. A different trend was noted for the output link, where markedly different slopes were observed in *Labeotropheus* reared in each treatment (Figure 12c; Table 3). Here animals reared in the benthic environment exhibited faster growth of the RA, and also reached larger sizes. There was a lot of variation in the length of this element from animals in both treatments, and thus the difference between slopes was not significant at the 0.05-level. That *Labeotropheus* from the benthic environment grew larger underscores the idea that these are highly specialized benthic foragers (Ribbink et al., 1983; Konings, 2007; Albertson & Pauers, 2019).

We also assessed whether foraging treatments induced more global changes in craniofacial geometry over time. Using 2-D landmark-based geometric morphometrics, we documented similar results. Specifically, we found that craniofacial developmental trajectories were distinct between *Maylandia* from each foraging treatment (trajectory shape, $p=0.0367$), whereas they were indistinguishable between treatments in *Tropheops* and *Labeotropheus* ($p>0.1$ for both). Plotting these trajectories in PC space (Figure 13) provided a visualization of these statistics. The first notable trend is that *Maylandia* from each time point occupied more of the PC plot than the other two species, whereas *Labeotropheus* time points all overlapped close to the 0,0 position. *Tropheops* were intermediate in terms of spread across the PC plot. Further, we noted slight differences in

mean shapes at each stage for *Maylandia* reared under benthic versus pelagic foraging conditions. In all species, ontogeny was largely captured by PC1, which characterized variation in eye size, eye position, relative head length, and craniofacial profile. In addition, 4 and 8 week *Maylandia* were distinguished along PC2, which likewise captured variation in relative eye size and head length. Thus, *Maylandia* exhibited the most dynamic and plastic patterns of growth, in terms of specific bone lengths as well as global craniofacial geometry.

Discussion

The evolution, genetic basis, and plasticity of a dynamic functional system

It is hard to overstate the importance of 4-bar linkage systems in the field of evolutionary morphology, which have been used to model the kinematics of fish feeding (Westneat, 1990), avian flight (Norberg et al., 1990; Nudds et al., 2007), and the raptorial appendage of mantis shrimp (Patek et al., 2007). Not only do such engineering principles provide a way to predict function from form, but they can also reveal aspects of morphology that may be more constrained by physics than others. For instance, a recent study showed that the evolution of kinematic transmission in both the fish opercle 4-bar system and the stomatopod raptorial appendage appears to be disproportionately driven by variability in the output linkage (Hu et al., 2017). In other words, changing the length of the RA may provide a more efficient means for selection to alter fish feeding kinematics.

We have long sought to better understand the genetic basis, development, and evolution of elements of the opercle 4-bar linkage system in cichlids (e.g., Albertson et al., 2005; Roberts et al., 2011; Hu & Albertson, 2014; Hu & Albertson, 2017). This

functional complex of bones and ligaments helps to drive lower jaw depression (Westneat 1991), varies between species in a way that predicts foraging niche adaptation (Roberts et al., 2011; Hu & Albertson, 2014, 2017), and has been shown to be plastic when animals are reared under different foraging/mechanical conditions (Hu & Albertson, 2017; Navon et al., 2020). Results from the current study complement and expand previous work in this system. First, we document a high degree of plasticity in the generalist forager, *Maylandia*, insofar as exhibiting early and more extensive gene expression differences between foraging treatments, as well as differences in growth trajectories at the anatomical level. These data are consistent with previously published data showing greater rates of bone deposition in *Maylandia* compared to *Tropheops* (Navon et al., 2020; Tetrault et al., 2023). Also similar to previous work (Parsons et al., 2014; Navon et al., 2020), we show that the specialized benthic foraging taxon, *Labeotropheus*, exhibits limited anatomical plasticity and consistently low gene expression across treatments over time. There is a hint of plasticity in this species in the length of the RA, which is consistent with a previous genetic mapping study where we found that the *Labeotropheus* allele was sensitive to foraging treatments at a locus that underlied variation in RA length (Parsons et al., 2016). *Tropheops* also exhibited more limited sensitivity of gene expression to foraging mode and no detectable difference in bone growth; although, RA length was generally longer in benthic foraging animals, which is consistent with previous data showing greater bone deposition in *Tropheops* in response to benthic foraging (Navon et al., 2020). Taken together, we suggest that these cichlid genus reside at different points along a plasticity axis, with *Maylandia* exhibiting the highest magnitude of plasticity across craniofacial bones, *Labeotropheus* developing a feeding

apparatus that is largely (though not completely) robust to foraging mode, and *Tropheops* residing somewhere in the middle (Parsons et al., 2014; Parsons et al., 2016; Navon et al., 2020; Tetrault et al., 2023).

The importance of pelagic foraging in driving plasticity and adaptive radiations

Another notable consensus from this body of research is that pelagic foraging appears to be driving plasticity, particularly in *Maylandia*. In previous work, this was seen as greater rates of bone matrix deposition, and higher relative expression of the Hh target, *ptch1,* when *Maylandia* individuals were reared under pelagic foraging conditions (Navon et al., 2020). In a recent genome-wide analysis, nearly 4x as many genes were differentially expressed between *Maylandia* and *Tropheops* when animals were reared in a pelagic versus benthic foraging environments. Here we showed that anatomical plasticity in *Maylandia* was associated with an early and dramatic increase in expression of environmentally sensitive and bone marker genes in *Maylandia* individuals required to forage with a pelagic mode (Figure 11). This may seem counterintuitive as bone mechanosensing is almost always associated with and studied in the context of high static loadings (Akhter et al., 1998; Gunter et al., 2013; Holguin et al., 2016; Muschick et al., 2011), which is more closely approximated by our benthic foraging challenge. We suggest that the pelagic treatment will challenge the feeding apparatus in a different way – e.g., through the (presumably) low amplitude, but high frequency action of rapidly opening and closing the oral jaws while suction feeding. In several independent experiments we now show that this action can have a more pronounced effect on bone, at both the transcript and tissue level, compared to biting/scraping food from rocks (Navon et al., 2020; Tetrault et al., 2023).

In the realm of freshwater ecology and evolution, the benthic habitat of lakes has long been recognized as an important driver of trophic segregation in fishes owing to a high level of heterogeneity (Bootsma et al., 1996; Schindler and Scheuerell, 2002); however, the vast open-water pelagic zone may also be considered novel when ancestrally riverine populations invade large lakes, the first step in many fish adaptive radiations (Gillespie & Fox, 2003; Wund et al., 2008; Matthews et al., 2010; Præbel et al., 2013; Doenz et al., 2019). Plankton drives energy flow in the pelagic habitat (Schindler and Scheuerell, 2002), and deep lakes support a greater abundance of plankton than rivers (e.g., Cardoso et al., 2012). Adaptations associated with locating (e.g., UV vision; Carleton et al., 2000) and foraging on (e.g., suction feeding) plankton are required for fishes to successfully invade this niche. Suction feeding involves several unique musculoskeletal and kinematic features relative to other modes of foraging (Liem, 1991; Wainwright et al., 2015); however, the "modulatory multiplicity" that characterizes cichlid feeding mechanisms (Liem, 1979; 1980), combined with plasticity of the underlying craniofacial bones (Bouton et al., 1983; Navon et al., 2020), positions cichlids to efficiently exploit (in the near term) and adapt (in the long term) to this trophic niche.

The idea that phenotypic plasticity in an ancestral population may bias the direction of phenotype evolution is known as the "flexible stem hypothesis" (West-Eberhard, 1998; 2003). Under this hypothesis, when a plastic population in one environment (e.g river) is exposed to a new and novel environment (e.g lake/pelagic), new patterns of phenotypic variation are exposed to selection. If the novel environments remain stable over time, the loci and/or alleles that control new phenotypic variants may be driven to fixation. Two key predictions underlie the flexible stem hypothesis. One is

that phenotypic patterns of divergence between species align with patterns induced by plasticity within species. Cichlids have undergone repeated evolution along the benthic-pelagic eco-morphological axis (Kocher, 2004), leading to predictable variation in a suite of foraging related traits (Cooper et al., 2010), which can be recapitulated in the lab by manipulating the mode by which animals are allowed to feed (e.g., Bouton et al., 2002; Parsons et al., 2014; 2016). For this reason the cichlid feeding apparatus has long been hypothesized to be a morphological "flexible stem" (West-Eberhard, 1998; 2003). The other prediction under the flexible stem hypothesis is that genes involved in plasticity will also underlie species differences (Gibert, 2017). Thus, the genes examined in this study provide molecular support for the flexible stem theory.

The proximate genetic basis of craniofacial plasticity: Where to go from here?

Our data show that craniofacial plasticity is associated with early "spikes" in expression of environmentally sensitive genes, but what might the roles for these genes tell us about how plasticity is regulated at the molecular/cellular level?

Kiaa0586 is required for primary cilium formation and without the Kiaa0586 protein, cilia axonemes fail to form, but still have intact basal bodies (Yin et al., 2009). Primary cilia are mechanosensors that sense and respond to fluctuations in environmental stimuli and at the center of this organelle is Hh signaling (reviewed in Bangs & Anderson., 2017). The Hh pathway is critical for bone formation in various areas of the mammalian skeleton, but of particular interest to us is its role in craniofacial bones (reviewed by Pan et al., 2013). We have recently implicated Hh signaling and cilia structure/function in cichlid bone formation and plasticity (Navon et al., 2020; Gilbert & Tetrault et al., 2021; Packard et al., 2023). *Kiaa0586* is required for both proper

craniofacial development and Hh signaling (Buxton et al., 2004; Davey et al., 2006). *Kiaa0586* was plastic in both *Maylandia* and *Tropheops*, but the timing was different, with the highest intraspecific variation in *Maylandia* at week 1, and *Tropheops* at week 2 (Figure 11a-d; Figure S2a; Table S6). *Labeotropheus* was not plastic at any time point for this gene. We also assessed expression of *ptch1*, which showed a similar, albeit less pronounced, pattern with plastic expression in *Maylandia* at 1 week. Hh signaling can regulate bone development in a number of ways, including cell-cycle regulation and differentiation of progenitor cells (Wu et al., 2004; Plaisant et al., 2009; 2011; Deng et al., 2019). Our previous genome-wide study using the same taxa and tissues implicated cell-cycle regulation (Tetrault et al., 2023), and consistently *cdc20* exhibits marked differential expression between environments in *Maylandia* at 1 week (Figure 11a; Figure S2g; Table S6). However, we also note that *ptch1* and the bone differentiation marker, *sp7*, cluster together at the 1 week time point (Figure 11a). It is therefore possible that Hh signaling is leading to accelerated bone growth in pelagic *Maylandia* through both cell division and differentiation. Further experiments looking at these cell behaviors immunohistochemically would be fruitful.

Some genes were plastic in multiple species but at different times, suggesting an importance in bone plasticity in general, but that the effects are time- and species-dependent. For example, *actr6* encodes an evolutionarily conserved actin-related protein that has been shown to localize to the nucleus and interact with heterochromatin proteins (Ohfuchi et al., 2006). Actr6 is predicted to be a member of the SWR1 chromatin remodeling complex, supporting both its structure and function (Willhoft and Wigley, 2020). Notably, SWR1 can act as both a repressor and activator of transcription, and as

part of this complex in plants Actr6 has been shown to have a negative effect on basal level transcription and a positive effect on environmentally induced transcription (Choi et al., 2016). Here *actr6* expression was plastic in *Maylandia* at weeks 1, 2, and 8 wks (Figure 11a,b,d; Figure S2b; Table S6), in *Tropheops* at 4 wks (Figure 11c; Figure S2b; Table S6), and not at all in *Labeotropheus*. In both *Maylandia* and *Tropheops actr6* was initially expressed at a higher level in the pelagic environment; however, in *Maylandia* it was expressed at a higher level in benthic animals at 2 and 8 weeks (Figure 11a,b,d; Figure S2b; Table S6). It is tempting to speculate that the higher initial expression of *actr6* under pelagic foraging conditions represents the "induced" condition associated with transcriptional activation and accelerated bone growth, whereas the higher expression observed later in benthic *Maylandia* represents the basal condition and transcriptional repression. Either way the potential changes in chromatin state associated with differential *actr6* expression would be a fruitful line of future inquiry.

While we did not find any clustering between genes across time points (Figure 11), *opg* remained somewhat of an outlier, especially at later time points and in the combined dataset (Figure 11c-e), indicating that this gene is acting differently than the others in the dataset. For example, contrary to all other markers, *opg* did not decrease to its lowest level at week 8, and instead exhibited relatively high levels of expression at week 8 across all three species (Figure 11e; Figure S2j; Table S6). In the context of bone remodeling, OPG is a negative regulator of osteoclastogenesis. It is secreted from osteoblasts, along with RANKL, and while RANKL binds to its receptor, RANK, on the surface of osteoclast progenitors to promote differentiation, OPG binds to RANKL, preventing the activation of RANK. The ratio of RANKL:OPG is considered an indicator

of bone remodeling activity (Mizuno et al., 1998; Yasuda et al., 1999; Wu et al., 2013). In *Labeotropheus* and *Tropheops*, this ratio remained consistently low over time, suggesting modest remodeling activity. Alternatively, the RANKL/OPG ratio in *Maylandia* was higher, particularly at weeks 1 and 2, which suggests that not only is more bone being deposited at these time points (e.g., high early expression of *sp7*), but that bone is being remodeled to accommodate environment-specific bone architectures. That *opg* expression peaks again in *Maylandia* at 8 wks, while *rankl* decreases in expression (i.e., decreasing the RANKL/OPG ratio), may suggest decreased remodeling activity and a shift to more isometric growth at this time point. Either way, the dynamic and unique pattern of expression of this gene should be followed-up in future studies aimed at characterizing the cytochemical basis of bone remodeling activity in these species.

Conclusions: Transcriptional dynamics of craniofacial plasticity

We took a set of marker genes previously characterized to be involved in bone formation/remodeling, combined with a set previously shown to be environmentally sensitive (Tetrault et al., 2023), and characterized expression patterns at multiple time points following the on-set of foraging challenges. The data showed markedly similar patterns over time in each species. Whereas the plastic taxon, *Maylandia,* was characterized by an early response of relatively high expression followed by a drop off in transcription over time, the canalized genus, *Labeotropheus,* exhibited relatively low levels of expression over time. Gene expression in *Tropheops* was characterized by patterns somewhere in between the other two species. In general, these data underscore the importance of time in the assessment of gene expression, in response to a shift in

foraging environment. Indeed, the effect of time was significant for every gene, and in all three species (Table 2), a result that is not surprising given the dynamic nature of bone development (Brunskill et al., 2014; Mork & Crump, 2015; Ahi, 2016).

Also of importance is the observation that the 1 week time point is where we observed bone the highest level of expression as well as the greatest number of genes differentially expressed within a species. This suggests that studies that examine the transcriptional basis of plasticity weeks or months after the start of the experiment (Tu et al., 2012; Gunter et al., 2013; Schneider et al., 2014; Parsons et al., 2016; Gibbons et al., 2017) may be missing important, early response activity. In fact, our data suggest that important expression dynamics may be occurring in a matter of days following the on-set of foraging challenges.

Finally, this work underscores the importance of pelagic foraging in driving craniofacial plasticity. In addition to implications insofar as the flexible stem evolution of pelagic eco-morphs (see above), it is important to consider the novelty of the pelagic environment in terms of current and future anthropogenic change of aquatic systems. In particular, the widespread construction of hydroelectric dams is leading to the creation of large reservoirs. Adaptation to pelagic modes of foraging will be critical for survival of fishes whose habitat changes from clear-water river systems to reservoir/lake (Gilbert et al., 2020), and so understanding the factors that enable plasticity is also critical. Our work, while limited in taxonomic scope, suggests that (a) some species will be better able to mount a plastic response than others, and (b) plasticity in response to novel pelagic foraging niches might be more efficient than that in response to newly created benthic habitats. All in all, there is still much to learn about the molecular regulation of

plasticity, but given its wide-spread importance across fields, we suggest that it should remain a top priority for biologists.

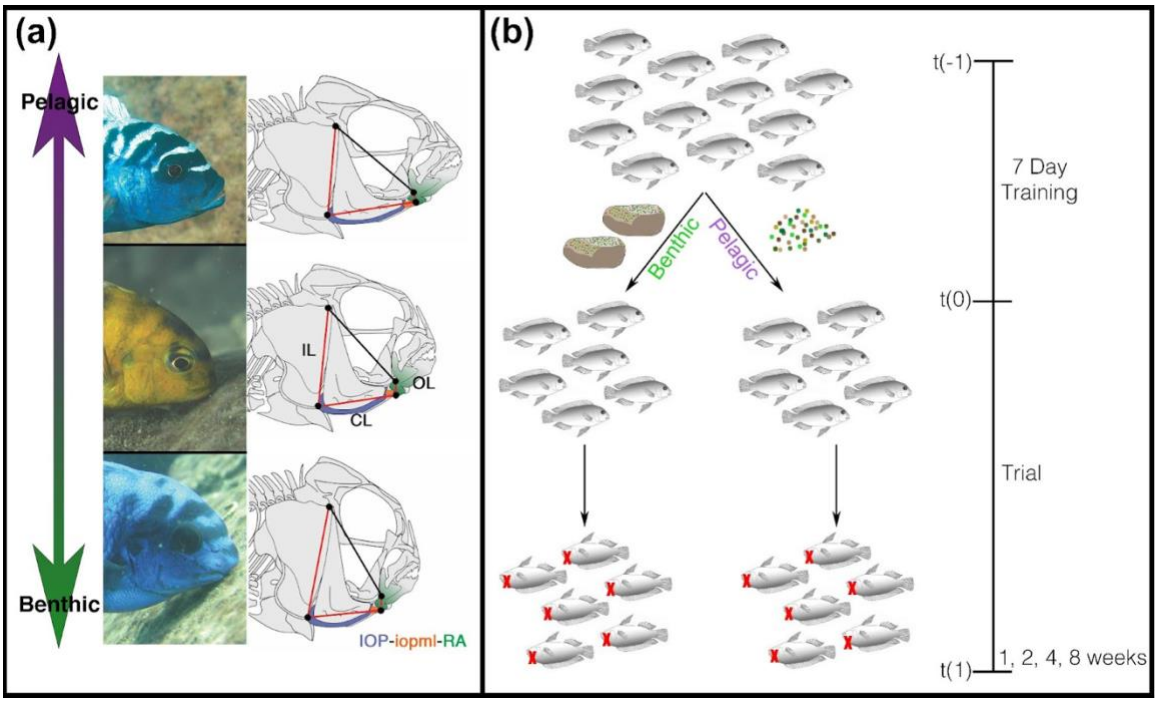

Figure 10: Cichlid time series experimental design. (a) African cichlids forage along the benthic-pelagic axis, and have craniofacial structures optimized for their foraging preference. Each skeletal diagram has the 4-bar linkage overlaid. The three movable linkages are in red, while the fixed linkage is shown in black. The input link (IL) is the height of the opercle bone, the coupler link (CL) is the length of the IOP bone and the IOP ligament, and the output link (OL) is the connection from the end of the CL to the jaw joint. *Labeotropheus* (bottom) are benthic specialists with a short coupler link (CL) and long output link (OL) adapted for scraping algae off of rocks. *Tropheops* (middle) are benthic generalists, with a longer coupler link and shorter output linkage, compared to *Labeotropheus*, which allows for a faster jaw rotation but this species prefers a benthic environment. *Maylandia* (top) are true generalists with the longest coupler and shortest output linkage, compared to *Labeotropheus*, which allows for a fast oral jaw rotation. (b) We fed all three species either on a benthic or pelagic diet challenge for 1, 2, 4, or 8 weeks with a one week training period to ensure all experimental animals were able to forage in the correct manner. Pelagic fish were given finely ground up flake food (75% algae; 25% yolk) to force animals to suction feed out of the water column, and a small amount of brine shrimp daily. Animals in the benthic environment were fed the same amount of finely ground flake food mixed with ground freeze dried brine shrimp pasted on lava rocks with food-grade agar so fish would have to bite and twist their food to pluck it from the rocks.

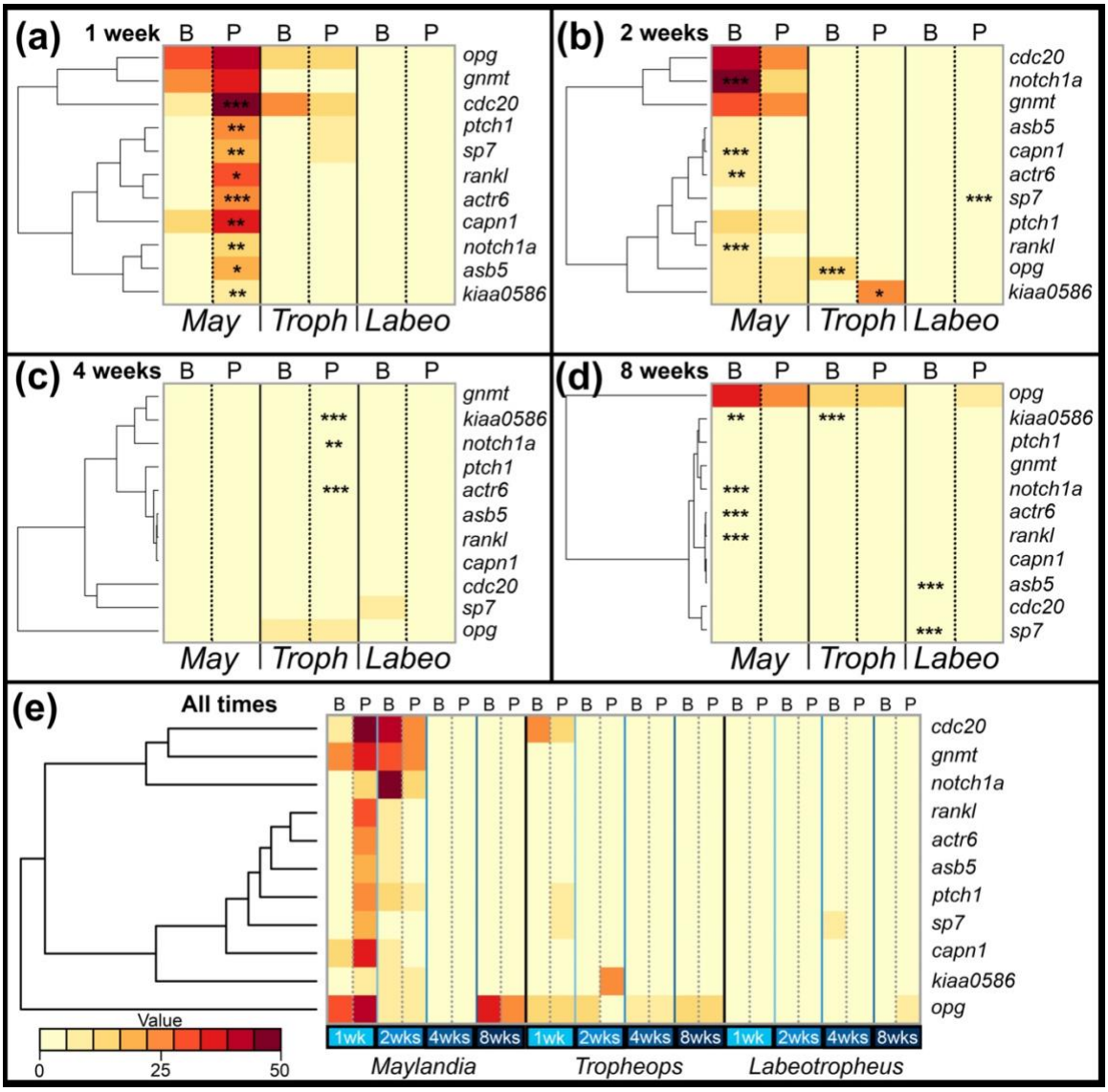

Figure 11: Gene expression is dynamic over time, with the early response being the most important. All panels present gene expression for all three species, *Labeotropheus* (*Labeo*), *Tropheops* (*Troph*), and *Maylandia* (*May*) at one or more timepoints. Solid lines separate species, while dotted lines separate benthic (B) and pelagic (P) treatments. Asterisks indicate significant differences in gene expression between environments, and are labeled on the treatment with higher average expression (*, **, and *** indicate significance at the <0.05, <0.01, and <0.001 levels, respectively) . Darker colors indicate higher expression levels than lighter colors (key in panel E). Positions of genes listed on the right of each heatmap are based on relatedness of the genes, as determined by the dendrogram associated with each map. Expression was calculated via the ΔCt method. Each biological replicate for each gene indicates the average expression of an individual as a percentage of the highest expression value for that gene. (A) Gene expression of week 1. No plasticity was observed in *Labeotropheus* or *Tropheops*, while all genes except *gnmt* were plastic in *Maylandia*. Plasticity in *Maylandia* always occurred with high expression in the pelagic environment. (B) Alternatively to week 1, week 2

expression showed plasticity in *Tropheops*, and limited plasticity in *Labeotropheus*. All plasticity in *Maylandia* at this time point was upregulated in the benthic environment. (C) Week 4 expression indicates plasticity only in *Tropheops*. However, many genes in *Maylandia* were just under the level of significance ($0.1>p>0.05$). Plasticity in *Labeotropheus* could not be determined because $n<3$ for the benthic environment. (D) Expression levels at 8 weeks show plasticity for all three species but expression was higher only in the benthic environment. (E) Expression over all time points, separated by species (solid black lines), then by week (solid blue lines), and further by environment (dotted gray lines; B,P).

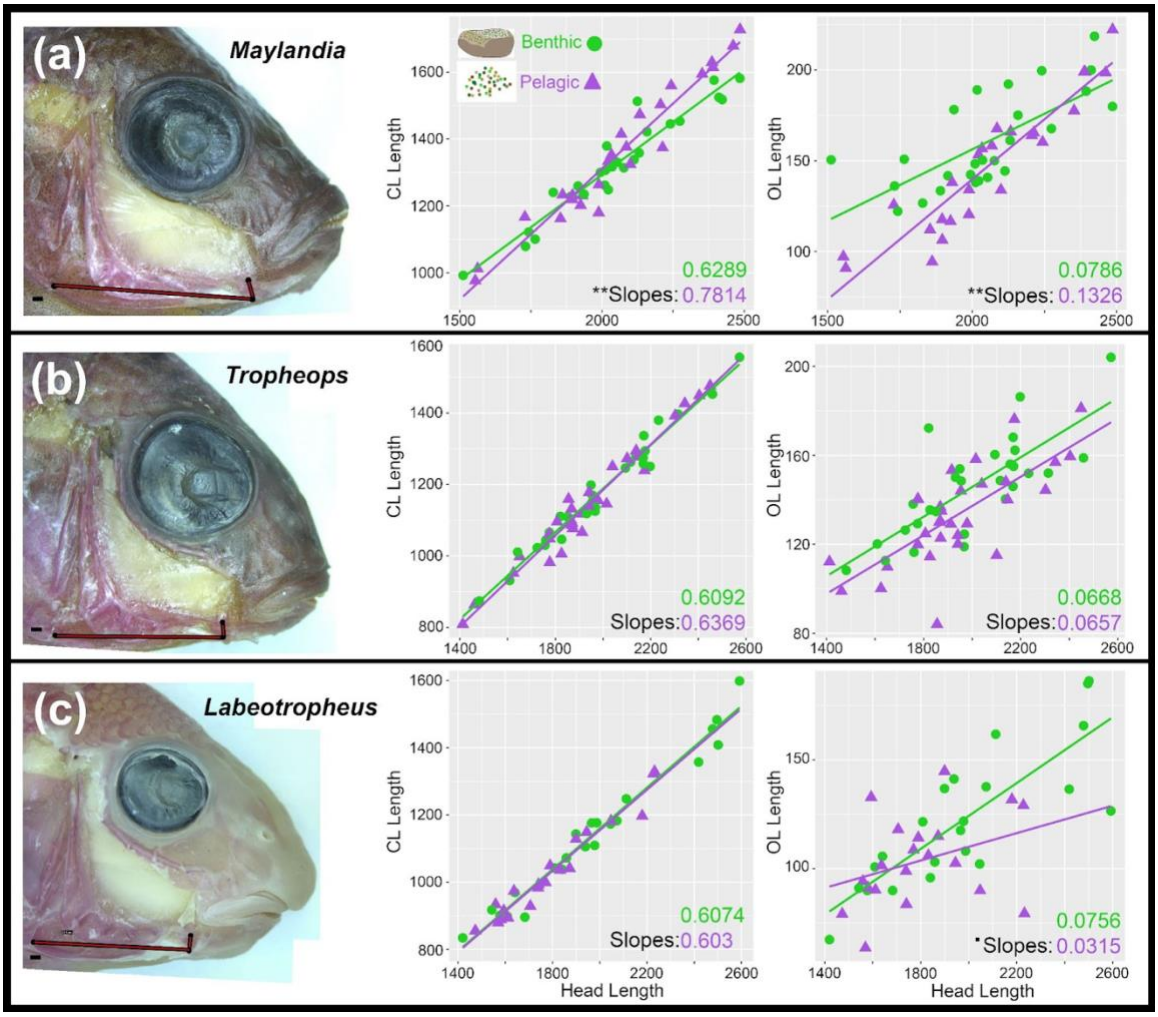

Figure 12: Morphological plasticity is dependent upon species and individual linkages. Representative images of Alizarin red stained LF (A), TO (B) and MG (C). Head length of each individual was plotted against either the coupler linkage length (middle) or output linkage length (right). Animals in the benthic treatment are represented by green circles and pelagic by purple triangles. Slopes for each species by treatment were calculated using a linear model and were used to compare slopes. Divergent slopes indicate plasticity in that particular linkage, which is apparent only in the output linkage for LF (A), and in MG for both linkages (C). While TO may appear plastic in the output linkage due to non-overlapping slopes, the slopes are nearly identical and indicate that TO are not plastic, but benthic feeders appear to be larger than pelagic feeders (B).

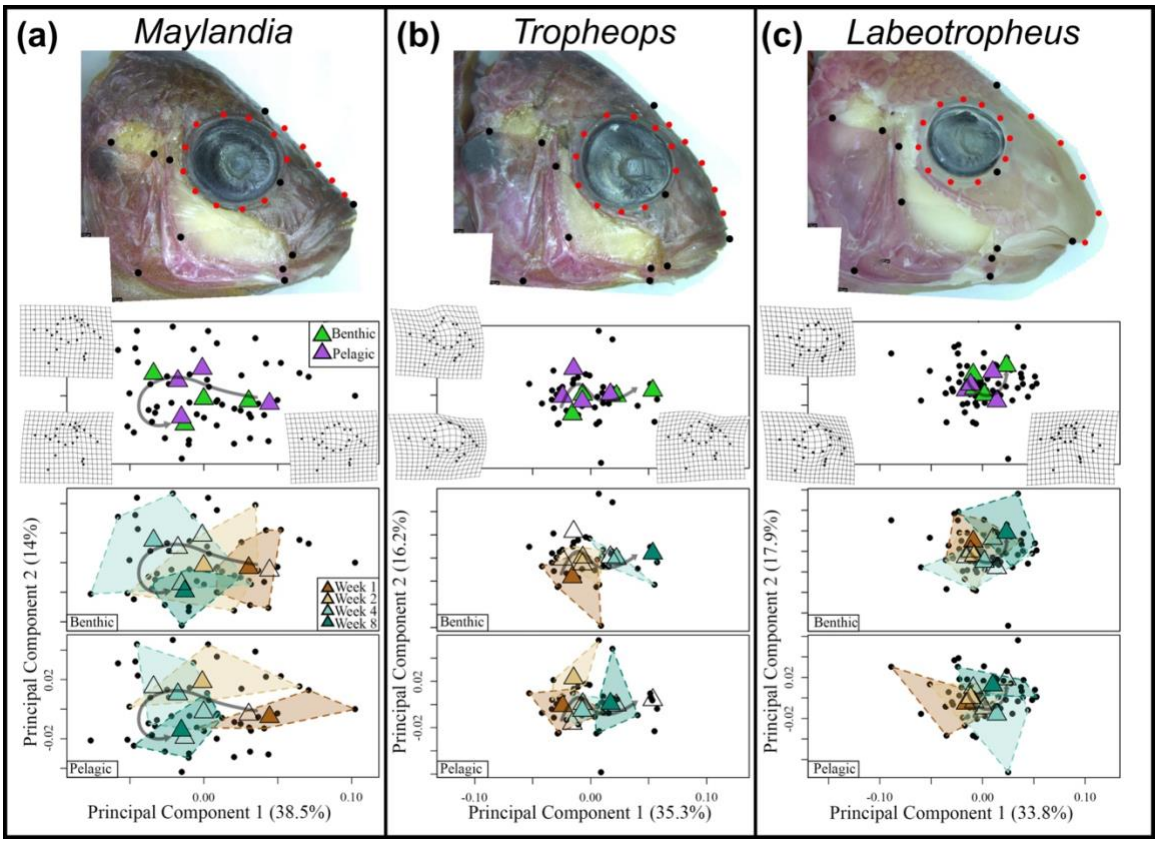

Figure 13: Landmarking scheme and trajectory analyses. Whole shape landmarking data for (a) Maylandia, (b) Tropheops, and (c) Labeotropheus. Fixed landmarks are denoted by black dots on the cleared and stained craniofacial profiles. Semilandmarks painting curves around the eye and along the slope of the head are in red. Trajectory analyses are superimposed onto PC space by treatment and by week for each species. Black points indicate individual animals. Colored triangles in the top three panels depict treatment (benthic=green, pelagic=purple), or time (week 1=dark brown, week 2=light brown, week 4=light teal, week 8=dark teal) in the remaining panels. Mean path is illustrated in a dark gray arrow on each panel. Deformation grids illustrate the outer bounds of each PC.

Table 2: Statistics from the ANOVA model assessing importance of species, treatment, and time in gene expression. There is an effect of species, time, and the interaction between them for all genes. Treatment was less prominent in determining gene expression differences. Darker cells indicate lower p-values.

	kiaa0586	*actr6*	*asb5*	*sp7*	*capn1-like*	*gnmt*	*cdc20*	*ptch1*	*notch1a*	*opg*	*rankl*
Species	0.04134	8.71E-09	1.04E-04	0.02371	2.00E-16	2.00E-16	3.12E-11	1.96E-07	1.14E-09	2.00E-16	1.76E-13
Treatment	0.03225	0.00648	0.054785	3.24E-04	0.035491	N/S	N/S	0.06242	0.07228	N/S	0.06194
Time	3.33E-06	1.69E-06	4.25E-04	5.35E-08	2.66E-15	3.29E-16	2.00E-16	4.45E-09	7.37E-11	2.00E-16	1.66E-12
Species:Treatment	0.07935	0.00295	N/S	0.037132	0.043118	N/S	N/S	0.07993	N/S	N/S	N/S
Species:Time	0.00471	1.47E-08	4.09E-04	1.66E-05	2.00E-16	2.00E-16	2.00E-16	0.00912	9.81E-15	2.21E-14	3.55E-13
Treatment:Time	0.00996	6.65E-05	0.003963	6.52E-06	8.04E-04	N/S	2.62E-05	7.58E-05	1.29E-04	0.0548	7.76E-04
Species:Treatment:Time	0.00178	9.06E-07	0.00365	0.0046	1.34E-04	N/S	9.38E-07	7.42E-05	1.04E-07	0.0558	0.00298

Table 3: Comparison of slopes between environments and species. (Top) Slopes from Figure 12. Statistically different slopes at α=0.05 are highlighted in gray. Darker shades indicate different significance levels. While *Labeotropheus* did not reach the level of significance for any linkage, the output link approached plasticity with p=0.0616. (Bottom) p-values are displayed for the comparison of slopes between species within a treatment. Cells are highlighted based on p-value. Notably, *Maylandia* grew faster for both the coupler and output linkages in the pelagic environment compared to both *Tropheops* and *Labeotropheus*. However, species were indistinguishable from each other for both linkages when fed benthically.

Treatment effects	**Coupler Link**		**Output Link**		**Input Link**		**Fixed Link**	
	Benthic	**Pelagic**	**Benthic**	**Pelagic**	**Benthic**	**Pelagic**	**Benthic**	**Pelagic**
Maylandia	0.6289	0.7814	0.0786	0.1326	0.761	0.761	0.747	0.839
Tropheops	0.6092	0.6369	0.0668	0.0657	0.587	0.668	0.815	0.814
Labeotropheus	0.6074	0.603	0.0756	0.0315	0.681	0.62	0.709	0.717

SpeciesxTreatment	**Coupler Link**		**Output Link**		**Input Link**		**Fixed Link**	
	Benthic	**Pelagic**	**Benthic**	**Pelagic**	**Benthic**	**Pelagic**	**Benthic**	**Pelagic**
May:Troph	0.8837	0.0036	0.8157	0.001	0.0013	0.0954	0.0891	0.695
May:Lab	0.8475	0.002	0.9849	1.00E-04	0.093	0.625	0.4209	0.0031
Lab:Troph	0.9987	0.7669	0.86	0.2124	0.1301	0.017	0.0008	0.0184

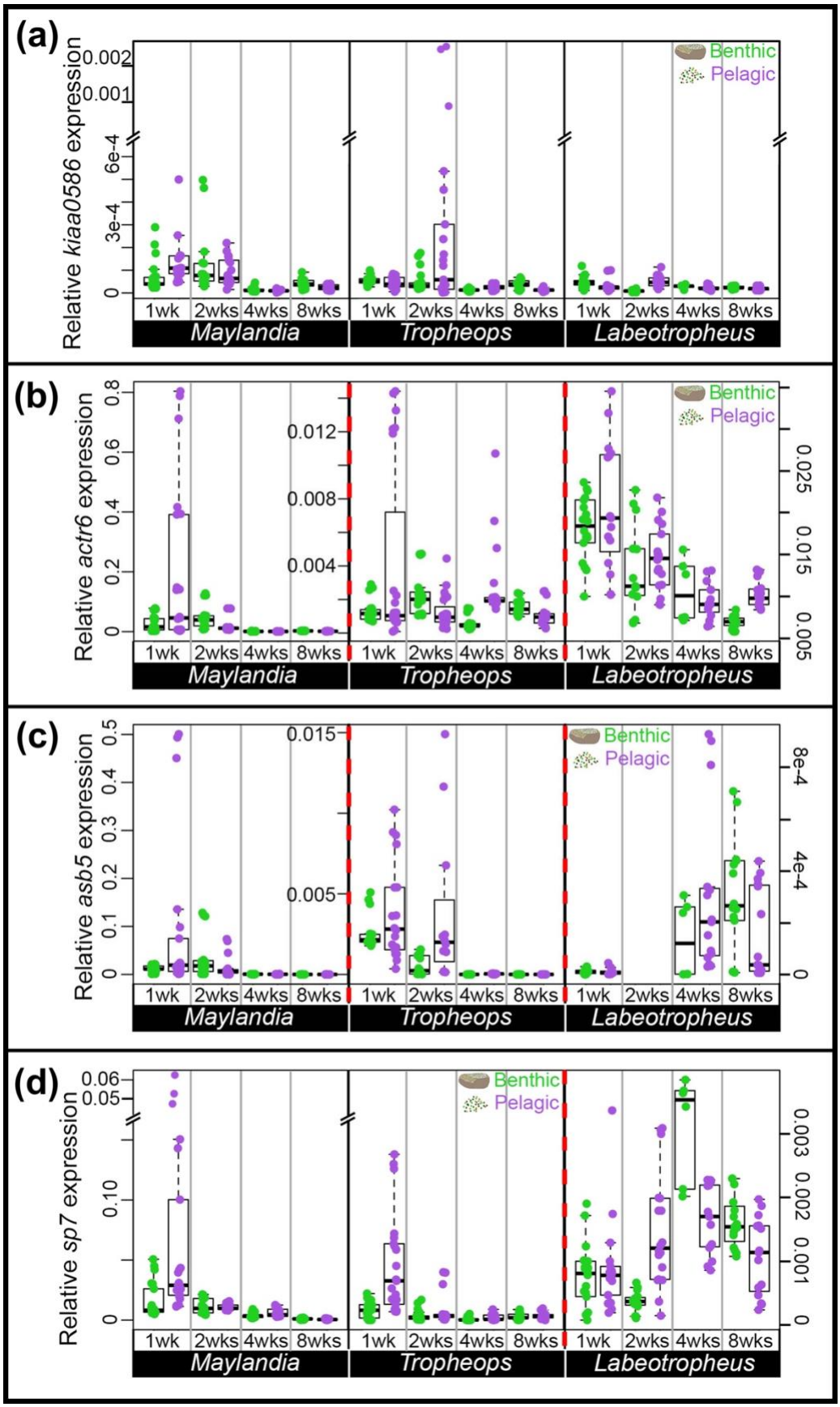
(a)
Relative kiaa0586 expression
0.002
0.001
6e-4
3e-4
0
Benthic
Pelagic
1wk 2wks 4wks 8wks 1wk 2wks 4wks 8wks 1wk 2wks 4wks 8wks
Maylandia
Tropheops
Labeotropheus
(b)
Relative actr6 expression
0.8
0.6
0.4
0.2
0
0.012
0.008
0.004
0.025
0.015
0.005
Benthic
Pelagic
1wk 2wks 4wks 8wks 1wk 2wks 4wks 8wks 1wk 2wks 4wks 8wks
Maylandia
Tropheops
Labeotropheus
(c)
Relative asb5 expression
0.5
0.4
0.3
0.2
0.1
0
0.015
0.005
8e-4
4e-4
0
Benthic
Pelagic
1wk 2wks 4wks 8wks 1wk 2wks 4wks 8wks 1wk 2wks 4wks 8wks
Maylandia
Tropheops
Labeotropheus
(d)
Relative sp7 expression
0.06
0.05
0.10
0
0.003
0.002
0.001
0
Benthic
Pelagic
1wk 2wks 4wks 8wks 1wk 2wks 4wks 8wks 1wk 2wks 4wks 8wks
Maylandia
Tropheops
Labeotropheus

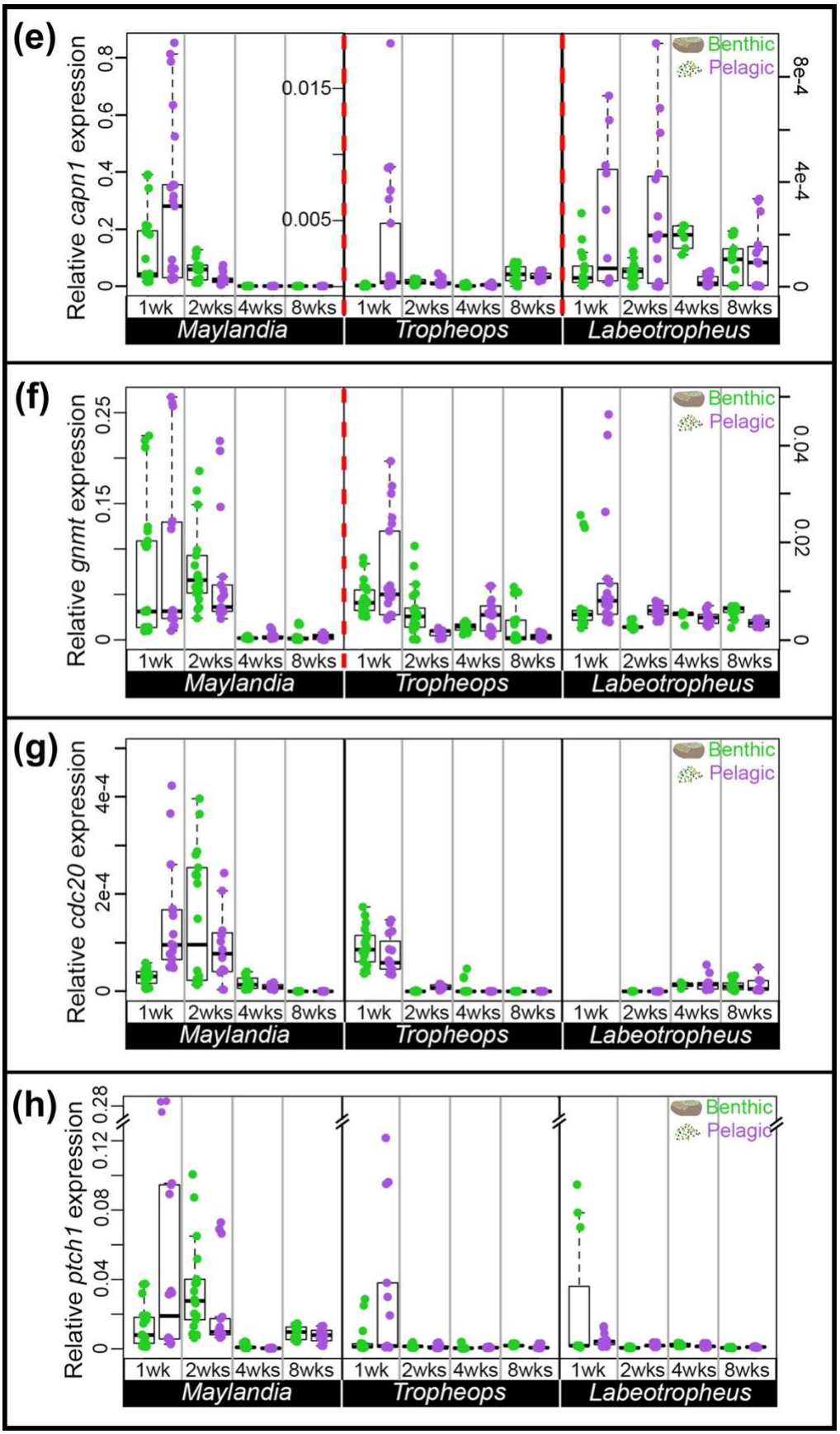
(e)
Relative capn1 expression
0
0.2
0.4
0.6
0.8
0.015
0.005
8e-4
4e-4
0
Benthic
Pelagic
1wk 2wks 4wks 8wks
Maylandia
Tropheops
Labeotropheus
(f)
Relative gnmt expression
0
0.15
0.25
0.04
0.02
0
Benthic
Pelagic
1wk 2wks 4wks 8wks
Maylandia
Tropheops
Labeotropheus
(g)
Relative cdc20 expression
0
2e-4
4e-4
Benthic
Pelagic
1wk 2wks 4wks 8wks
Maylandia
Tropheops
Labeotropheus
(h)
Relative ptch1 expression
0
0.04
0.08
0.12
0.28
Benthic
Pelagic
1wk 2wks 4wks 8wks
Maylandia
Tropheops
Labeotropheus

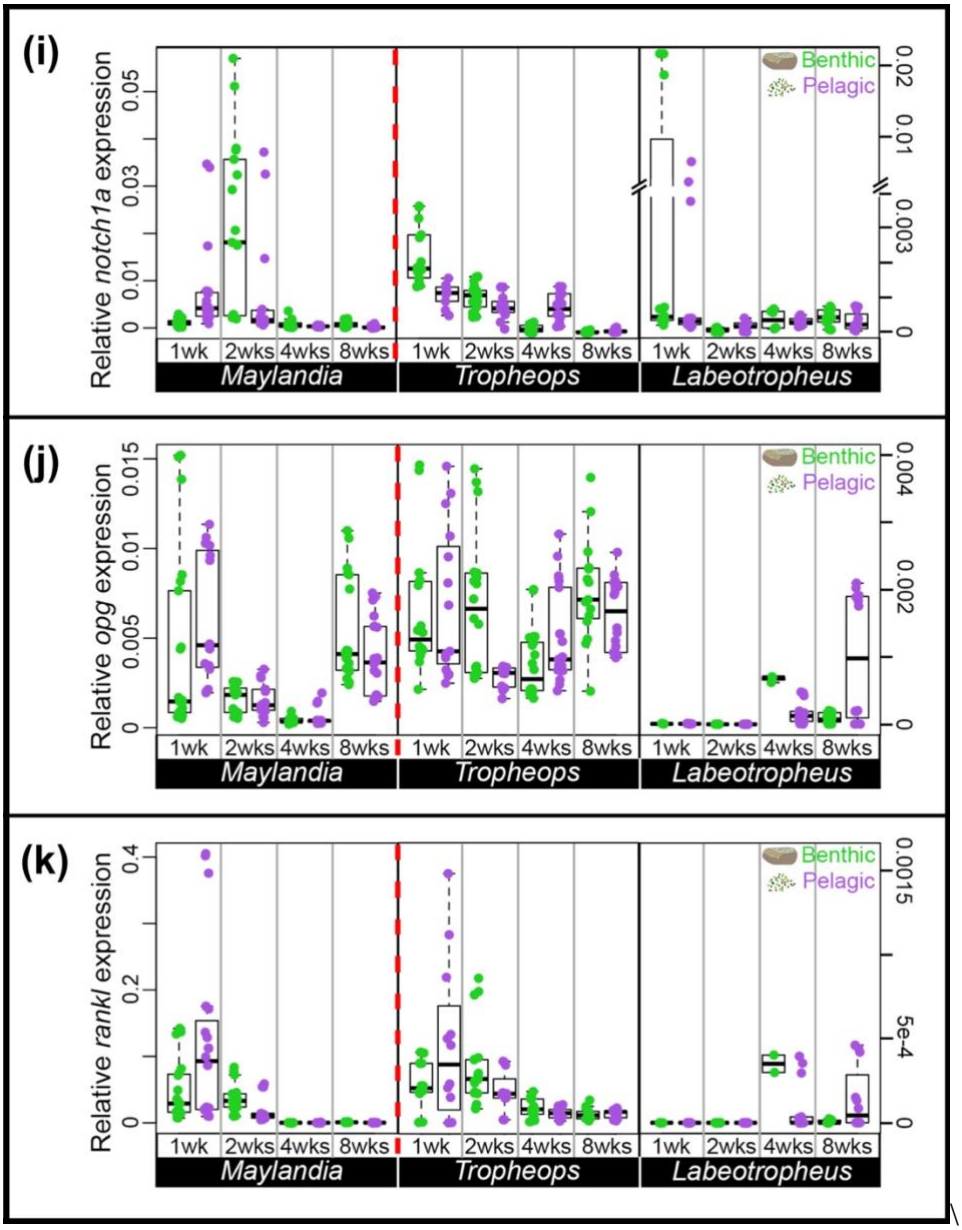

Figure S2: Expression of each gene over time. Expression of (a) *kiaa0586* (b) *actr6* (c) *asb5* (d) *sp7* (e) *capn1-like* (f) *gnmt* (g) *cdc20* (h) *ptch1* (i) *notch1a* (j) *opg* (k) *rankl* in *Maylandia*, *Tropheops*, and *Labeotropheus*. Each gene is separated by species (thick black bar) and further by time (gray bars). Red dotted bars indicate y-axis values are different between the two bordering species. Benthic points are in green, pelagic in purple.

Table S4: **Sample size of each species:week:treatment for qPCR and anatomical work.**

			qPCR n	Anatomy n
Maylandia	Week 1	Benthic	7	7
		Pelagic	7	7
	Week 2	Benthic	6	6
		Pelagic	6	6
	Week 4	Benthic	7	7
		Pelagic	5	6
	Week 8	Benthic	6	6
		Pelagic	6	6
Tropheops	Week 1	Benthic	7	7
		Pelagic	8	9
	Week 2	Benthic	7	7
		Pelagic	8	8
	Week 4	Benthic	7	8
		Pelagic	7	8
	Week 8	Benthic	6	7
		Pelagic	6	7
Labeotropheus	Week 1	Benthic	6	6
		Pelagic	6	6
	Week 2	Benthic	5	6
		Pelagic	5	5
	Week 4	Benthic	2	5
		Pelagic	5	5
	Week 8	Benthic	5	4
		Pelagic	4	4

Table S5: qPCR cichlid primer sequences.

Gene	Primer sequence (5'-3')
actb2 For	GTATGTGCAAGGCCGGATT
actb2 Rev	TTCTGACCCATACCCACCAT
actr6 For	GCAAATCCCGTCTGTTACGC
actr6 Rev	CATAGTCCTCCCGCATCACC
asb5 For	CAGTGTGATGGTACCCGTCC
asb5 Rev	CACAAAACGAGCAGCTCAGAAA
capn1-like For	ATGTTTAGGGTTGGGACTCCAG
capn1-like Rev	GGTGACAACCAACTGATCCCT
cdc20 For	GGCTCCTGTATCAGTTCGCT
cdc20 Rev	AGGCGAATGGTCTCATCTGC
gnmt For	GTGTCGGACCAGTGTTTTGC
gnmt Rev	AGCCCAAAGAGATGAACGCA
kiaa0586 For	CCTGGATCAGCAGGTTAAGCA
kiaa0586 Rev	CTGATGGCAAGGCAGAAAAGG
notch1a For	CAGATGCGAGCAGGACATAA
notch1a Rev	ACAGGTGCCACCATTAAAGC
opg For	CCAAACCGGCGATGAAACTG
opg Rev	ACGTTGGTTGTTCAGCTTGC
ptch1 For	TTCTGATGCTGGCCTATGCA
ptch1 Rev	CCCCTGAGACTTGGCACAGT
rankl For	GTCTGTTTCTCTCCGGCTACC
rankl Rev	CCAGGTCCCAGACTCAATGC
sp7 For	GGCCGCATCTATTCTGGAGG
sp7 Rev	GGCAGTCTTACCGGGTGTAG

Table S6: Plasticity in gene expression by time point for each species. Darker shades of gray indicate a lower p-value. May=*Maylandia*, Troph=*Tropheops*, Lab=*Labeotropheus*. B=Benthic, P=Pelagic.

Kiaa0586	**1 week**		**2 weeks**		**4 weeks**		**8 weeks**	
MayP:MayB	0.003031	P>B	N/S	N/A	N/S	N/A	0.00156	B>P
TrophP:TrophB	N/S	N/A	0.01805	P>B	7.93E-05	P>B	1.90E-06	B>P
LabeoP:LabeoB	N/S	N/A	N/S	N/A	-	-	N/S	N/A
Actr6								
MayP:MayB	1.02E-04	P>B	0.001275	B>P	N/S	N/A	4.00E-07	B>P
TrophP:TrophB	N/S	N/A	N/S	N/A	1.00E-07	P>B	0.06248	B>P
LabeoP:LabeoB	N/S	N/A	N/S	N/A	-	-	N/S	N/A
Asb5								
MayP:MayB	0.02123	P>B	N/S	N/A	N/S	N/A	N/S	N/A
TrophP:TrophB	N/S	N/A	N/S	N/A	N/S	N/A	N/S	N/A
LabeoP:LabeoB	N/S	N/A	-	-	-	-	3.90E-06	B>P
Sp7								
MayP:MayB	0.001597	P>B	N/S	N/A	N/S	N/A	N/S	N/A
TrophP:TrophB	N/S	N/A	N/S	N/A	N/S	N/A	N/S	N/A
LabeoP:LabeoB	N/S	N/A	3.34E-05	P>B	-	-	0	B>P
Capn1-like								
MayP:MayB	0.002369	P>B	7.00E-07	B>P	N/S	N/A	N/S	N/A
TrophP:TrophB	N/S	N/A	N/S	N/A	N/S	N/A	N/S	N/A
LabeoP:LabeoB	N/S	N/A	N/S	N/A	-	-	N/S	N/A
Gnmt								
MayP:MayB	N/S	N/A	N/S	N/A	N/S	N/A	N/S	N/A
TrophP:TrophB	N/S	N/A	N/S	N/A	0.09024	P>B	N/S	N/A
LabeoP:LabeoB	N/S	N/A	N/S	N/A	N/S	N/A	N/S	N/A
Cdc20								
MayP:MayB	2.40E-06	P>B	N/S	N/A	N/S	N/A	N/S	N/A
TrophP:TrophB	N/S	N/A	N/S	N/A	N/S	N/A	N/S	N/A
LabeoP:LabeoB	-	-	N/S	N/A	-	-	N/S	N/A
Ptch1								
MayP:MayB	0.00492	P>B	0.07215	B>P	0.06524	B>P	N/S	N/A
TrophP:TrophB	N/S	N/A	N/S	N/A	N/S	N/A	N/S	N/A
LabeoP:LabeoB	N/S	N/A	N/S	N/A	-	-	N/S	N/A
Notch1a								
MayP:MayB	0.00768	P>B	5.97E-04	B>P	0.06897	B>P	4.12E-05	B>P
TrophP:TrophB	N/S	N/A	N/S	N/A	0.003031	P>B	N/S	N/A
LabeoP:LabeoB	N/S	N/A	N/S	N/A	-	-	N/S	N/A
Opg								
MayP:MayB	N/S	N/A	N/S	N/A	N/S	N/A	0.09952	B>P
TrophP:TrophB	N/S	N/A	6.24E-04	B>P	0.0761	P>B	N/S	N/A
LabeoP:LabeoB	N/S	N/A	N/S	N/A	-	-	N/S	N/A
Rankl								
MayP:MayB	0.01565	P>B	9.52E-05	B>P	N/S	N/A	0	B>P
TrophP:TrophB	N/S	N/A	N/S	N/A	N/S	N/A	N/S	N/A
LabeoP:LabeoB	N/S	N/A	N/S	N/A	-	-	N/S	N/A

CHAPTER IV

CILIARY ROOTLET COILED-COIL 2 (*crocc2*) IS ASSOCIATED WITH EVOLUTIONARY DIVERGENCE AND PLASTICITY OF CICHLID JAW SHAPE

Gilbert, M.C*., Tetrault, E.R.*, Packard, M., Navon, D., & Albertson, R.C. (2021). *Molecular Biology and Evolution*, *38*(8), 3078-3092.

Introduction

Plasticity is a core concept in the extended evolutionary synthesis

The Modern Synthesis of the 1930s and 1940s united Darwin's theory of natural selection with Mendelian genetics to explain the origin and maintenance of adaptive variation within populations, and has since been the prevailing paradigm in evolutionary biology (Mayr 1993). The Modern Synthesis set out a largely gene-centric view of adaptation wherein new variation arises in a population through genetic mutation, and natural selection leads to the differential survival of variants. In recent decades, however, it has become apparent that several elements are missing from the Modern Synthesis (Pigliucci 2007), including a consideration for previously unrecognized sources of variation, such as development (Waddington 1959; Jamniczky et al. 2010) and the environment (West-Eberhard 1989, 2003). In other words, the mechanisms for how phenotypic variation arises and is maintained within populations are not yet well understood (Hendrikse et al. 2007). These conceptual omissions have led to the idea that the field is in need of an Extended Evolutionary Synthesis (Mayr 1993; Pigliucci 2009).

Within the context of the Extended Evolutionary Synthesis, phenotypic plasticity has emerged as a core concept as it can have a potent effect on the degree and type of genetic variation that is exposed to natural selection (Mayr 1993; Pigliucci 2005, 2008;

Laland et al. 2014). Operationally, plasticity is the capacity of a single genotype to produce two or more phenotypes in response to environmental stimuli (Bradshaw 1965), which may increase fitness in fluctuating environments (West-Eberhard 1989; Schlichting and Pigliucci 1998). Phenotypic plasticity also has the potential to influence several evolutionary phenomena, including the origins of novel traits (Moczek 2008), speciation (Price et al. 2003; West-Eberhard 2005; Pfennig et al. 2010), and adaptive radiations (West-Eberhard 2003; Wund et al. 2008). Although plasticity is often considered separate from (or even opposite to) genetics, it is important to note that the two are inextricably linked, and that plasticity manifests due to the sensitivity of (genetically encoded) molecules and/or pathways to environmental input (Pigliucci 2005). In other words, if phenotypic variance is due to the combined effects of genetics, the environment, and their interaction (i.e., P=G+E+GxE), then plasticity may be considered the interaction term (GxE). A genetic basis for plasticity is supported by its heritability (reviewed by, Scheiner 1993), but many questions remain, including what are the specific genetic components of plasticity and at what level (e.g., nucleotide, transcript, protein) do they confer environmental sensitivity (Pigliucci 2005; Gibert 2017). This uncertainty about the genetic nature of plasticity has hindered progress into understanding the mechanisms through which plasticity may evolve (Via et al. 1995). Thus, phenotypic plasticity is recognized as an important process in evolution, but we still lack an understanding of many fundamental aspects of its biology (Ehrenreich and Pfennig 2016; Schneider and Meyer 2017).

The cichlid jaw as a flexible stem

Over the past two decades, we and others have worked to reveal the genetic bases for jaw shape differences among cichlid species (e.g., Albertson et al. 2003, 2005; Parnell et al. 2012; Powder et al. 2014; Hu and Albertson 2017; Irisarri et al. 2018). In addition, plasticity is well documented for the cichlid jaw. Specifically, when reared in the lab on diets that imposed distinct functional demands on the feeding apparatus, cichlids will develop distinct oral jaw morphologies (Bouton et al. 2002; van Snick Gray and Stauffer 2004). Notably, variation in cichlid feeding morphology induced by alternate feeding regimes can be strikingly similar to patterns of natural craniofacial variation among species (Parsons et al. 2014). Repeated lacustrine cichlid radiations are defined by a conserved primary axis of craniofacial variation that involves differences in head depth and jaw length/rotation, traits that are intimately associated with adaptations to alternate benthic and pelagic trophic habitats (Cooper et al. 2010), and it is this pattern of variation that is typically observed in studies of developmental plasticity of the cichlid jaw (Bouton et al. 2002; Parsons et al. 2014). Moreover, similar patterns of craniofacial plasticity have been observed in several other fish lineages when fed alternate benthic/pelagic diets (Parsons and Robinson 2006, 2007; Wund et al. 2008), which suggests a common mechanism may be at work.

The combination of morphological diversity and developmental plasticity has led to the assertion that the cichlid jaw represents a morphological “flexible stem” (West-Eberhard 2003). The flexible stem hypothesis of adaptive radiation postulates that patterns of developmental plasticity in an ancestral lineage will generate independently derived radiations along similar eco-morphological axes (West-Eberhard 1989, 2003). In other words, the nature of developmental plasticity in an ancestral population can

influence the direction of adaptive radiations by determining what genetic variation is exposed to selection through its phenotypic expression. Under this hypothesis, repeated evolution along a conserved benthic-pelagic eco-morphological axis in cichlids is the result of sorting, and ultimately fixing, genetic variation that is exposed to selection via plasticity. If true, we would expect that the same loci that underlie evolutionary divergence in cichlid jaw shape will also regulate plasticity of the structure (Gibert 2017). Here, we test this prediction.

Materials and Methods

Species and husbandry

Both cichlids and zebrafish were used for this project. All cichlids were raised in 10 gal glass aquaria on standard flake food until 2 months of age, before being transferred to 40 gal glass aquaria. A single LF female was crossed to a single TRC male, creating a hybrid mapping population that was used for pedigree mapping. These species differ in craniofacial geometry and plasticity (Parsons et al. 2014; Albertson and Pauers 2019; Navon et al. 2020). A full-sibling F1 family was interbred to produce 25 F2 families, which were interbred to generate 265 F3 individuals used in this study. At 2 months, F3 families were split into two diet treatments, pelagic or benthic. For more detailed methods on these treatments and this cross, see previously published papers by Parsons and colleagues (Parsons et al. 2014, 2016). Briefly, a combination of flake food, algae wafers, and freeze-dried daphnia was ground and either sprinkled directly into the water column (pelagic treatment) or mixed with a ~1–1.5% food-grade agar (Carolina Biological Supply Co., Burlington, NC) solution and spread over lava rocks (benthic treatment). Fish were raised to ~7 months of age on each diet, euthanized with MS-222

according to approved IACUC protocols, fixed in 4% PFA, and stored in 75% ethanol. Prior to fixation, flank muscular tissue was taken for DNA extraction. Animals were dissected to reveal functionally salient bones and muscles, and imaged using a digital camera (Olympus E520).

Zebrafish were raised in 2.8-l plastic aquaria on a diet of rotifers from 5- to 12-day postfertilization, and then on a combination of GM-300 (Skretting) and brine shrimp thereafter. For the foraging experiment (details below), zebrafish in the pelagic treatment received GM-300 sprinkled directly into the water column, whereas benthic fish received GM-300 mixed with a ~1% food-grade agar solution spread over the rough side of 2-in ceramic tiles. *Crocc2* mutant alleles were obtained from the Zebrafish International Resource Center (ZIRC). Allele 20707 consists of an ENU induced C > T nonsense mutation mapped to exon 8 that encodes a premature stop codon at amino acid 272. Allele 20708 contains a C > T nonsense mutation in exon 14 that creates a premature stop at amino acid 585. Fish harboring either allele yield comparable bone phenotypes; only 20707 phenotypes are reported here. Both alleles were contributed to ZIRC by the Stemple Lab (Busch-Nentwich et al. 2013) and map positions are based upon Zebrafish genome assembly GRCz11.

Pedigree Mapping (data generated by RCA)

QTL mapping methods and results are described elsewhere (Parsons et al. 2016; Zogbaum et al. 2021). Briefly, genomic DNA was extracted from flank muscle tissue using DNeasy blood and tissue kits (Qiagen Inc., CA), digested with the SbfI restriction enzyme, processed into RAD libraries as described (Chutimanitsakun et al. 2011), barcoded and sequenced using an Illumina HiSeq 2000 (Illumina, San Diego, CA) and

single-read (1x100 bp) chemistry. We focused on a locus for lower jaw mechanical advantage, which mapped to an interval on linkage group (LG) 21, with a peak genotype phenotype association at a marker on physical scaffold 31 at 2,946,476 bp (Figure 15a). Since an F3 hybrid cross allows for a relatively higher number of recombination events and mapping resolution, we used additional, unmapped, RAD-seq SNPs to assess genotypic effects along this scaffold at increasingly fine scales, using makers every ~0.5 Mb (Figure 15c) and ~0.1–0.2 Mb (Figure 15d). In addition, genetic divergence between wild caught LF and TRC (imported directly from the lake) was explored, using a panel of 3,087 RAD-seq SNPs, and FST values following Nei (1987) and calculated in the R package HIERFSTAT. These fishes were genotyped following the same RAD procedures and SNP calling pipeline, and at the same time as the hybrids.

Immunohistochemistry (data generated by MP)

Immunostaining was performed with mouse anti-acetylated alpha tubulin (1:500; Sigma T6793) or rabbit anti-gamma tubulin (1:500; Sigma T6557). Amplification of T6793 signal was performed using donkey anti-mouse Biotin (1:100) and Alexa 488 Streptavidin Conjugate (1:1,000) (Jackson Immunoresearch). Donkey anti-rabbit Alexa 594 was used to visualize gamma tubulin antibodies. Briefly, animals were anesthetized and sacrificed using MS222 (Western Chemical, Inc.) and fixed for 1.5 h in 4% paraformaldehyde, pH 7.4, at room temperature. For young zebrafish, 4dpf larval samples were permeabilized in acetone at 20°C for 20 min followed by 1% Triton X-100 in PBS for 1 h, and blocked in 5% donkey serum (Jackson Immunoresearch) in 0.1% Triton X 100 in PBS. For adult zebrafish, samples were embedded in 1.5% agar/5% sucrose and 20 μm cryosections were blocked for 1 h before immunostaining. All Washes were

performed in 0.1% PBS-Tween 20, pH 7.4. To prevent photobleaching, all samples were mounted using Vectashield with DAPI (H-1200; Vector Labs).

Geometric morphometrics (data generated by MCG)

Adult zebrafish were cleared and stained using traditional methods (Potthoff 1984; Taylor and Van Dyke 1985). All dissections, and subsequent imaging, were performed using a Leica M165 FC microscope, and attached Leica DFC450 camera (Leica Camera AG, Wetzlar, Germany). We imaged the lateral profile of the lower jaw, and dorsal surface (when premaxillae are protruding) of the kinethmoid (Hernandez et al. 2007) for morphological analyses. Geometric morphometric data were collected using Stereomorph (Olsen and Westneat 2015) in R (R Core Team 2018). In total, we summarized the lower jaw using six fixed and four semilandmarks (sliding) and the kinethmoid using four fixed and eight semilandmarks (see Rohlf and Slice 1990; Gunz and Mitteroecker 2013, for more information on fixed/semilandmarks).

Morphological data were aligned via generalized Procrustes superimposition (Goodall 1991) and then analyzed via ANOVA to test for significance differences in mean shape between homozygous genotypes for both the lower jaw and kinethmoid. In all analyses, we compared null models (shape~size) to full models (shape~size+genotype) to control for the effects of size. Tests were conducted utilizing a randomized residual permutation procedure (RRPP) and the data were subjected to 10,000 random permutations (Collyer and Adams 2018; Collyer et al. 2015). All morphological analyses were performed using Geomorph v3.1 (Adams et al. 2015, 2018).

Quantitative real-time PCR and network analysis

We purified RNA from homogenized whole heads of zebrafish excluding eyes and brain, between the ages of 3 and 15 months, in Trizol (Invitrogen) using phenol chloroform. We standardized resulting cDNA to 70 ng/ll using a High-Capacity cDNA Reverse Transcription Kit (Applied Biosystems). To determine relative gene expression levels, we used a 10-ll total reaction in triplicate using a QuantStudio3 Real-Time PCR System (Applied Biosystems). Each gene assessed was compared with expression levels of b-actin to determine relative expression levels via the DDCT method (Livak and Schmittgen 2001). Sample size was n= 5 for all genes in each age group/genotype except 10- to 15-month (i.e., old) mutant ptch2 where n=4. We used ANOVA for statistical analyses in R.

In order to determine the covariation of gene sets in our quantitative real-time PCR (qPCR) data set, we constructed gene networks in R. First, we used pairwise partial correlations with the ppcor package using the Pearson method to account for multicollinearity (Table 5). We next used the iGraph package to perform and visualize network analyses for each data set. These analyses weight the relationships between each gene based on the pairwise partial correlation value strengths. Correlations with a P value below 0.15 were included in the construction of the gene networks (Figure 19). The number of lines between each pair of genes indicates the strength of the covariation between them (i.e., five lines represents stronger correlation than 2).

Bone deposition analysis (data generated by DN)

Bone deposition experiments are described in detail elsewhere (Navon et al. 2020). Briefly, fish were anesthetized using MS-222 in cool water during injections and handling. They were injected with alizarin red (50 mg-fluorochrome/kg fish) at the first

timepoint and with calcein green (0.5 mg-fluorochrome/kg fish) at the second timepoint, approximately 5 weeks apart. One week after the final fluorochrome injection, fish were euthanized with a lethal dose of MS-222 and stored in 95% ethanol at 4°C. Craniofacial bones and flank scales were dissected from the head and body, cleaned of surrounding soft tissue, and flat mounted on glass slides. Cichlid bones were imaged with a Zeiss Axioplan2 fluorescent apotome microscope. Zebrafish bones were imaged with a Leica M165 FC microscope, and attached Leica DFC450 camera. All elements were imaged in triplicate using a red fluorescent filter, a green fluorescent filter, and a DCIM brightfield view. Trunk scales were flat mounted and imaged in the same way. Bone deposition was quantified by calculating the distance between the red and the green fluorochrome labels in each bone using Photoshop. Bone deposition was standardized for individual growth rate by regressing bone growth on scale growth and taking the residual values for downstream analysis. A series of ANOVAs using treatment and species (cichlids) or genotype (zebrafish) were performed in R (R Core Team 2018). Tukey's post hoc analyses (i.e., TukeyHSD) were performed to identify significant pairwise differences.

Results and Discussion

Genetic variation in *crocc2* is associated with functionally salient aspects of cichlid jaw shape

We generated a hybrid mapping pedigree by crossing two cichlid species that differ in jaw shape as well as their ability to remodel their jaws under different environmental conditions (Parsons et al. 2014; Navon et al. 2020). The first species, *Labeotropheus fuelleborni* (LF hereafter), is an obligate algal scraper, with a robust

craniofacial skeleton and limited plasticity. The second, *Tropheops* sp. "red cheek" (TRC), is a more generalized benthic forager, with smaller jaws and greater plasticity. With this genetic cross, we mapped variation in feeding architecture under distinct, ecologically relevant feeding regimes, whereby families were split and progeny were made to feed with either "biting" or "sucking" modes of feeding, mimicking a major ecological axis of divergence (see Parsons et al. 2016 for details). Results from this study demonstrated that the craniofacial G–P map is strongly influenced by the environment, as most quantitative trait loci (QTL) were specific to one environment (Parsons et al. 2016; Zogbaum et al. 2021). Among the environmentally sensitive loci was a QTL for the mechanical advantage of jaw closing, which is defined as the height of the ascending arm of the articular bone (e.g., articular process, AP), relative to overall jaw length (Figure 14). In cichlids, this bony process is where a major muscle involved in jaw closing inserts (the second subunit of the adductor mandibulae, A2), establishing this structure as the in lever for this functional system. A longer AP relative to jaw length, predicts greater mechanical advantage and a stronger bite. Lower jaw mechanical advantage tracks closely with feeding ecology in a range of vertebrate taxa (Westneat 2004; Manabu 2010; Roberts et al. 2011; Dumont et al. 2012; Casanovas-Vilar and van Dam 2013; Arbour and López-Fernández 2014), and is thought to drive evolutionary diversification (Dumont et al. 2014); however, its genetic basis is largely unknown (but see Albertson et al. 2005; Powder et al. 2014).

In this genetic cross, relative AP height mapped to LG21 in the benthic/biting environment (but not the pelagic/suction feeding environment) (Parsons et al. 2016; Figure 15a). Fine mapping across the physical scaffold associated with the QTL interval

showed that the peak genotype–phenotype association occurred at a SNP (i.e., G/A) within the *ciliary rootlet coiled-coil 2* (*crocc2*) gene (Figure 15b–d). A genome scan for divergent loci between natural populations of the parental species used in this cross (i.e., LF and TRC) demonstrated that these species possess alternate *crocc2* alleles (i.e., F_{ST}=0.95; Figure 15d; full data set published in Albertson et al. 2014). Notably, the SNP that underlied divergence within our mapping pedigree and between natural populations corresponded to a nonsynonymous change within *crocc2* (Figure 15b). This gene encodes an important structural component of the primary cilia, the ciliary rootlet. The alanine residue at position 963 appears to be conserved across African cichlids, but is a valine in LF, the obligate benthic forager with a long AP and low magnitudes of plasticity (Figure 15b). In addition, the A963V change is predicted to alter protein function based on a PolyPhen-2 (Adzhubei et al. 2013) protein prediction algorithm score of 0.904 (scores approaching 1.0 are considered functionally relevant), making this gene a robust candidate for regulating bone shape differences in cichlids.

Crocc2 encodes a large protein composed almost entirely of coiled-coil domains (Yang et al. 2002). This structural motif forms alpha-helices through hydrophobic interactions, wherein the polypeptide chain coils in order to bury hydrophobic residues and expose polar side chains (reviewed by Woolfson [2005]). The pairing of coiled-coil proteins occurs through heptad repeats, usually denoted as *abcdefg*, where *a* and *d* represent the hydrophobic residues (Figure 15e; Figure S3c), and interactions between opposing *a* and *d* residues represent the main hydrophobic seam in dimer formation (Woolfson 2005). In addition, residues that flank the hydrophobic seam in the alpha-helix, *e* and *g*, contribute to the specificity and stability between helices via ionic

interactions (e.g., salt bridges). Coiled-coils are dynamic and flexible structural motifs, which participate in myriad biological functions.

In the cilium, Crocc2 monomers homodimerize to form filamentous rootlets, which originate from the basal body and extend proximally toward the cell nucleus (Figure 15a, inset). Rootlets are thought to provide structural support for cilia by integrating the cilium with actin filaments (Yang et al. 2005). Cells lacking rootlets are structurally unstable and degenerate over time (Yang et al. 2005; Mohan et al. 2013). Notably, the

A963V change in African cichlids is predicted to affect this structural motif. Specifically, this change occurs in a stretch of residues where the heptad repeat is interrupted twice in African cichlids with the A allele (black arrowheads, Figure 15e). The V allele in LF is predicted to re-establish the heptad repeat across this region (Figure 15e). Consistent with this, the stability of the dimerization between helices is predicted to be higher with the V allele (Tm=95ºC), compared to the A allele (Tm=85ºC) (bCIPA, Mason et al. 2006). Notably, dimerization between the two different alleles is predicted to be the least stable (Tm=80ºC), which suggests that hybrids could be at a disadvantage if dimerization of this protein serves a core function. Collectively, these data suggest that this polymorphism may affect protein structure and cilia integrity/stability, with the V allele acting to increase stability.

When extending the Crocc2 sequence comparison across additional fish species several notable patterns emerged (Figure S3). First, we found that all perciform species examined (n=15) possessed either an A or V at this position, and further that all ray-finned fishes possessed a nonpolar, hydrophobic amino acid (Figure S3b). In addition, the

A/V poly- morphism noted in noncichlid perciforms was associated with the same G/A nucleotide polymorphism. Thus, all species within this order seem to have one of two nucleotides at this position, leading to either an A or V, and correspondingly a stretch of Crocc2 characterized by interrupted or contiguous heptad repeats, respectively (Figure S3c). The functional significance of this pattern with respect to bone/jaw shape remains unclear. On one hand, this region of the protein is characterized by increased variation in the continuity of the coiled-coil motif (relative to flanking regions), and so it may represent an area more permissive of variation, and therefore a potential target of selection. On the other hand, no obvious pattern emerges in terms jaw morphology when comparing species with continuous (e.g., LF, orangethroat darter, Antarctic dragonfish) versus interrupted (e.g., TRC, damselfishes, threespine stickleback) heptad repeats across this region. It is worth noting, however, that Crocc2 is a relatively large protein (>1,600aa in cichlids), and so it may be that the consequences of variation in amino acid sequence on bone biology has less to do with any one region of the protein, and more to do with the number and/or integrity of coiled-coil motifs across the entire protein, especially when making broad taxonomic comparisons. This could represent a fruitful line of future inquiry. Within African rift lake cichlids, however, where amino acid sequence homology is high (>95%), this particular mutation, and its predicted structural consequences, are more likely to have a direct effect on jaw/bone shape.

Rates of bone matrix deposition are canalized in the African cichlid species with the divergent *crocc2* allele

In the context of plasticity, a mutation that influences the integrity of a structural protein could provide a mechanism through which genetic assimilation occurs. We know from previous work that the cichlid species with the divergent *crocc2* allele, LF, exhibits

reduced craniofacial plasticity, relative to TRC, in response to alternate feeding regimes (Parsons et al. 2016; Navon et al. 2020). To determine the degree to which this finding holds specifically within the AP, we subjected LF and TRC to alternate feeding regimes, and then assessed rates of bone matrix deposition in the AP using two different fluorochromes injected at the beginning and end of the experiment (described in Navon et al. [2020]). We expected the generalized forager, TRC, to deposit more bone on the AP in the benthic/biting, compared with the pelagic/suction feeding, environment. Furthermore, we expected the obligate benthic foraging species, LF, to deposit relatively high rates of bone matrix deposition in both environments, consistent with the assimilation of a "biting" bone geometry. Our results support these predictions (Figure 16). We found a significant species-by-treatment effect in terms of matrix deposition (F=4.108, P=0.0137), with pairwise differences noted for TRC (TukeyHSD, P=0.0177) but not LF (TukeyHSD, P=0.9345) reared in different environments. These results show that bone formation is canalized in LF, resulting in consistently high levels of bone matrix deposition on the AP, and greater mechanical advantage of jaw closing.

Taken together, our results in cichlids suggest roles for *crocc2* in regulating species-specific bone geometry and plasticity, and that both phenotypes are related to differential mechanosensing. To test this hypothesis, we utilized the zebrafish system.

Crocc2 is required for the maintenance of primary cilia

Bone is a dynamic tissue that can sense and respond to its mechanical environment, and the primary cilia on bone cells are thought to play critical roles in mediating this process (Xiao et al. 2006; Papachroni et al. 2009; Nguyen and Jacobs 2013). Mice lacking functional cilia in bone precursor cells exhibit normal larval skeletal

patterning, but impaired growth (Qiu et al. 2012), as well as a reduced ability to form bone in response to mechanical loading (Temiyasathit et al. 2012). Unlike the axoneme and basil body, roles for the ciliary rootlet in bone biology are unknown. The limited data on this structure suggest that rootlets are important for maintaining ciliary integrity over time (Yang et al. 2005). Consistently, we found that zebrafish *crocc2* mutants possessed primary cilia as larvae (e.g., 4 days), but exhibited a dramatic reduction in cilia number, compared to wild-type (WT) siblings, as adults (e.g., >12 months) (Figure 17). Based on these data as well as known roles for the primary cilia and bone mechanosensing, we predicted that *crocc2* mutants will exhibit bone phenotypes that include 1) dysmorphic skeletal architecture in areas of high mechanical stress, 2) degenerative bone homeostasis, and 3) a reduced ability to mechanosense.

Jaw defects in *crocc2* mutants localize to regions of adaptive morphological variation in the cichlid jaw

We found that homozygous recessive *crocc2* mutants were viable through adult stages, enabling the analysis of bone phenotypes throughout life history stages. Consistent with our prediction, patterning of the *crocc2* craniofacial skeleton appeared relatively normal, but shape was distinct, especially at adult stages. A geometric morphometric analysis of craniofacial shape revealed key differences in foraging related bones, specifically in regions with direct mechanical input (e.g., attachment points for tendons and ligaments) (Figure 18). For instance, variation that distinguished mutant and WT jaw shapes was largely limited to the size and shape of the coronoid process (CP, Figure 18a,b). In zebrafish, this structure represents the point of insertion for the A2 muscle (Figure 14), and is functionally analogous to the region of the cichlid jaw that

maps to the *crocc2* locus. Thus, genetic/genomic mapping in cichlids and mutagenesis in zebrafish are consistent in implicating *crocc2* in the formation of nonhomologous but functionally equivalent structures of the jaw.

Shape defects were also noted in other bony elements. For example, the kinethmoid, which drives zebrafish jaw protrusion through a complex arrangement of ligamentous attachments, exhibited a unique shape in mutants (Figure 18c,d). Regions of this bone most affected in *crocc2* mutants include the rostral- and caudal-most surfaces, which serve as attachment sites for ligaments that connect the kinethmoid to the neurocranium and premaxilla, respectively (Staab and Hernandez 2010). In all, *crocc2* appears to be required to maintain bone integrity in zebrafish, especially in areas subjected to mechanical stress.

Crocc2 is required for bone homeostasis

We next examined bone growth and homeostasis in *crocc2* mutants at the transcript level. Specifically, we performed quantitative RT–PCR on freshly dissected craniofacial bones from mutant and WT animals at two different stages, young (3–5 months) and aging (10-15 months) adults. We used a panel of known and presumptive bone markers for this analysis (n=10, Table S7), and reasoned that if 1) cilia are required for normal bone growth and homeostasis, and 2) *crocc2* mutants lose cilia over time, then we should observe a mis-regulation of bone marker genes in older, compared with younger, mutant animals.

When considering the expression of individual bone marker genes, we found evidence for mis-regulation (Table 4; Figure S4). ANOVA models indicated significant effects of genotype on gene expression for three osteoblast markers (including *col10a1*),

and all three Hedgehog (Hh) markers. Hh signaling was assessed given that members of this pathway localize to the primary cilia (Goetz et al. 2009), and that it plays important roles in bone development and homeostasis (reviewed by Long 2011; Alman 2015). Genotype was not significant for osteoclast markers, nor the mature chondroblast marker, *col2a1a*. Age also had a significant effect on the expression levels of 3/4 osteoblast genes, 2/3 Hh markers, as well as the osteoclast marker, *csf1ra*. Genotype-by age was significant for the osteoblast markers, *runx2b* and *AP*, as well as for the Hh target gene, *ptch2*. The significant GxA effect for *runx2b* appeared to be driven by relatively higher expression in young mutant bones and lower expression in old mutant bones (Figure S4). For *AP*, higher expression was documented in older mutant fish, compared with old WT and young mutants, whereas for the Hh markers, *ptch1* and *ptch2*, mutants exhibited relatively lower expression than WT at both stages (Figure S4).

As bone homeostasis requires the coordinated expression of multiple genes, we next sought to assess the degree to which these genes exhibited coordinated expression in mutant and WT animals. Specifically, we performed partial correlations analyses on expression data within mutant and WT animals at both life-history stages, and report correlation coefficients and P values for all pairwise comparisons with the effect of the other variables removed (Table 5). Among young adults, differences between genotypes were modest, with mutant exhibiting 8/45 significant ($P < 0.05$) pairwise correlations, compared with 11/ 45 in similarly aged WT siblings (Table 5). Further, of the 11 significant correlations in WTs, only three were shared with mutants. This pattern was reflected in a network analyses of expression data, where both WT and mutant animals were characterized by four modules of correlated gene expression; however, the

composition of genes within each module was different, as was the overall strength of correlation in gene expression, which was higher in WT bone (i.e., a greater number of lines connecting traits, Figure 19a,b).

Differences in correlated gene expression were substantially greater in older adults, with mutants exhibiting 17/45 significant pairwise correlations, compared with 31/45 significant correlations in age-matched WT animals (Table 5). These data suggest a far more integrated expression network of bone markers in WT versus crocc2 mutants, an assertion that was supported by the network analyses (Figure 19c,d). Four modules were recovered for older WT animals, which were characterized by a high degree of correlation both within and between modules. Alternatively, gene expression in older mutants was characterized by two distinct modules, consistent with a dissociated gene network. This idea was supported by the spatial localization of TRAP and AP activities in WT versus *crocc2* mutants. In WT animals the enzymatic signature of bone resorption (i.e., TRAP) and deposition (i.e., AP) was typically colocalized (Figure 19c, inset), as expected based on the literature (e.g., Albertson and Yelick 2007; Cooper et al. 2013), and the interconnected expression of these two factors in the network (e.g., linked by various bone markers, Figure 19c). Alternatively, TRAP and AP activities were conspicuously distinct in *crocc2* mutants (Figure 19d, inset), consistent with their dissociated expression in network-space (Figure 19d).

All in all, these genetic data complement the analysis of *crocc2* bone phenotypes (e.g., Figure 18), and suggest that dysmorphic bone shape in *crocc2* mutants is underlain by mis-regulated marker gene expression.

Crocc2 is required for bone plasticity

To more explicitly test the hypothesis that *crocc2*-induced bone defects are due to impaired mechanosensing, we subjected fish to alternate feeding regimes intended to impose different functional demands on the craniofacial skeleton (Figure 20), similar to what was performed in cichlids (Figure 16). We then assessed rates of bone matrix deposition in the coronoid process (CP) of animals reared in different environments (Figure 20b,c). Our expectation was that WT animals would exhibit greater rates of CP bone deposition in the benthic foraging treatment where fish were required to leverage food from the substrate. We predicted further that this plastic response would be limited in *crocc2* mutants. Our data supported both predictions: Rates of bone matrix deposition were higher in the CP from WT fish reared in the benthic versus pelagic treatment, and this response was absent in mutants (Figure 20d). Thus, mutant fish reared in the benthic environment appear to have lost the ability to deposit bone in response to increased mechanical load. More generally, these results are consistent with the hypothesis that dysmorphic bone phenotypes in *crocc2* mutants arise due to impaired mechanosensing.

During this analysis, we noted variation in CP shape, consistent with the results from the shape analysis described above. We therefore explored CP shape in these experimental animals, and found that it was distinct between treatments (Treatment: Z=2.470, P=0.003) and genotypes (Genotype: Z=2.197, P=0.005), and that there was a significant interaction effect between these two variables (Genotype-by-Treatment: Z=2.194, P=0.006). In addition, by quantifying shape using both fluorochrome labels, we were able to track shape over time, and document a significant effect of this variable on CP shape (Time: Z=2.96, P=0.001). Another notable outcome of this analysis was that WT shape, across time and treatments, exhibited relatively less variation compared with

that across mutants, which occupied a far greater range of shape space (Figure S5). This qualitative assessment was supported by quantitative tests of morphological disparity, which showed that mutants exhibited 2x the disparity as WT animals (0.0238 vs. 0.0119, respectively; P=0.065). Increased disparity in mutant CP shape may be related to mis-regulated bone homeostasis (e.g., Figure 19).

Conclusion

Adaptive radiations and the root of flexible stems

Adaptive radiations constitute a major source of biodiversity on this planet, and have played a central role in our understanding of evolutionary processes. One attribute of adaptive radiations that has long intrigued and confounded biologists is their repeated, almost stereotypical, nature. For example, stem lineages that recurrently invade a novel environment (e.g., marine to freshwater among threespine stickleback) often diverge along highly predictable eco-morphological axes. Although similarities in ecological opportunity may explain some of these patterns, the extent to which replicate adaptive radiations are consistent has led to the proposition that other mechanisms may be at work. One notable hypothesis suggests that phenotypic plasticity in the stem lineage has the potential to bias the direction of adaptive radiations. Formalized as the flexible stem hypothesis (West-Eberhard 2003), this theory sets out to provide a mechanistic explanation for the repeated nature of adaptive radiations—for example, as an ancestral population is exposed to a novel environment, new phenotypic and genetic variants will be exposed to natural selection as individuals within the population mount a plastic response. Over time, those cryptic genetic variants that enable animals to more effectively exploit new resources may become fixed (i.e., genetic assimilation, sensu

Waddington 1953), thereby biasing the direction of evolution along the eco-morphological axis established by the initial plastic response. Thus, if ancestral patterns of plasticity are similar across taxa, then the genetically fixed evolutionary responses should reflect that similarity. One empirical sign of such flexible stem evolution is predicted to be molecular similarity between morphological plasticity and evolution (Gibert 2017; Navon et al. 2020). Our work seeks to detect such signals.

We first set out to study cryptic genetic variation underlying cichlid jaw shape, with a focus on loci that underlie variation within distinct foraging environments. Fine-mapping implicated the *crocc2* locus, and functional studies in zebrafish supported the assertion that this gene is necessary for load-induced bone growth and remodeling. These results are consistent with the broader literature on the primary cilia and bone remodeling (Xiao et al. 2006; Papachroni et al. 2009; Qiu et al. 2012; Temiyasathit et al. 2012; Nguyen and Jacobs 2013). However, whereas the overwhelming majority of studies focus on the basal body, axoneme, and other more distal components of primary cilia, ours is unusual in implicating the proximal rootlets in bone biology. Whether the effect is due to ciliary integrity or a more nuanced, and as yet undescribed, role for the rootlets remains to be determined. Regardless of the specific mechanism, we showed that the African cichlid species with the divergent *crocc2* allele exhibited an assimilated phenotype—that is, high levels of bone matrix deposition regardless of mechanical environment. In the context of variation in the coiled-coil motif, this raises the interesting question of whether the number and/or integrity of the motif (i.e., fewer interruptions) might influence mechanosensing. In zebrafish, the loss (or reduction) of Crocc2 function resulted in reduced plasticity, supporting critical roles for this molecule in mechanosensing. In LF,

loss of plasticity was associated with a putative gain-of-function polymorphism, where Crocc2 is characterized by fewer disruptions in the motif and correspondingly higher homodimerization affinity. Taken together, these insights suggest that the ability of bone cells to mechanosense may actually require a degree of interruption in the Crocc2 coiled coil motif. In other words, this region of interrupted heptad repeats may serve to "sensitize" Crocc2/rootlets to environmental input. If true, this configuration may be actively selected for in African cichlids, several of which are known to be plastic in head/jaw shape (Parsons et al. 2014; Gunter et al. 2017; Hu and Albertson 2017; Navon et al. 2020). This work constitutes the second in a set of experiments aimed at understanding the molecular basis of plasticity. The other has focused on Hh signaling (Parsons et al. 2016; Hu and Albertson 2017; Navon et al. 2020), which is notable given the close association between the primary cilium and the Hh signal transduction pathway. Members of the Hh pathway localize to the cilium (Yuan et al. 2015), and cells lacking cilia are unable to transduce a signal in response to the Hh ligand (Haycraft et al. 2005; Berbari et al. 2009). Thus, cilia have been said to constitute the "Hh signal transduction machine" (Goetz et al. 2009). Given the conservation of molecular mechanisms across vertebrates, understanding how, or if, Hh signaling and rootlets interact to effect bone biology in general, and mechanical load-induced plasticity in particular, could be a fruitful line of study. More generally, we suggest that the Hh-cilia signaling mechanism represents a robust molecular candidate for flexible stem evolution of the cichlid jaw.

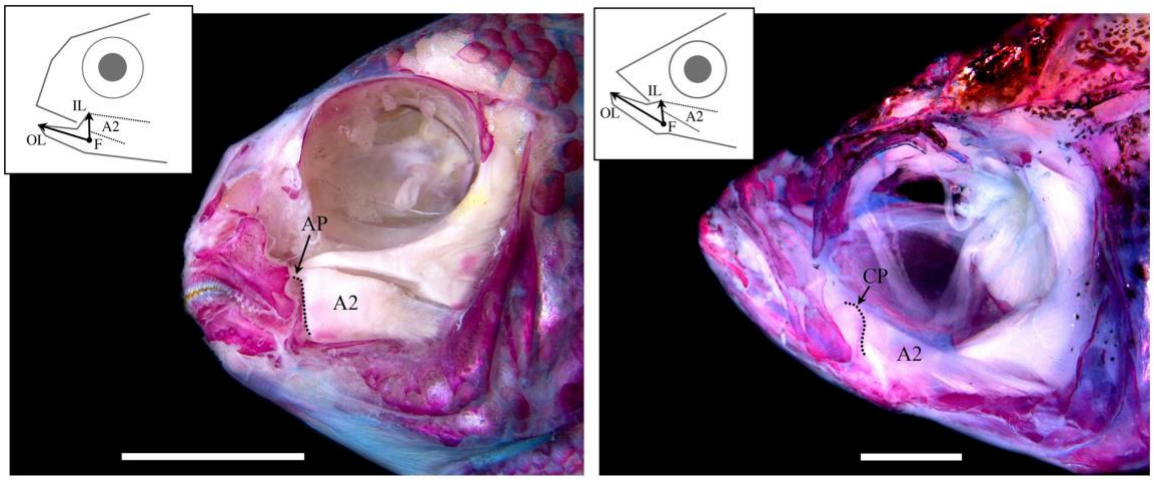

Figure 14: Functional anatomy of the cichlid and zebrafish head. A dissected and alizarin red stained head of a representative cichlid, Tropheops sp. “red cheek”, is depicted at left, and a zebrafish is shown at right. Craniofacial bones are red, and muscles are white. The lever mechanism that defines the mechanical advantage of jaw closing is illustrated for each species, whereby the jaw joint acts as the fulcrum (F), jaw length is the out-lever (OL), and a dorsally projecting bony process, on which the second subunit of the adductor mandibulae (A2) inserts, acts as the in-lever (IL). In cichlids, the in-lever is the ascending arm of the articular (AP), whereas in zebrafish it is the coronoid process (CP). Thus, in each species, this functional system is comprised of nonhomologous bony processes. Scale bar equals 1 cm in the cichlid image (left), and 1 mm in the zebrafish image (right).

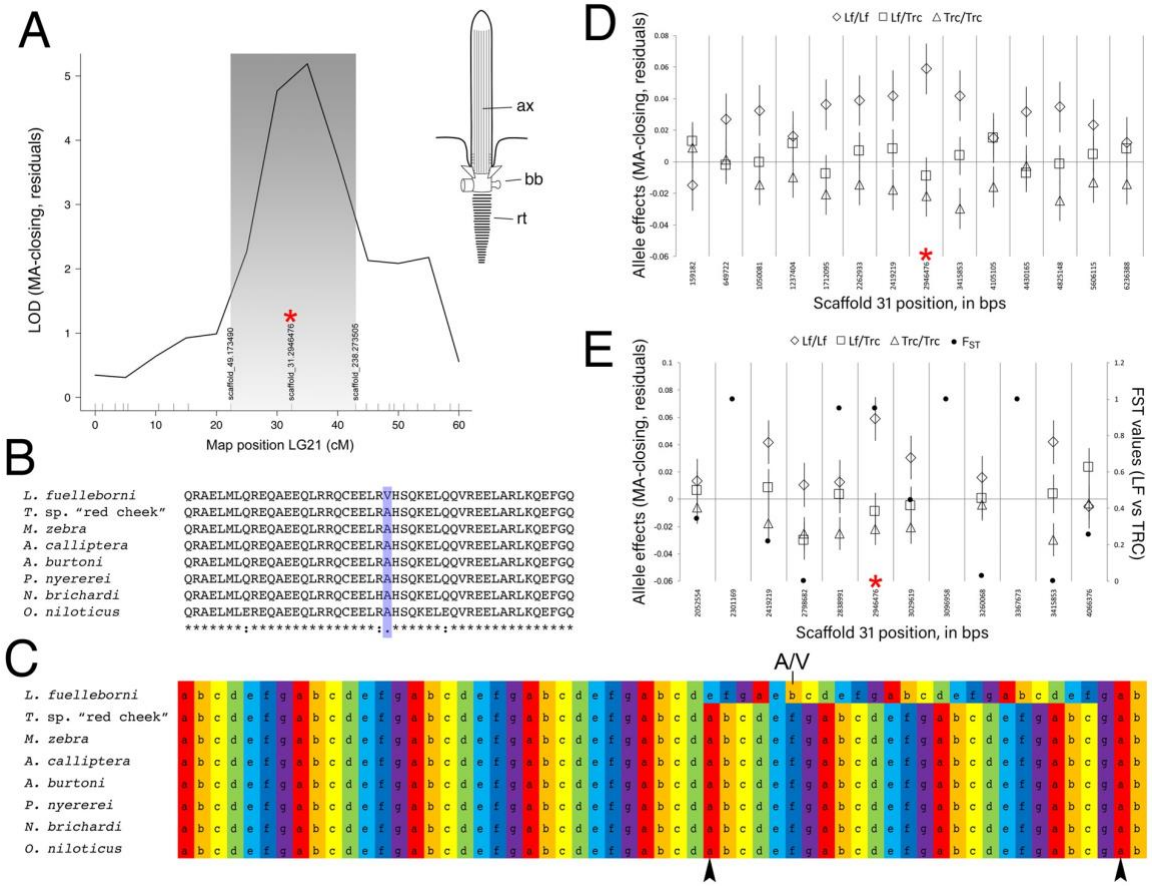

Figure 15: Mapping of lower jaw mechanical advantage in cichlids. The QTL for relative height of the articular process (i.e., mechanical advantage of jaw closing, "MA-closing") maps to LG21 and peaks over a marker on physical scaffold number 31 (A). A schematic of a primary cilium is shown in (A) as well, where "ax" is the axoneme, "bb" is the basal body, and "rt" illustrates the striated rootlet. The SNP at the QTL peak (red asterisk) encodes a nonsynonymous (A/V) polymorphism within Crocc2, where the A allele is conserved across African cichlids (B), and is associated with two predicted interruptions (arrowheads, C) in the heptad repeat (i.e., denoted, and color-coded, a–g). The V allele in LF is predicted to result in contiguous heptad repeats in this region of the protein (C). With additional markers every ~0.5 Mb, we queried the phenotype–genotype relationship along scaffold 31, and show that the peak association remains at ~2.9 Mb (red asterisk, D). We sought to refine the interval even further using markers every ~100-200 kb, between ~2–4 Mb on scaffold 31, and find that the peak association holds at the crocc2 SNP (red asterisk, D). Further, this marker is nearly alternatively fixed between - wild populations of LF and TRC (e.g., FST = 9.5).

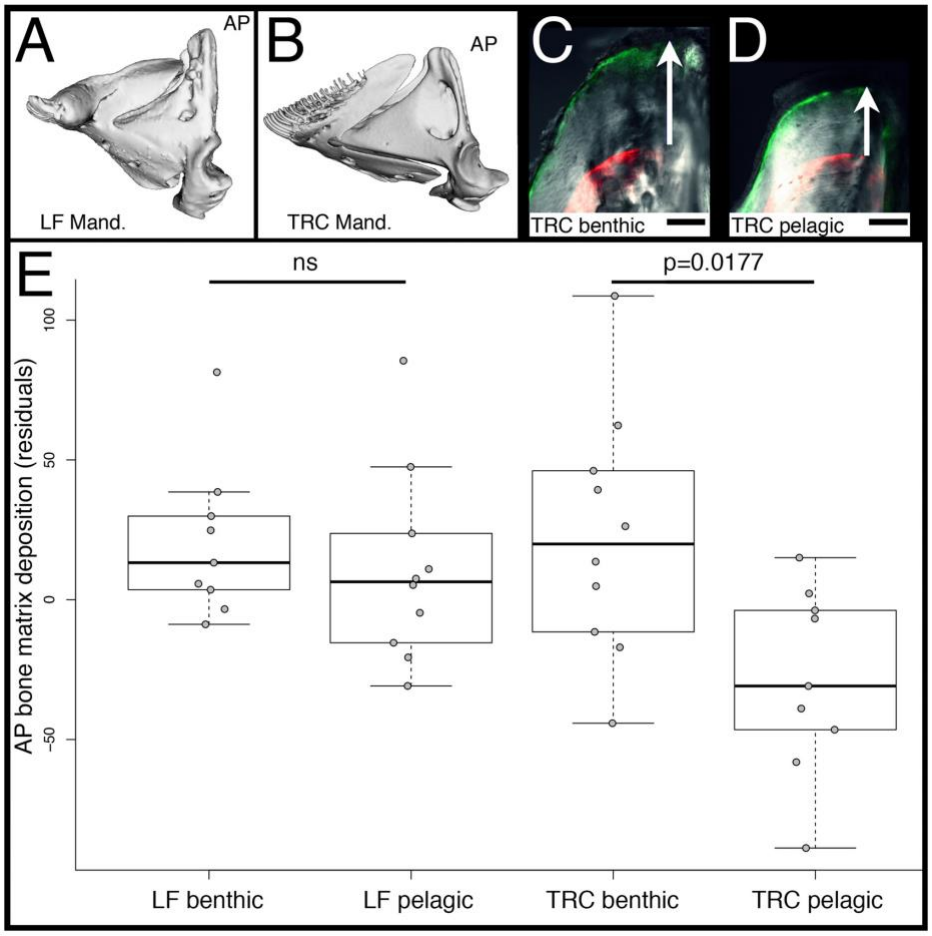

Figure 16: Rates of bone matrix deposition in cichlids. Mandibles of LF (A) and TRC (B) are shown, and the ascending arm of the articular bone (AP) is labeled. The tip of the AP in TRC reared in either a benthic/biting (C) and pelagic/sucking (D) environment is shown. Panels (C and D) are overlays of bright field, GFP, and RFP illumination. The RFP filter shows where alizarin red was incorporated into the bone. GFP is the calcein green label 5 weeks later. The distance between labels (white arrows) represents the amount of matrix deposited during that time. Scale bars equal 50 μm. Quantification of the rates of bone matrix deposition are shown in (E). Significance was determined via an ANOVA followed by a Tukey's multiple comparison test.

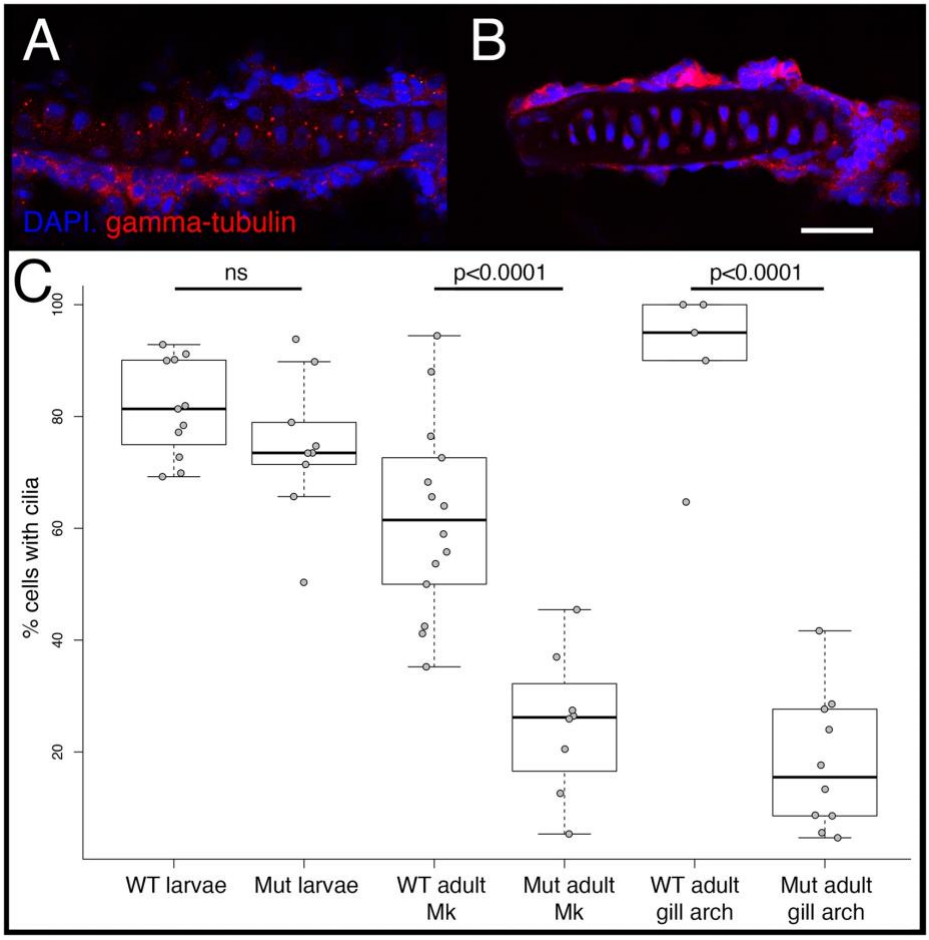

Figure 17: Cilia number in WT and mutant zebrafish. Cilia were visualized via immunohistochemistry using either anti-gamma-tubulin (shown), which labels the basal bodies, or anti-alpha acetylated-tubulin (not shown), which labels the axoneme, and imaged via confocal microscopy. Representative images are shown for the gill arch cartilage in WT (A) and full-sibling crooc2 mutants (B). Scale bar equals 20 μm. Quantification of cilia number per cartilage, calculated as the percentage of nondividing cells containing cilia, is shown in (C). Significance was determined via an ANOVA followed by a Tukey's multiple comparison test. In larval (4dpf) fish, each data point represents a count from a different cartilage across n = 3 WT and n = 3 crocc2 mutant animals. In adults (>12 months), data points represent counts from different sections of Meckel's cartilage (i.e., Mk), or from different gill arch cartilages. Sample sizes for adults are also n = 3 for each genotype.

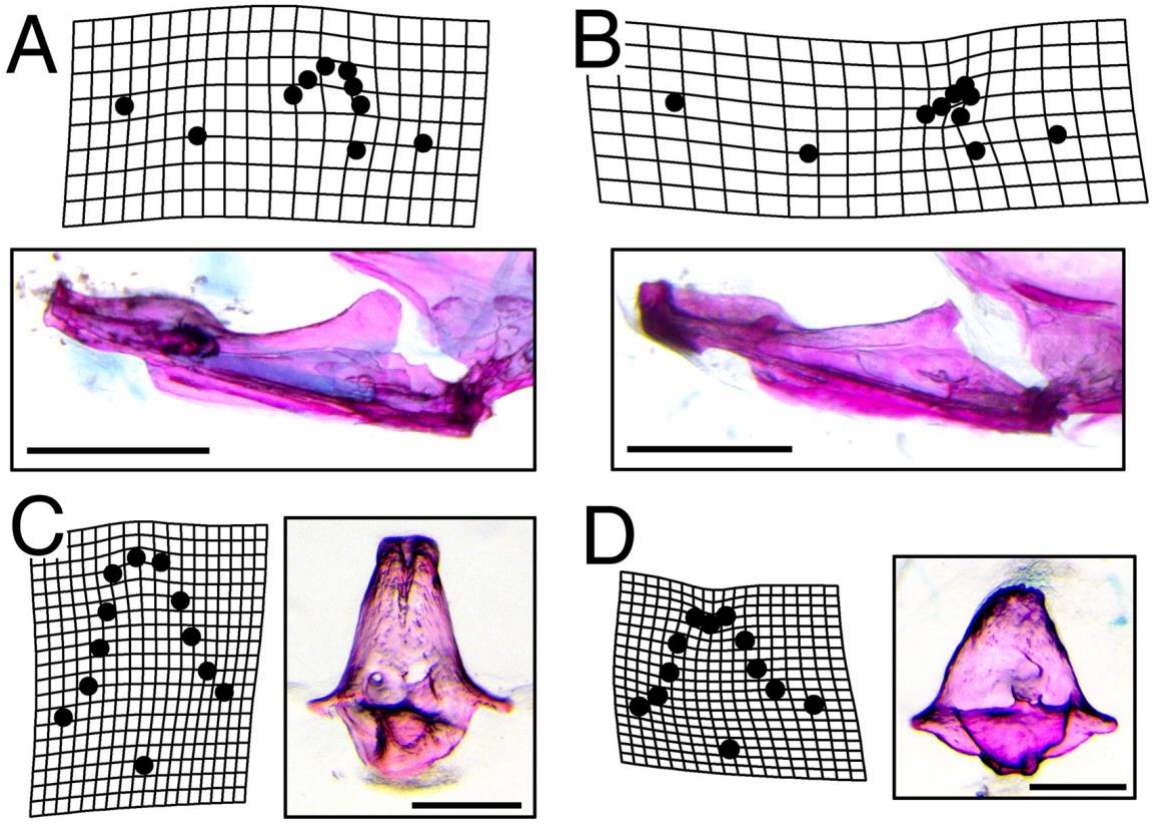

Figure 18: Dysmorphic bone geometry in crocc2 mutants. A geometric morphometric shape analysis was performed on various element of the feeding apparatus in WT and crocc2 mutant fish. Mutants exhibit distinct mandible shapes compared to WT siblings, with the most conspicuous differences occurring in the size and shape of the coronoid process (B vs. A). Scale bars in (A) and (B) equal 1 mm. Shape differences were also noted for the kinethmoid, with mutants exhibiting an overall shortening of the element in the dorsal–ventral dimension (D vs. C). Scale bars in (C) and (D) equal 200 μm. Deformation grids represent commonly seen phenotypes in the mandible, and exaggerated mean shapes in the kinethmoid. Procrustes ANOVA with post-hoc pairwise comparisons of group means (procD.lm, advanced.procD.lm), was significant for mandible mean shapes at $P = 0.02$, and for kinethmoid means at $P = 0.12$.

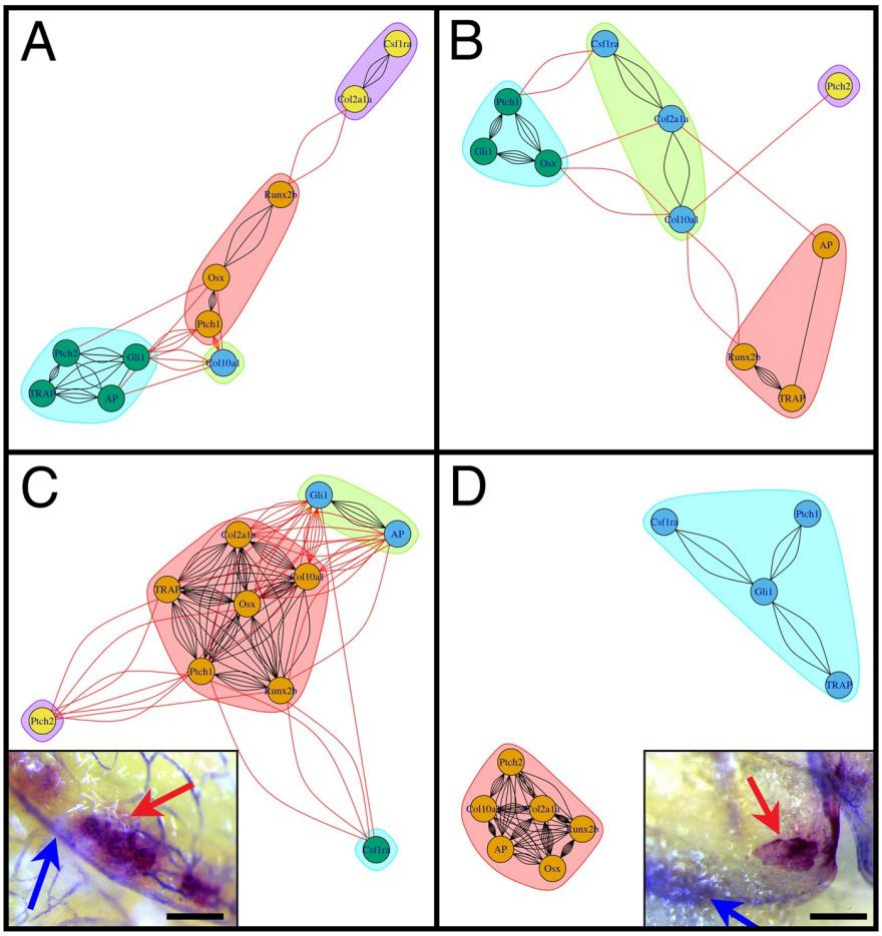

Figure 19: Mis-regulation of the bone marker gene expression in crocc2 mutants. Network output of partial correlations (from Table 5). Red lines represent correlations between genes in different modules, whereas black lines represent correlations within modules. Colors denote distinct modules in each analysis. Panel (A) illustrates the interaction between bone marker expression in WT animals at the young adult stage (3–5 months), whereas panel (B) shows data for comparably staged mutants. Note that, although there are a greater number of correlations in WT versus crocc2 mutant animals, both networks are characterized by four interconnected modules. Covariation of gene expression in old adult (10–15 months) bone is shown for WT (C) and mutant (D) animals. WT zebrafish show a relatively high number of correlations both within and between modules, consistent with a tightly integrated gene network. Alternatively, mutants show a dissociated pattern characterized by two distinct modules, which is reflected in in vivo patterns of bone cell activity (insets, C and D). In WT bone (i.e., interopercle), TRAP and AP are generally in close approximation, whereas in mutants these factors are often expressed in distinct areas of the bone. Scale bars equal 200 µm.

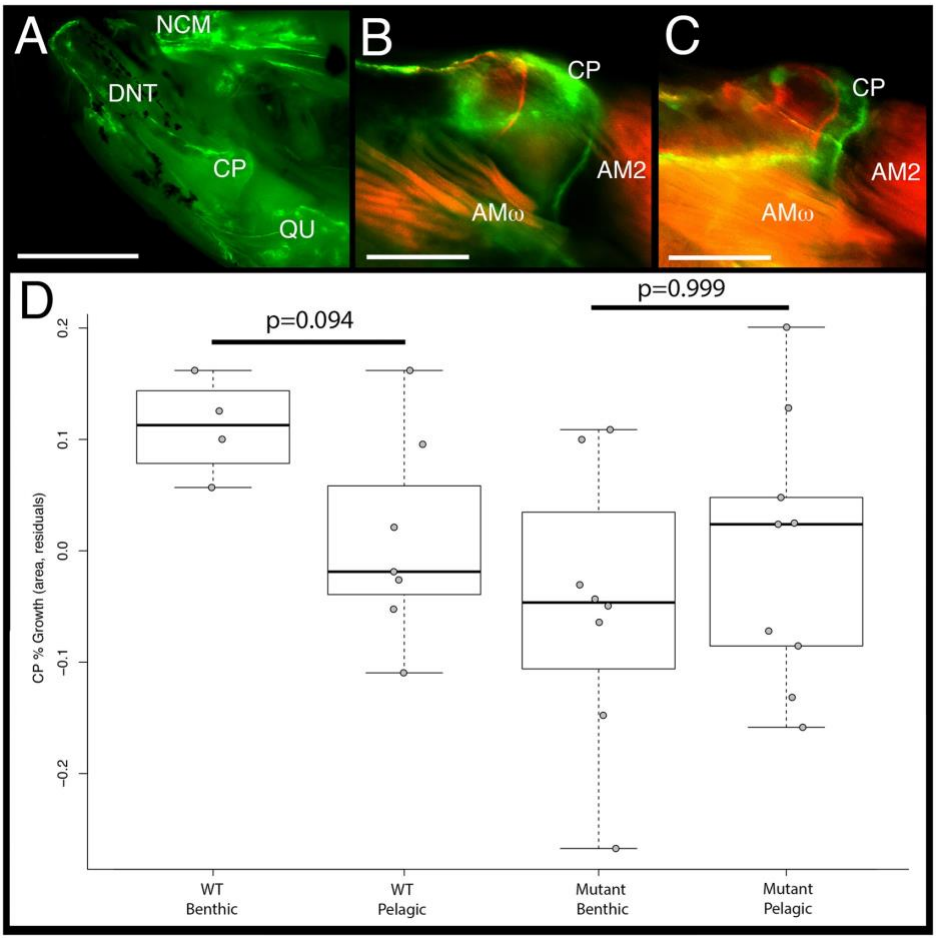

Figure 20: Rates of bone matrix deposition do not respond to environmental stimuli in crocc2 mutants. Bone deposition rate was measured as the ratio between the area of the coronoid process (CP) at time 0 (red label) over the area at time 1 (green label) in WT and crocc2 mutant zebrafish reared under alternate foraging regimes. Panel (A) shows the medial view of the oral jaw skeleton, under GFP illumination, depicting the anterior neurocranium (NCM), dentary (DNT), CP, and quadrate (QU). Scale bar for (A) equals 1 mm. Panel (B) depicts a composite image of red and green fluorochromes in the CP of a WT animal, whereas panel (C) shows the CP of a crocc2 mutant. Two subdivisions of the adductor mandiblae can be seen in (B and C)—AM2 and AMω. Scale bars in (B) and (C) equal 200 μm. Panel (D) presents the results of a comparison of bone deposition rates. Pairwise significance was assessed via an ANOVA followed by a Tukey's multiple comparison test.

Table 4: Expression differences of bone marker genes.

Osteoblast markers:	***Runx2b***		***Osx***		***AP***	
	F-value	**P-value**	**F-value**	**P-value**	**F-value**	**P-value**
Genotype	5.982	0.0163	2.796	0.0982	5.994	0.01621
Age	*31.757*	*1.78E-07*	3.23	0.0759	*11.466*	*0.00104*
GxA	*22.254*	*8.20E-06*	0.908	0.3435	*10.043*	*0.00206*
Osteoclast markers:	*Csf1ra*		*TRAP*			
	F-value	P-value	F-value	P-value		
Genotype	2.824	0.097185	1.567	0.214		
Age	*13.951*	*3.73E-04*	2.589	0.111		
GxA	1.557	0.216196	0.381	0.539		
Chondroblast markers:	*Col10a1**		*Col2a1a*			
	F-value	P-value	F-value	P-value		
Genotype	3.986	0.048744	0.045	0.8317		
Age	*12.967*	*5.06E-04*	4.929	0.0291		
GxA	0.009	0.925719	0.217	0.6424		
Hedgehog markers:	*Ptch1*		*Ptch2*		*Gli*	
	F-value	P-value	F-value	P-value	F-value	P-value
Genotype	6.758	0.0111	*18.683*	*6.39E-05*	5.373	0.0233
Age	*6.351*	*1.37E-02*	*18.93*	*5.80E-05*	0.845	0.361
GxA	1.09	0.2996	4.324	0.0422	0.04	0.8415

Note.—Expression of genes involved in bone/cartilage development was assessed in WT and mutant animals at two life-history stages, young adult (3–5 months) and old adult (10–15 months). The ANOVA

model was (expression ~ genotype × age), and the effects of genotype, age, and their interaction are presented. Marker genes are organized by general function. *Col10a1* has an asterisk next to it, because it plays roles in both endochondral and dermal bone formation in fishes. Values with significance after Bonferroni-correction are italicized.

Table 5: Covariation in the expression of bone marker genes

Young WT Bone										
	runx2b	***col10a1***	***AP***	***TRAP***	***osx***	***ptch1***	***col2a1a***	***csf1ra***	***gli1***	***ptch2***
runx2b		0.413	0.637	0.757	*0.022*	0.480	0.080	0.869	0.830	0.343
col10a1	0.200		0.119	0.630	0.114	*0.003*	0.654	0.558	*0.040*	0.124
AP	−0.116	0.370		*0.004*	0.098	0.509	0.200	0.814	0.115	*0.040*
TRAP	0.076	−0.118	*−0.622*		0.356	0.649	0.922	0.426	*0.025*	*0.007*
osx	*0.523*	0.375	−0.391	−0.224		*0.002*	0.293	0.872	0.804	0.123
ptch1	−0.172	*−0.637*	0.161	−0.112	*0.659*		0.866	0.778	*0.005*	0.916
col2a1a	0.411	−0.110	0.308	0.024	−0.254	0.041		*0.009*	0.205	0.596
csf1ra	−0.041	0.143	0.058	0.194	0.040	0.069	*0.585*		0.310	0.395
gli1	0.053	*0.475*	0.374	*0.511*	−0.061	*0.612*	−0.305	0.246		*0.019*
ptch2	0.230	−0.365	*−0.476*	*−0.601*	−0.366	−0.026	−0.130	0.207	*0.531*	

Young Mutant Bone

	runx2b	*col10a1*	*AP*	*TRAP*	*osx*	*ptch1*	*col2a1a*	*csf1ra*	*gli1*	*ptch2*
runx2b		*0.026*	0.176	*0.000*	0.420	0.169	0.425	0.205	0.754	0.244
col10a1	*−0.474*		0.177	0.664	*0.030*	0.448	*0.052*	0.785	0.734	0.132
AP	0.299	0.299		0.145	0.482	0.913	0.123	0.304	0.161	0.597
TRAP	*0.746*	0.098	−0.322		0.860	0.307	0.822	0.158	0.910	0.727
osx	0.181	*0.462*	−0.158	−0.040		*0.002*	0.083	0.928	*0.000*	0.845
ptch1	0.304	0.171	−0.025	−0.228	*0.622*		0.251	0.060	*0.000*	0.736
col2a1a	0.179	*0.419*	0.339	−0.051	−0.378	−0.256		*0.015*	0.553	0.521
csf1ra	−0.281	0.062	−0.229	0.312	−0.020	0.407	*0.512*		0.452	0.537
gli1	−0.071	−0.077	−0.309	−0.026	*−0.702*	*0.768*	0.134	−0.169		0.657
ptch2	−0.259	−0.332	0.119	0.079	−0.044	0.076	−0.144	0.139	0.100	

Old WT Bone

	runx2b	*col10a1*	*AP*	*TRAP*	*osx*	*ptch1*	*col2a1a*	*csf1ra*	*gli1*	*ptch2*
runx2b		*0.028*	*0.051*	*0.008*	*0.001*	*0.000*	*0.013*	0.078	0.151	0.063
col10a1	*−0.549*		*0.007*	*0.001*	*0.000*	*0.005*	*0.000*	0.735	*0.000*	0.230
AP	*−0.496*	*−0.641*		0.175	*0.005*	0.229	*0.011*	0.182	*0.003*	0.630
TRAP	*−0.633*	*−0.735*	−0.357		*0.000*	*0.000*	*0.001*	0.195	*0.051*	*0.051*
osx	*0.752*	*0.832*	*0.664*	*0.904*		*0.002*	*0.000*	0.590	*0.004*	0.087
ptch1	*0.771*	*0.663*	0.319	*0.781*	*−0.708*		*0.000*	0.083	*0.049*	*0.037*
col2a1a	*0.606*	*0.867*	*0.618*	*0.768*	*−0.772*	*−0.775*		0.674	*0.005*	0.221
csf1ra	−0.453	0.092	0.351	−0.342	0.146	0.447	0.114		0.131	0.679
gli1	−0.376	*−0.873*	*−0.701*	*−0.496*	*0.681*	*0.499*	*0.664*	0.394		0.433
ptch2	−0.475	−0.318	−0.131	*−0.495*	0.441	*0.525*	0.324	−0.112	−0.211	

Old Mutant Bone										
	runx2b	*col10a1*	*AP*	*TRAP*	*osx*	*ptch1*	*col2a1a*	*csf1ra*	*gli1*	*ptch2*
runx2b		*0.025*	*0.011*	0.664	*0.000*	0.747	*0.000*	0.843	0.211	0.124
col10a1	*−0.699*		*0.000*	0.648	*0.025*	0.400	*0.005*	0.636	0.529	*0.006*
AP	*0.761*	*0.954*		0.498	*0.029*	0.740	*0.004*	0.586	0.298	*0.020*
TRAP	−0.157	−0.165	0.243		0.408	0.225	0.850	0.807	0.117	0.668
osx	*0.926*	*0.698*	*−0.685*	0.295		0.715	*0.000*	0.942	0.207	0.117
ptch1	0.117	0.300	−0.121	−0.422	−0.133		0.470	0.713	0.072	0.379
col2a1a	*0.967*	*0.807*	*−0.822*	0.069	*−0.915*	−0.259		0.674	0.343	*0.022*
csf1ra	−0.072	−0.172	0.197	0.089	0.027	−0.134	0.152		0.127	0.252
gli1	0.433	0.226	−0.366	0.528	−0.437	0.590	−0.336	0.516		0.824
ptch2	0.519	*0.795*	*−0.715*	−0.155	−0.528	−0.312	*−0.709*	0.400	−0.081	

Note.—Partial correlation coefficients (below diagonal) and *P* values (above diagonal) are shown for both genotypes at young (3–5 months) and old (10–15 months) stages. Values are italicized if significant at the ~0.05-level.

Figure S3: Sequence variation in Crocc2 across fishes. Amino acid sequence around the coding mutation identified in our genetic cross is highly conserved across African cichlids, but sequence homology begins to breakdown when other perciform and ray-finned fish species are included in the alignment (A-B). Notably, whereas all other African cichlids examined have an Alanine (A) at position 963, *Labeotropheus* has a Valine (V), which is similar to New World cichlids as well as most other perciform species. In fact, all perciforms possess either an A or V, and all fish species possess a non-polar, hydrophobic amino acid at this position (blue shade, B). While considerable sequence variation exists across this stretch of amino acids, the resulting coiled-coil motif

is largely conserved, especially toward the N-terminus (C). The V in *Labeotropheus* results in few interruptions (black arrowheads) in heptad repeats (i.e., a- g) compared to other African cichlids (C). This region of Crocc2 is also associated with greater predicted structural variation, which suggests that this portion of the protein may be less constrained, and/or a target of natural selection. All Crocc2 sequences were obtained from NCBI and the Ensembl genome browser.

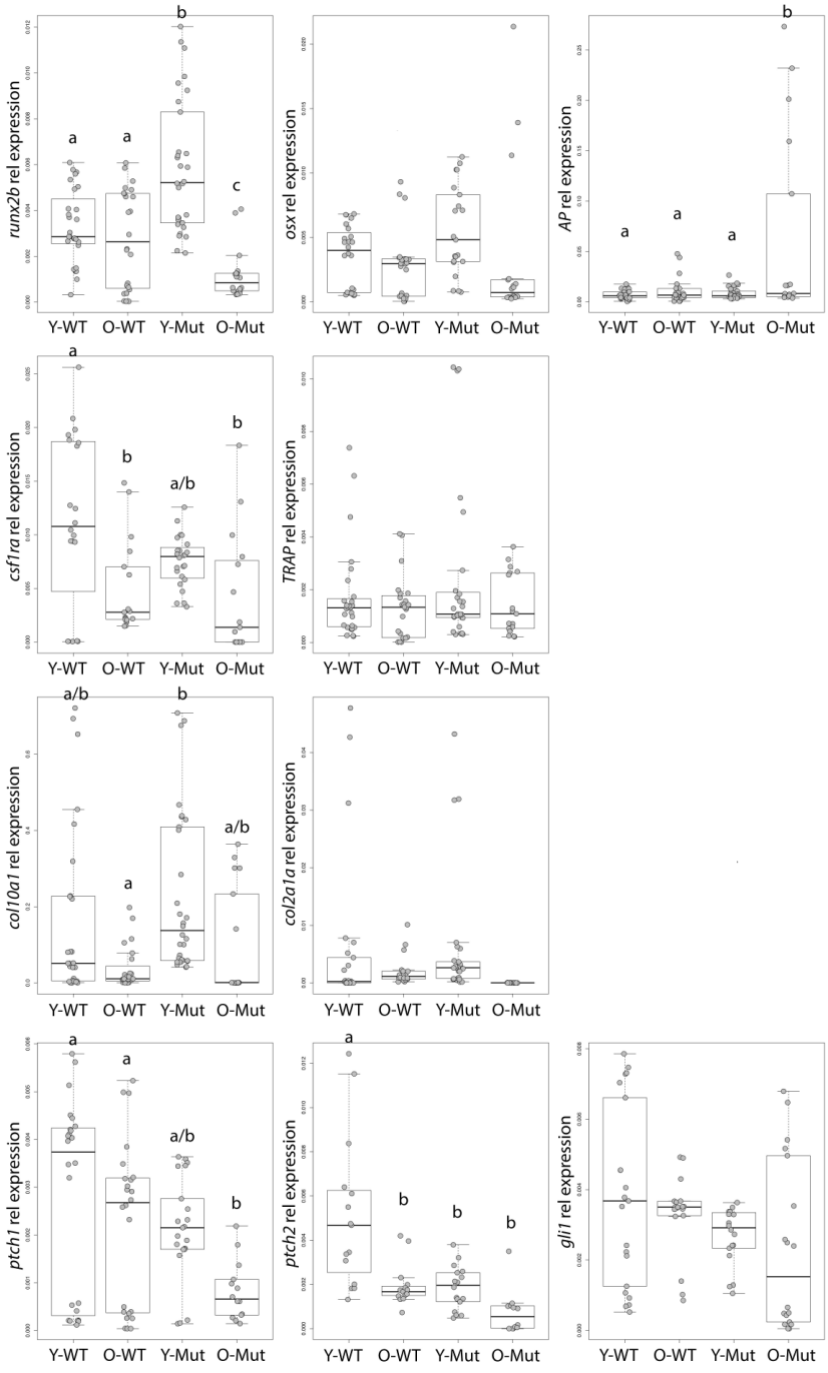

Figure S4: Expression results from bone marker genes. Full results are shown for quantitative RT-PCR, organized in the same pattern as Table 4. Relative expression levels are shown for young adult WT (Y-WT), old adult WT (O-WT), young adult *crocc2* mutants (Y-Mut), and old adult *crocc2* mutants (O-Mut). Letters above the box plots refer to statistical groupings as determined by ANOVA followed by a Tukey's multiple comparison test. Graphs with no letters, did not exhibit any significant pair-wise differences.

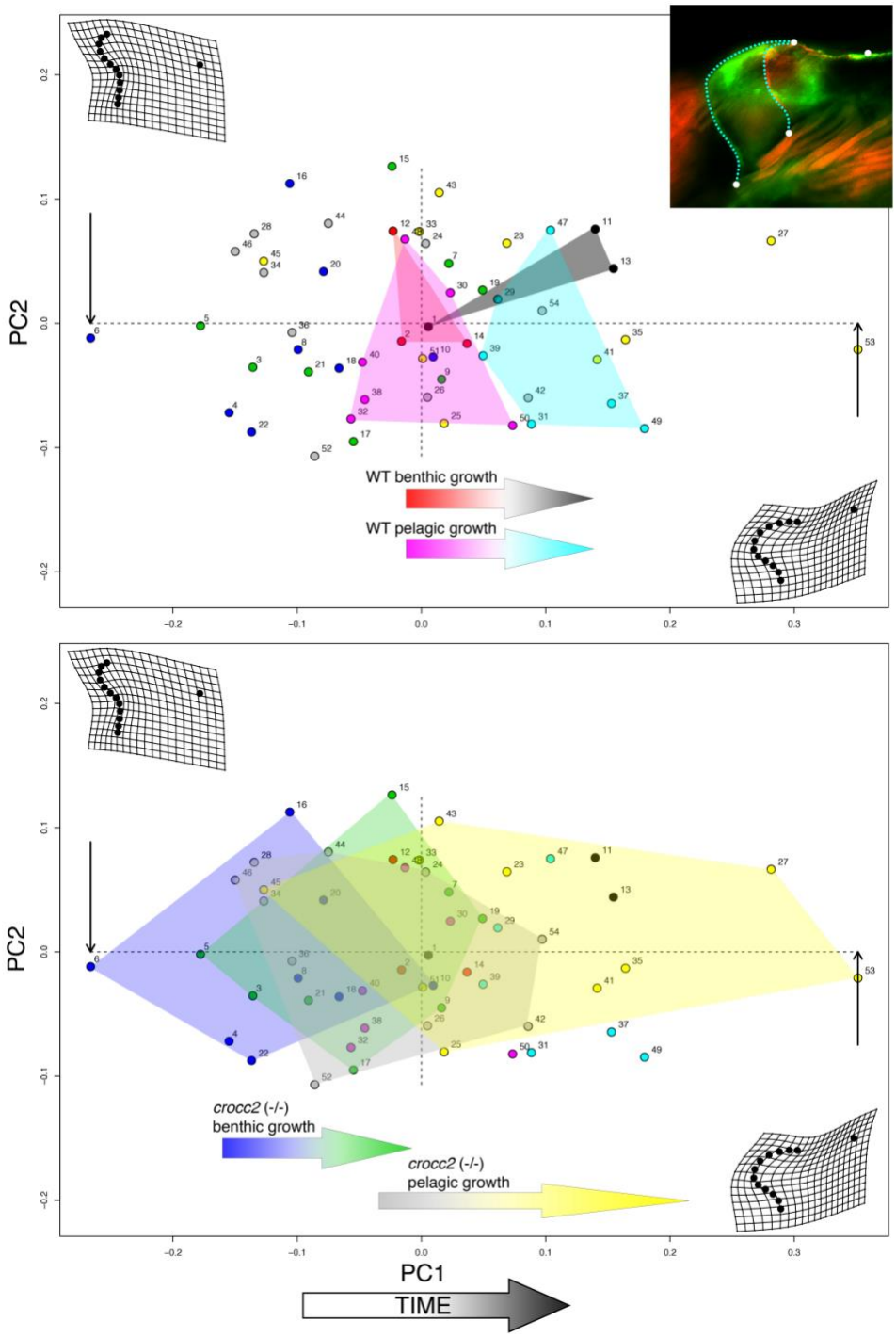

Figure S5: Shape analysis of the CP in *crocc2* and WT zebrafish across environments. Shape space from a morphometric analysis on CP shape. PC1 accounts for 63% of the variation, and mainly captures variation in growth over time, such that shape at time 0 (determined using the red fluorochrome, Alizarin Red) is associated with more negative PC1 scores, whereas shape at time 1 (green fluorochrome, Calcein Green) is associated with more positive PC1 scores. PC2 accounts for 17% of the variation in CP shape. The inset at top illustrates the digitizing scheme, with landmarks depicted as white

dots and semi-landmarks arrayed along the blue dotted line. Note that each animal is measured twice - once for T0 shape (red), and once for T1 shape (green). In shape space, T1 and T0 are numbered consecutively, such that samples 1 and 2 correspond to individual one at times 1 and 0, respectively.

Table S7: Primer sequences for zebrafish bone markers and the housekeeping gene, b-actin.

Danio rerio **qRT-PCR Primer Sets**	
Gene Name	**Sequence (5'-3)'**
Runx2b For	CAAACACCCAGACCCTCACT
Runx2b Rev	GTATGACCATGGTGGGGAAG
Osx For	GCGTCGATTCTGGAGGAG
Osx Rev	AATCTCGGACTGGACTGGTG
AP For	CAGTGGGAATCGTCACAACAA
AP Rev	CAACACAGTGGGCATAAGCA
Csf1ra For	GGCCAGCATAAGAACATCGT
Csf1ra Rev	CGTCATGGGTTCTGGAAAGT
TRAP For	CGTCCACTGACCACAGGAAGA
TRAP Rev	AAGGATCCTGACGTCTGATTGA
Col10a1 For	CCTGTCTGGCTCATACCACA
Col10a1 Rev	AAGGCCACCAGGAGAAGAAG
Col2a1a For	ATCCCATCATTTCACCTGGA
Col2a1a Rev	TCTGTCCCTTTGCACCAAGT
Ptch1 For	GCCGCATCCCAGGCCAACAT
Ptch1 Rev	CGTCTCGCGAAGCCCGTTGA
Ptch2 For	CATCCCATTCAAGGAGAGGA
Ptch2 Rev	GGCAGGGAATATCAGCAAAA
Gli1 For	GTCATCCGCACCTCTCCAAA
Gli1 Rev	ATGGTGCCCACAGACAGATG
B-Actin For	CAACAGGGAAAAGATGACACAGAT
B-Actin Rev	CAGCCTGGATGGCAACGT

CHAPTER V

GNMT AS A CANDIDATE FOR CICHLID SPECIES CRANIOFACIAL SHAPE DIFFERENCES

Tetrault, E.R., & Albertson, R.C.

Introduction

Getting to the genomic regulation of species shape differences is important in understanding the molecular basis of adaptations. Malawi cichlids are a hyperdiverse family of fishes, with variation in body size and depth, coloration, brooding style, among other things, due to the rapid speciation rates in Lake Malawi (Streelman et al., 2003; Navon et al., 2017; Roberts et al., 2017; Albertson et al., 2018; Marconi et al., 2023). Though extensive, much of the variation in this group is centered along the benthic-pelagic axis, and these fish have adapted their craniofacial profiles and jaws to feed efficiently along this axis. Benthic fishes feed by scraping algae off of rocks, with short jaws typically downturned with tricuspid teeth, and a steep, rounded sloped head (Westneat, 1991; Streelman et al., 2003), adapted for power. On the opposite end of this axis, pelagic foragers have longer jaws that are upturned, and fewer rows of bicuspid teeth, optimal for suction feeding from the water column (Westneat, 1991; Streelman et al., 2003). We previously described a large number of genes involved in the differences in cichlid species' craniofacial bones by using a combination of RNA-seq and ATAC-seq data to understand with more confidence a suite of factors that have expression differences (i.e differentially expressed and differentially accessible) between species in a given environment (Tetrault et al., 2023). While subsets of genes were identified where expression differences were specific to a particular foraging environment, another subset included 13 genes that were differentially expressed in both the benthic and pelagic

foraging environment. In other words, the effects of these genes appeared to be robust to the environment, an assertion that we validated in chapter 3 using qPCR. We consider these factors to be promising candidates in regulating species-specific bone shapes.

In the context of my dissertation, it was not plausible to follow-up on all 13, and so we sought to prioritize this list. We first looked to see which of these factors were in the top-100 (out of over 5000) differentially expressed genes. This reduced the number to 6, including *b3galt1*, *b3galt2*, *fam3c*, *thx*, *tnfrsf6b*, and *gnmt*. We then cross-referenced these to other genetic and genomic datasets. Multiple previous QTL analyses repeatedly implicate an interval on linkage group 19 (LG19) as an important regulator of lower jaw shape, specifically global shape of the jaw, the height of the RA, and the mechanical advantage of jaw opening (Albertson et al., 2003; 2005; Figure 21a). In addition, both morphological integration and modularity of the lower jaw are associated with LG19 (Parsons et al., 2012; Hu et al., 2014). In addition, population branch statistic (PBS) measurements, which uses genome-wide pairwise FST values among three populations (in this case three cichlid species) to determine whether one allele appears more frequently in one population than another, suggests that LG19 contains a divergent allele in *Maylandia* (Figure 21b). Together, these data implicate LG19 as a hotspot for the regulation of traits associated with the lower jaw, especially the RA. These multiple datasets accumulated over 20 years point to *glycine N-methyltransferase* (*gnmt*), which lies near all QTL and PBS data on LG19, as a top candidate to look into.

Expression levels from RNA-seq libraries indicated that the generalist species, *Maylandia*, had higher *gnmt* levels compared to *Tropheops*, a benthic generalist (Figure 21c). A separate experiment looking at expression dynamics over time supports the

genome-wide data, with higher expression in *Maylandia* at multiple timepoints following the onset of foraging trials (Figure 21c).

Gnmt encodes a methyltransferase in the methionine cycle (Figure 22a), which involves a series of reactions important to many biological processes, but particularly for our purposes DNA methylation (Zhang, 2018) and bone metabolism (Vijayan et al., 2014; Plummer et al., 2016). In this cycle, the adenosyl group from ATP is transferred to methionine, forming S-adenosylmethionine (SAM). Methyltransferases, such as *gnmt*, then catalyze the removal of the methyl group from SAM, leading to the formation of S-adenosylhomocysteine (SAH) (Luka et al., 2009). S-adenosyl-L-homocysteine hydrolase (SAHH) converts SAH to homocysteine, which is further transformed to methionine to restart the methionine cycle.

The ratio of SAM to SAH is considered the methylation index, with a high ratio leading to hypermethylation, and a low ratio suggesting hypomethylation. Research suggests that changes to the SAM/SAH ratio and resulting changes in methylation are typically underlain by levels of SAH (reviewed in Zhang, 2018), due to SAH being a potent methylation inhibitor. However, methylation and SAM/SAH ratios are largely tissue-specific (Chen et al., 2010). *Gnmt* transgenic *Drosophila*, in which *gnmt* expression is elevated, produced animals with low levels of SAM, high concentrations of SAH, and a low methylation index (Obata et al., 2014). In cellular models, high *gnmt* also leads to decreased SAM, as well as lower cell viability and cell number (Huidobro et al., 2013). Methionine supplementation in rats is correlated with Gnmt protein levels and activity, as well as increases in the concentrations of both SAM and SAH (Rowling et al., 2002). High *gnmt* expression is associated with high levels of DNA methylation in

developing zebrafish (Fang et al., 2013). While methionine is linked to methylation via the pool of available SAM and SAH, it also has been shown to elicit other epigenetic changes, such as increasing the expression of miRNAs (Plummer et al., 2017). However, how methionine affects methylation is age- and tissue-dependent, and gene-specific (Tremolizzo et al., 2002; Sanchez-Roman et al., 2011; Mattocks et al., 2017).

Methionine also plays important roles in bone morphology, density, and bone cell differentiation. For example, methionine restricted mice present with low bone mass (Ables et al., 2012), decreased bone mineral content and bone size (Ouattara et al., 2016), and reduced expression of bone cell differentiation and activity genes (Ouattara et al., 2016; Plummer et al., 2016). Conversely, methionine supplementation increases bone density, presumably via a decrease in bone resorbing cell markers and activity in rats (Vijayan et al., 2014). It is thought that this increase in bone works through downregulation of the TLR4/NF-kB signaling pathway in osteoclast precursor cells (Vijayan et al., 2014), which is involved in cell survival and proliferation.

Based on previous data, as well as known roles for *gnmt* in methylation and the methionine cycle, we prioritized this gene for future study. As a first step, we performed a SAM & SAH ELISA to determine whether measures differ between species.

Materials and Methods

Species and treatment

Cichlids were housed at equal density in 40-gallon glass aquaria on a 14hour/10hour light/dark cycle at 28°C and fed a flake food diet (75% algae, 25% yolk) until the onset of an experiment. When animals were of similar size in one tank (3-4 cm),

they were given a pelagic-like diet for 2 weeks, consisting of finely ground flake food and supplemented with live brine shrimp.

SAM/SAH assay

We assessed levels of SAM/SAH, the relative concentrations of which give us the methylation index of a sample, using the SAM and SAH ELISA combo kit (Cell Biolabs, Inc). The IOP-RA complex and liver were dissected from each *Maylandia* (n=9,5), and *Tropheops* (n=3, IOP-RA only). Tissues were homogenized in 1X PBS using a dounce homogenizer and stored at -80°C until assay preparation. Briefly, SAM and SAH conjugates were added to a 96-well protein-binding plate to and stored overnight, covered, at 4°C to allow for binding. All wells were washed 3x with PBS the following day. Homogenized samples and anti-SAM or anti-SAH antibodies were added to the corresponding wells for 1 hour at room temperature. Wells were washed 3x with wash buffer, incubated with a secondary antibody for 1 hour at room temperature, and washed again 3x with wash buffer. Substrate solution was then added and left to develop for 2-30 minutes. When color change was apparent across all wells, stop solution was added to stop the reaction. Absorbance measurements were immediately taken at 450nm in a plate reader. As this is a competitive binding assay, in which the antibodies preferentially binds SAM and SAH in tissue samples, which gets washed away, compared to the corresponding conjugate that is bound to the plates, higher absorbance readings are indicative of a lower concentration of SAM or SAH.

Results

SAM/SAH levels are tissue dependent

We assayed protein levels of SAM and SAH in both the IOP-RA complex and the liver in *Maylandia*, as the IOP-RA is a tissue of interest, and the liver is where much data on SAM and SAH are collected. For *Tropheops*, we were only able to obtain values for the IOP-RA, and had only 3 individuals.

Only [SAH] showed significant differences between tissues in *Maylandia* (Figure 22b,c). However, levels of both SAM and SAH in the IOP-RA complex were lower than what was confidently detectable given kit parameters. In addition, we had a low sample size and high degrees of variation between individuals, particularly in *Tropheops*. This, coupled with the sensitivity of the ELISA, makes it difficult to determine whether what we see is biologically relevant or an artifact of the assay itself, and therefore, solid conclusions cannot be made about levels of SAM and SAH in this complex.

Discussion

Concentrations of both SAM and SAH were very low in the tissues we were interested in and difficult to detect with the parameters set by the kit. Higher levels were obtained in the liver due to the abundant literature in this tissue, but we thought it best to go with a tissue-specific approach. For this to be successful, both IOP-RA complexes from one or more animals would need to be pooled together to generate a high enough concentration for detection. However, this may not be the best way to go about assessing methylation. Besides the experimental issues faced with the SAM/SAH ELISA, SAM and SAH levels are an indication of the pool of methyl groups available to be used for methylation. While much previous research links the ratio of these proteins to DNA

methylation, there is no evidence that this is the only type of methylation affected (e.g histone methylation). Further experiments should focus on luminometric methylation assay (LUMA). This assay uses methylation sensitive and insensitive restriction enzymes for DNA cleavage and pyrosequencing for quantification of genome-wide DNA methylation. LUMA gives a more accurate measurement of methylation than the SAM/SAH ELISA. However, given that methylation data can conflict between global levels and specific sites (Tremolizzo et al., 2002; Sanchez-Roman et al., 2011; Mattocks et al., 2017), then it may not be a matter of levels of global methylation, but perhaps the regions being methylated are different. In that case, reduced representation bisulfite sequencing (RRBS), or whole-genome bisulfite sequencing (WGBS), could be used to determine areas of high methylation. This assay couples bisulfite treatment, which converts unmethylated, but not unmethylated cytosines to uracils, and sequencing to map methylation across the genome.

While *gnmt* is responsible for the conversion of SAM to SAH and in turn methylation, it is part of the more broad methionine cycle. The methionine cycle has implications in bone deposition, density, and size. We did try a fluorometric methionine quantification assay (Abcam, ab234041) using both IOP-RA complexes from each animal, however methionine levels were undetectable. Upon trouble-shooting, we found the manufacturer of the methionine kit recommends a large amount of starting material (i.e 10^6 cells). Previous experiments using ATAC-seq (Tetrault et al., 2023) in which we quantified the number of cells in each IOP-RA complex to be at an average of $6.5x10^4$ for juvenile cichlids of the size used in this experiment. A single biological replicate would

then need to be pooled from both the left and right complex from a number of individuals in order to get a detectable signal indicating presence of methionine.

A cichlid *gnmt* transgenic model would be a fruitful line of study to really understand the effects of *gnmt* on species shape differences, more specifically those linked to DNA methylation signatures and bone homeostasis. A CRISPR knockout model could be made using a gRNA that introduces a premature stop codon, specifically in a *Maylandia* species, as there was higher expression of *gnmt* compared to *Tropheops* (Figure 21c) and QTL analyses implicating LG19 were from hybrids of a *Maylandia* and *Labeotropheus* cross. Lower levels of *gnmt* from the knockout model would presumably give a more benthic shape phenotype (like *Tropheops* or *Labeotropheus*). From there, we could assess the molecular regulation of shape differences, using LUMA to determine genome-wide methylation levels, WGBS for identifying specific sites of methylation, and qPCR to assess downstream RNA targets of any major pathways.

Instead of looking at methionine levels in different species, we could dose pelagic and benthic diets with differing concentrations of methionine and observe bone growth over time, looking at a combination of methionine manipulation and mechanical loading on bone shape and homeostasis. As methionine treatment increases bone density and decreases bone resorption activity (Vijayan et al., 2014), and restriction decreases transcription of bone depositing cell markers (Plummer et al., 2016), we would expect an increase in bone deposition and the cells responsible for this process, as well as increased transcription of major bone-positive genes. With restriction, we would intend on seeing the opposite: a higher number of osteoclasts (or at least fewer osteoblasts), and high bone resorption markers and activity. Whether this is methylation-dependent could be

determined via site-specific assays, like RRBS, which gives information about specific promoters that are methylated.

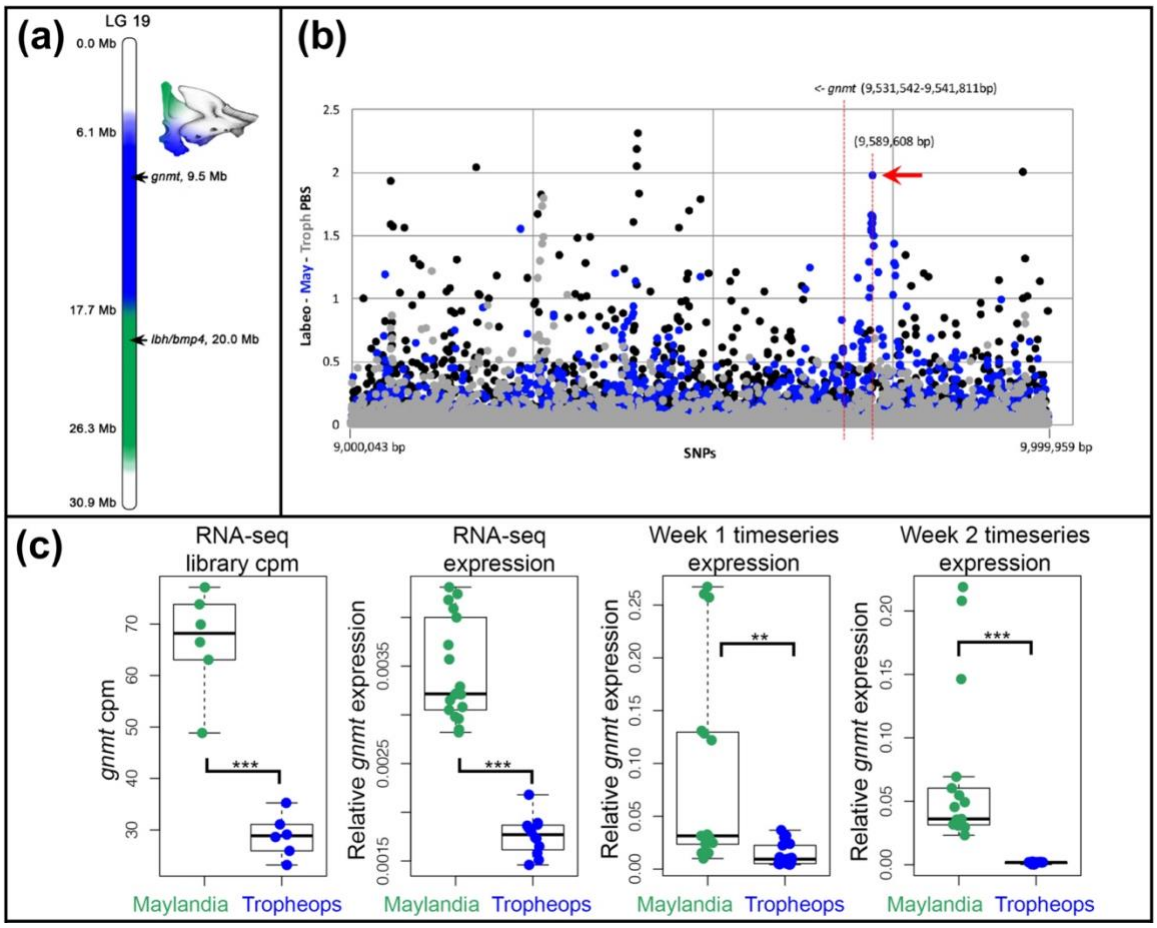

Figure 21: *Gnmt* has been implicated as important for species differences in multiple separate experiments. (a) Multiple QTL on linkage group 19, containing *gnmt*, was found for the retroarticular process, which is a part of the same tissues used in experiments from panel (c). (b) PBS analysis also suggests there is an SNP right upstream of *gnmt* in *Maylandia*, compared to both *Tropheops* and *Labeotropheus*. (c) *Gnmt* was upregulated in *Maylandia* compared to *Tropheops* in RNA-seq experiments (first panel), validated in the same tissue in the same species (second panel), and in both weeks 1 and 2 in the timeseries experiments (third and last panels, respectively. Tissues from these experiments are partially composed of the same area of tissue as panel (a).

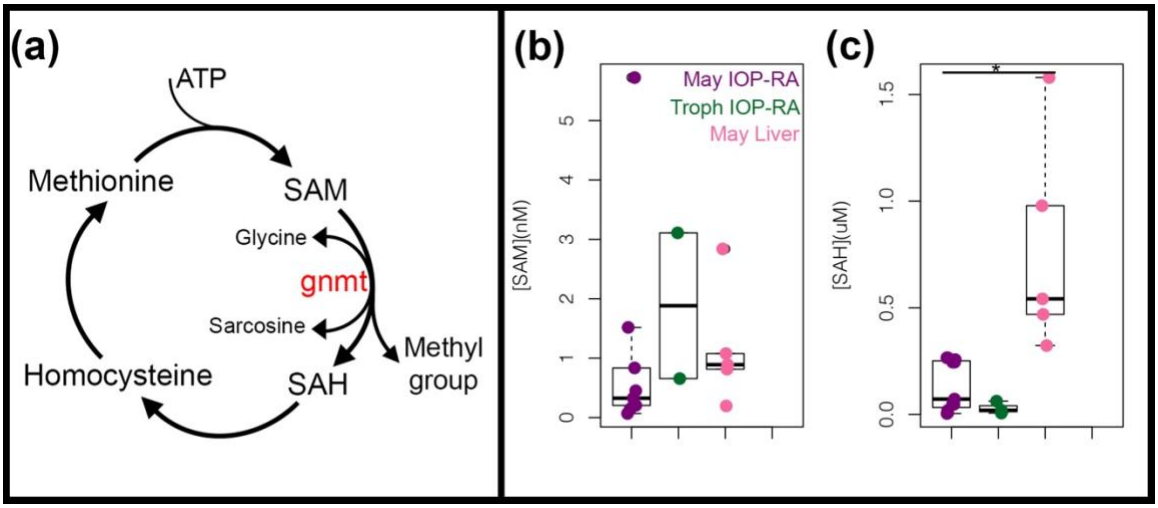

Figure 22: The methionine cycle and SAM/SAH levels in different tissues. (a) The methionine cycle. ATP is transferred to methionine forming SAM. *Gnmt* converts SAM to SAH by removing a methyl group. Levels of (b) SAM, and (C) SAH protein expression in *Maylandia* IOP-RA complex (purple) and liver (pink), and *Tropheops* IOP-RA (green).

CHAPTER VI

GENERAL CONCLUSIONS

HH signaling as a predictor of plasticity

HH signaling localizes to the primary cilium, and high HH signaling can be attributed to high levels of mechanosensing. Lack of HH signaling wipes out the plastic response from alternate foraging treatments in a manner similar to species that are not inherently plastic, like *Labeotropheus* (Navon et al., 2020). It is possible that the primary cilium in some species triggers HH signaling but does not in others, and that HH signaling sensitizes bone cells to respond to mechanical inputs. Compared to other cichlid species, such as the plastic species *Maylandia*, the *Labeotropheus* allele of the *crocc2* gene is associated with constant high levels of bone deposition. The predicted reestablishment of the heptad repeat of the *crocc2* allele in *Labeotropheus* may create a stronger rootlet structure of the primary cilium leading to the high bone deposition rates regardless of environmental input, compared to the ancestral allele which allows for a plastic response dependent upon the mechanical stimulus. This is supported by the consistently low levels of HH-related genes (*KIAA0586*, *ptch1*) in *Labeotropheus* across multiple timepoints paneled in this dissertation, compared to *Maylandia* and *Tropheops*. Given the intimate connection between HH signaling and cell cycle/proliferation, and supported by the work of this dissertation, it is likely that cell proliferation is one mechanism by which the increased bone deposition occurs. Taken together, HH signaling can be a relatively confident predictor of the plastic potential of a species.

Cell cycle and methylation in plasticity and species shape differences

While data on the specific mechanisms by which more bone is created in cichlid plasticity is not available at this time, given the work in this dissertation, it is reasonable to assume that cell proliferation and/or cell differentiation are part of the cause. At least in *Maylandia*, cell cycle is prominently implicated in the plastic response, particularly in the pelagic environment. Because progression through the cell cycle is required for cell division and therefore proliferation, it is likely that proliferation of progenitor cells is responsible for the increased bone deposition in this species. This is apparent given the specific genes found in the analysis directly related to cell proliferation (e.g. *ccna2*, *cdca5*). However, more work testing this directly is needed to make a solid conclusion, such as *in vivo* EdU labeling to assess cell populations that are actively proliferating.

Besides plasticity, we found evidence of the genetic regulation of species differences. It is likely that species shape variation, at least in specific craniofacial bones that are sensitive to mechanical input, in part come from transcriptional differences in levels of cell-cycle related genes, and/or regulation of methylated DNA. Multiple analysis suggest cell cycle is important for *Maylandia* shape compared to *Tropheops*, regardless of the environment of rearing, whereas cell differentiation was implicated in *Tropheops* shape under the same conditions. It is possible that different species use different mechanisms of increasing bone cell number/type, which would be an interesting future direction to parse out.

In addition to cell cycle, epigenetic mechanisms such as DNA methylation were implicated in species shape differences. *Gnmt*, a methyl transferase, was found to be differentially expressed and accessible between *Tropheops* and *Maylandia* in both

benthic and pelagic foraging environments. This was supported in further experiments at multiple timepoints showing that *Maylandia* had higher *gnmt* gene expression, and in independent QTL and PBS analyses. This highly suggests a role of DNA methylation in regulating craniofacial shape differences, and the specific levels and locations of this epigenetic regulation could be a fruitful line of study. It is probable that many of the downstream differences in gene expression across all chapters of this dissertation come in part from changes in methylation status across the genome.

Time is a major factor in gene expression regulation

A major theme of this dissertation is the role of time in gene expression regulation. In chapter 2, genes that were differentially expressed at 2 weeks with continued accessibility changes at 4 weeks were identified, suggesting that foraging treatment stimulates expression changes in certain species at least out to 2-4 weeks after onset of treatment. In chapter 3, genes were found to be most highly expressed after 1-2 weeks of foraging challenge, with a later drop off in expression levels at 4 weeks, continuing to 8 weeks. In addition, other work suggests that the genetic profile is dependent upon the onset/duration of foraging treatment (Gunter et al., 2013; Schneider et al., 2014). Chapter 4 confirmed an early consistent gene network but later gene network disintegration characterized by lower levels of expression, specifically when mechanosensory organelles are disrupted. This suggests an important factor may be age in assessing transcriptional profiles.

Because the body of work in this dissertation show the highest level of expression and largest number of differentially expressed genes early on (i.e. 1-2 weeks), it is likely that plasticity studies that assess gene regulation later on, such as 1 year+ after foraging

onset are missing the regulation of the early plastic response, and more so identifying genes involved in homeostasis and long term maintenance of bone shapes and the plastic response. Taken together, this suggests that the time of environmental input can greatly affect the regulation of a phenotype.

The new genotype-phenotype map

Considering the new contributions to the field, the genotype-phenotype map from Jamniczky et al. (2010) can be modified to include the effect of time on a resulting phenotype (Figure 23). Taking the timing and loss of cilia rootlet experiments together, we now know that the timing of mechanical stimulation greatly affects the transcriptional profile and plastic response of cichlid fishes. Plasticity is characterized by early, strong bursts of expression of mechanosensitive genes, followed by a decline over time. When the cilia rootlet is compromised, the transcriptional network early on is relatively stable, but disintegrates over time. However, it is likely that in the case of non-plastic species like *Labeotropheus*, the structurally stable primary cilium is less sensitive to environmental stimuli and has a locked-in transcriptional pattern that follows, regardless of time. Selection then acts on those fish that are best adapted to their novel environment, which alters the genotype. All in all, the genotype and the environment are inseparable, as they both influence the phenotype. While the genotype contains the genes, the environment and the timing of the environmental stimuli alters the expression of those genes, which then, via selection, feeds back onto the genotype.

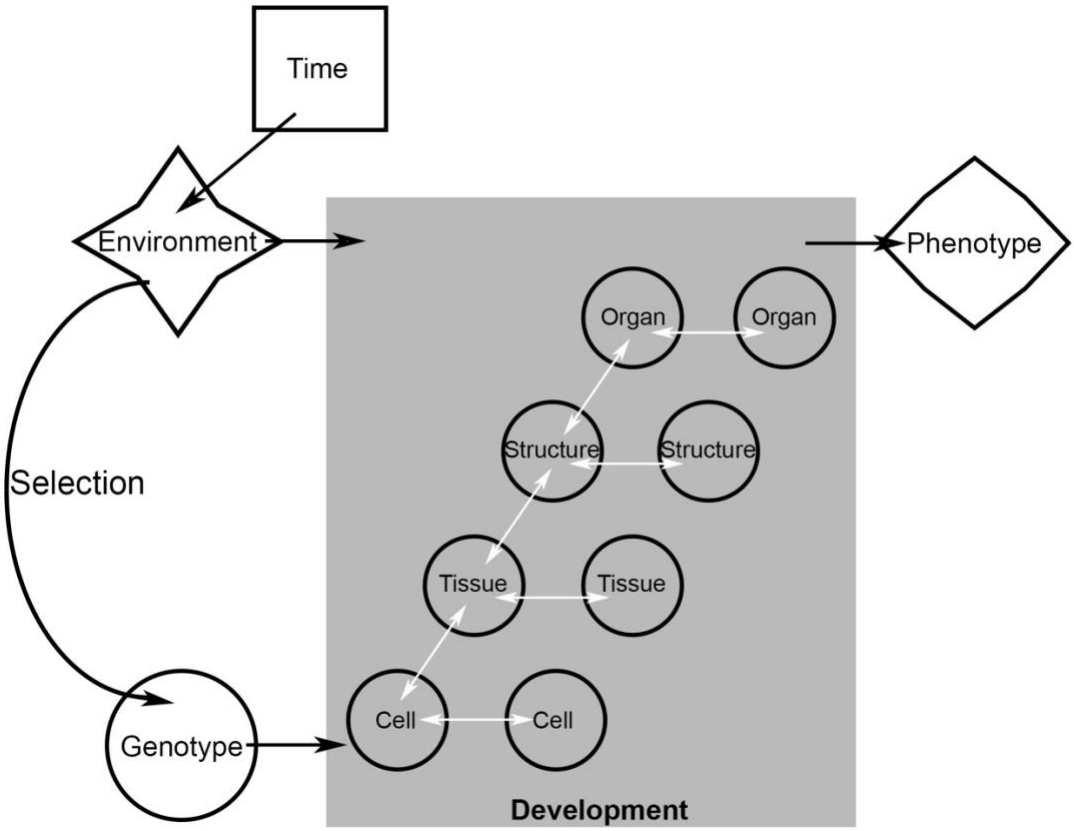

Figure 23: New genotype-phenotype map considering new contributions to the field.

APPENDICES

APPENDIX A. Fgf signaling in cichlid scale shape variation.

Albertson, R.C., Kawasaki, K.C., Tetrault, E.R., & Powder, K.E. (2018). Genetic analysis in Lake Malawi cichlids identify new roles for Fgf signaling in scale shape variation. *Communications Biology, 1*: 55.

Cichlid scale shapes differ between species and along different positions on the body. QTL analysis identified over 40 significant loci associated with scale shape variation in scales on two specific locations on the body, one hotspot being around the gene *fgfr1b*. Using qRT-PCR, we found that scales that were taller in the dorsal-ventral axis, as in *Tropheops*, had higher levels of *fgfr1b* gene expression compared to *Labeotropheus*, which has shorter scales. In addition, regenerated scales have a pronounced uptick in *fgfr1b* expression, again more so in *Tropheops* compared to regenerated *Labeotropheus* scales. This contributed to one figure in the main paper.

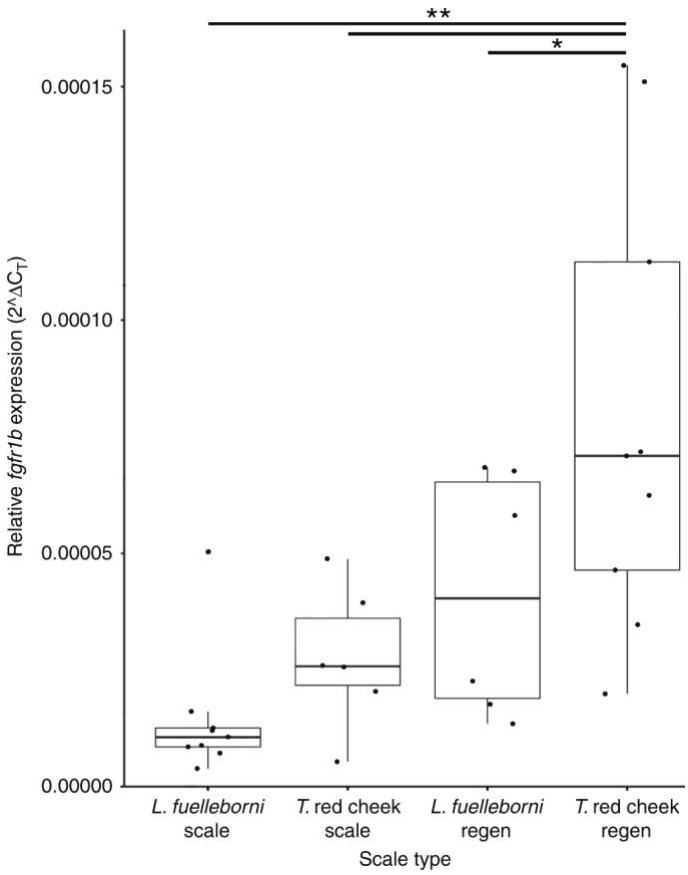

Figure A1: Quantitative rtPCR results for scale tissues. Box and whisker plot showing expression levels relative to the housekeeping gene, *beta actin*. All data points are shown as black dots. Error bars extend to the maximum and minimum values for each group, not including outliers. The center of each box depicts the median, and the upper and lower hinges correspond to the third and first quartiles, respectively. Relative expression is calculated via the comparative C_T method. Along the x-axis, species names followed by "scale" indicates expression in tissue around normally growing scales. Species names followed by "regen" indicates expression in scales after one week of regeneration. Asterisks indicate significance at the $p < 0.05$ (*) and $p < 0.01$ (**) levels.

APPENDIX B: HH signaling in bone deposition in Malawi Cichlids.

Navon, D., Male, I., Tetrault, E.R., Aaronson, B., Karlstrom, R.O., & Albertson, R.C. (2020). Hedgehog signaling is necessary and sufficient to mediate craniofacial plasticity in teleosts. *Proceedings of the National Academy of Sciences of the United States of America*, *117*(32), 19321-19327.

The cichlid species *Maylandia zebra* and *Tropheops sp. red cheek* were subjected to alternate foraging treatments for 5 weeks. We assessed ptch1 expression levels in the opercle and found that expression levels tracked with rates of bone deposition. MZ pelagic feeders and TRC benthic feeders exhibited higher rates of both bone deposition and *ptch1* expression levels. This work contributed as one supplemental figure.

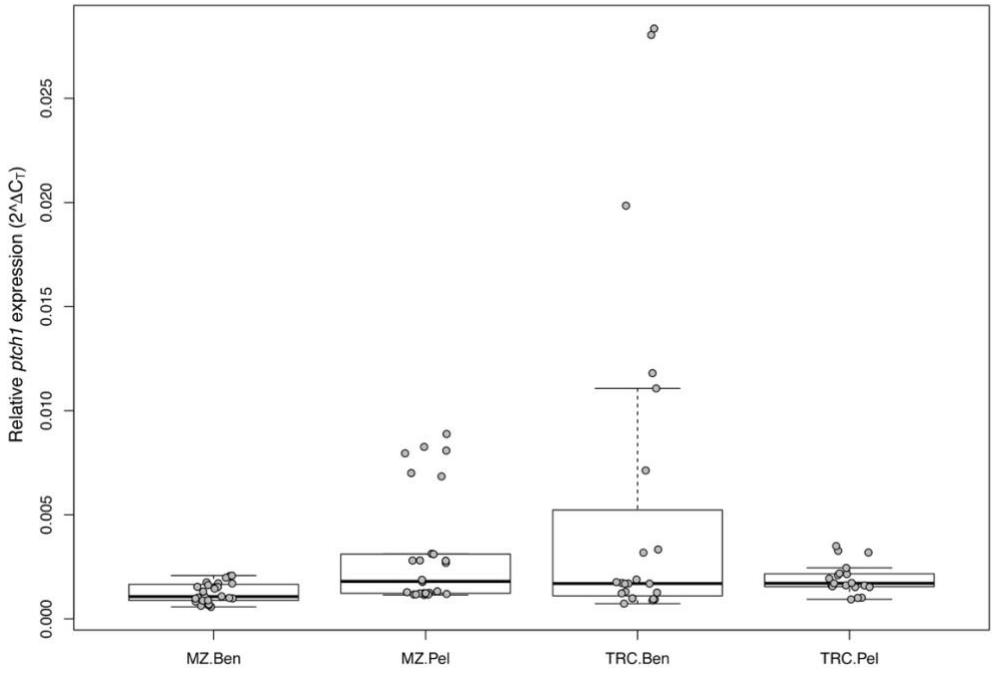

Figure A2: Relative expression of *ptch1* in the opercle bones of two species of cichlids, MZ and TRC, across diet treatments. Higher expression was observed in MZ reared in the pelagic environment, where greater rates of matrix deposition were documented, compared to those reared in the benthic environment [n=8,9 (ben, pel); p = 0.0014]. In

TRC, greater rates of matrix deposition were documented in the benthic environment, and this treatment is also where higher *ptch1* expression was observed [n=8,7 (ben, pel); p = 0.057].

APPENDIX C: HH signaling target gene expression in HH transgenic zebrafish lines.

Navon, D., Male, I., Tetrault, E.R., Aaronson, B., Karlstrom, R.O., & Albertson, R.C. (2020). Hedgehog signaling is necessary and sufficient to mediate craniofacial plasticity in teleosts. *Proceedings of the National Academy of Sciences of the United States of America, 117*(32), 19321-19327.

We assessed transcript levels of *ptch1, ptch2, gli1,* and *hhip* in wild type and two transgenic HH signaling lines, one that increases signaling upon heatshock, and one that decreases signaling with heatshock. Overall, we see increases in signaling output in the Shh transgenic line compared to WT. Gli2DR transgenic fish had similar or dampened expression compared to WT. This work contributed as one supplemental figure.

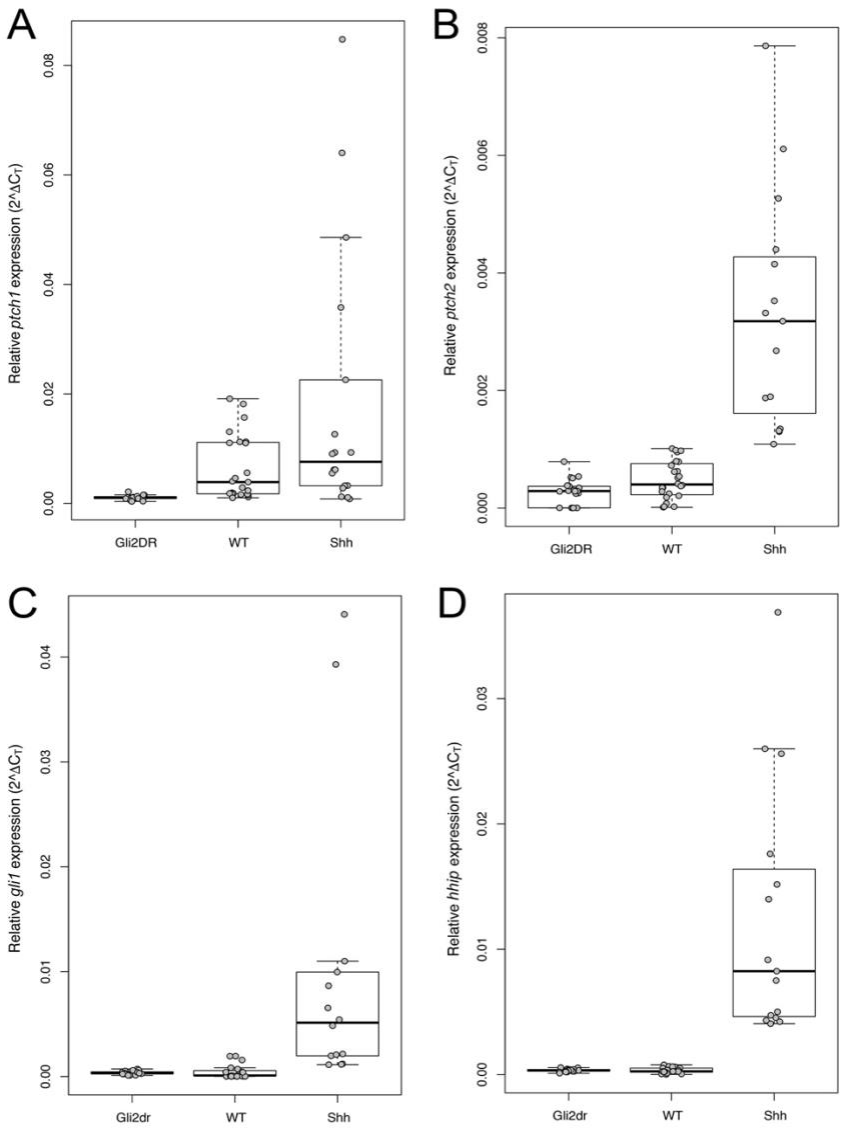

Figure A3: Relative expression of the Hh transcriptional targets, *ptch1* (**A**), *ptch2* (**B**), *gli1* (**C**), and *hhip* (**D**) in the opercle series of bones from three different zebrafish lines: wild- type [n=8,8,7,6 (*ptch1, ptch2, gli1, hhip*); "WT"], *(Tg(hsp70l:gli2aDR-EGFP))* [n=5,7,8,8 (*ptch1, ptch2, gli1, hhip*); "GliDR"], and *(Tg(hsp70l:shha-EGFP))* [n=6,5,5,5 (*ptch1, ptch2, gli1, hhip*); "Shh"]. WT fish represent animals with endogenous levels of all genes. We note relatively higher levels of *ptch1* and *ptch2,* in WT bone relative to *gli1* and *hhip.* When heatshocked, GliDR fish express a dominant-negative form of the *gli2a* transcription factor, thereby repressing Hh signaling. Shh fish express *shha* when heatshocked, which encodes a Hh ligand, thereby expanding Hh signaling. These effects were originally validated via qPCR in larval zebrafish (30). We confirmed that transgene activities resulted in altered transcriptional output of Hh signaling targets in adult craniofacial bones. The effect of genotype on *ptch1* ($F = 6.328$, $p = 0.0034$), *ptch2* ($F = 46.08$, $p < 0.0001$), *gli1* ($F = 10.89$, $p = 0.0001$), and *hhip* ($F = 30.05$, $p = 1.89e-09$) levels

was highly significant for all Hh targets, although the trend is largely driven by animals with expanded Hh signaling especially for *gli1* and *hhip*.

APPENDIX D: Expression of *crocc2* in mutant vs WT animals.

Packard, M.C., Gilbert, M.C., Tetrault, E.R., & Albertson, R.C. (2023). Zebrafish *crocc2* mutants exhibit divergent craniofacial shape, misregulated variability, and aberrant cartilage morphogenesis. *Developmental Dynamics*, *252*(7), 1026-1045.

We assessed the role of the primary cilium rootlet component, *crocc2*, in cartilage morphogenesis. To ensure that gene expression of *crocc2* was reduced in mutant animals compared to their WT siblings, I performed qPCR on the heads of juvenile (1-2 mos.) zebrafish. We found that expression was reduced, as expected. This work contributed to one supplementary table.

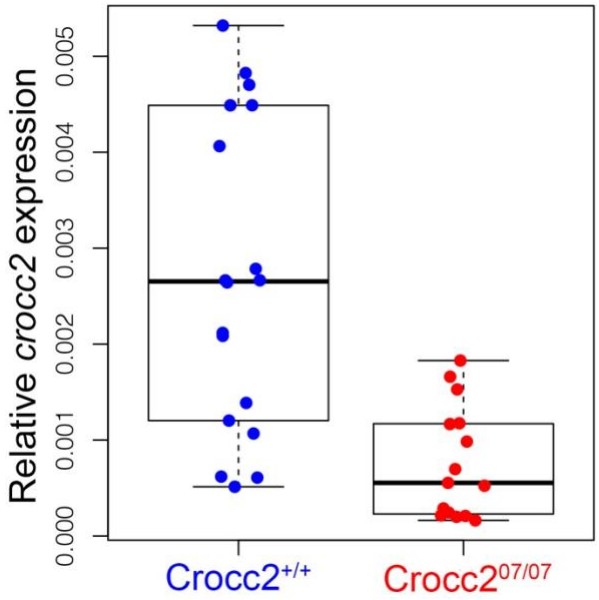

Figure A4: Expression of *crocc2* is significantly reduced in mutants compared to WT siblings.

REFERENCES

Ables, G. P., Perrone, C. E., Orentreich, D., & Orentreich, N. (2012). Methionine-restricted C57BL/6J mice are resistant to diet-induced obesity and insulin resistance but have low bone density. *PLoS ONE*, *7*(12), 1–12. https://doi.org/10.1371/journal.pone.0051357

Adams, D., Collyer, M.L., & Kaliontzopoulou, A. (2018). *Geomorph: software for geometric morphometric analysis*.

Adams, D.C., Collyer, M.L., Otarola-Castillo, E., & Sherratt, E. (2015). *R: package, geomorph: software for geometric morphometric analysis*. Available from: https://cran.r-project.org/web/packages/geomorph/index.html.

Adzhubei, I., Jordan, D.M., & Sunyaev, S.R. (2013). Predicting functional effect of human missense mutations using PolyPhen-2. *Current Protocols in Human Genetics*, Chapter 7:Unit 7.20.

Ahi, E. P., Kapralova, K. H., Pálsson, A., Maier, V. H., Gudbrandsson, J., Snorrason, S. S., … Franzdóttir, S. R. (2014). Transcriptional dynamics of a conserved gene expression network associated with craniofacial divergence in Arctic charr. *EvoDevo*, *5*(1), 1–19. https://doi.org/10.1186/2041-9139-5-40

Ahi, E. P., Steinhäuser, S. S., Pálsson, A., Franzdóttir, S. R., Snorrason, S. S., Maier, V. H., & Jónsson, Z. O. (2015). Differential expression of the aryl hydrocarbon receptor pathway associates with craniofacial polymorphism in sympatric Arctic charr. *EvoDevo*, *6*(1), 1–18. https://doi.org/10.1186/s13227-015-0022-6

Ahi, E. P., Walker, B. S., Lassiter, C. S., & Jónsson, Z. O. (2016). Investigation of the effects of estrogen on skeletal gene expression during zebrafish larval head development. *PeerJ*, *2016*(3), 1–29. https://doi.org/10.7717/peerj.1878

Ahi, E. P. (2016). Signalling pathways in trophic skeletal development and morphogenesis: Insights from studies on teleost fish. *Developmental Biology*, *420*(1), 11–31. https://doi.org/10.1016/j.ydbio.2016.10.003

Akhter, M. P., Cullen, D. M., Pedersen, E. A., Kimmel, D. B., & Recker, R. R. (1998). Bone response to in vivo mechanical loading in two breeds of mice. *Calcified Tissue International*, *63*(5), 442–449. https://doi.org/10.1007/s002239900554

Al-Bari, A. A., & Al Mamun, A. (2020). Current advances in regulation of bone homeostasis. *FASEB BioAdvances*, *2*(11), 668–679. https://doi.org/10.1096/fba.2020-00058

Albertson, R. C., Kawasaki, K. C., Tetrault, E. R., & Powder, K. E. (n.d.). Genetic analyses in Lake Malawi cichlids identify new roles for Fgf signaling in scale shape variation. *Communications Biology*, (2018). https://doi.org/10.1038/s42003-018-0060-4

Albertson, R. C., & Kocher, T. D. (2006). Genetic and developmental basis of cichlid trophic diversity. *Heredity*, *97*(3), 211–221. https://doi.org/10.1038/sj.hdy.6800864

Albertson, R. C., & Pauers, M. J. (2019). Morphological disparity in ecologically diverse versus constrained lineages of Lake Malaŵi rock-dwelling cichlids. *Hydrobiologia*, *832*(1), 153–174. https://doi.org/10.1007/s10750-018-3829-z

Albertson, R. C., Powder, K. E., Hu, Y., Coyle, K. P., Roberts, R. B., & Parsons, K. J. (2014). Genetic basis of continuous variation in the levels and modular inheritance of pigmentation in cichlid fishes. *Molecular Ecology*, *23*(21), 5135–5150. https://doi.org/10.1111/mec.12900

Albertson, R. C., Streelman, J. T., & Kocher, T. D. (2003). Directional selection has shaped the oral jaws of Lake Malawi cichlid fishes. *Proceedings of the National Academy of Sciences of the United States of America*, *100*(9), 5252–5257. https://doi.org/10.1073/pnas.0930235100

Albertson, R. C., Streelman, J. T., Kocher, T. D., & Yelick, P. C. (2005). Integration and evolution of the cichlid mandible: The molecular basis of alternate feeding strategies. *Proceedings of the National Academy of Sciences of the United States of America*, *102*(45), 16287–16292. https://doi.org/10.1073/pnas.0506649102

Albertson, R. C., & Yelick, P. C. (2007). Fgf8 haploinsufficiency results in distinct craniofacial defects in adult zebrafish. *Developmental Biology*, *306*(2), 505–515. https://doi.org/10.1016/j.ydbio.2007.03.025

Alexa, A., & Rahnenführer, J. (2007). Gene set enrichment analysis with topGO. *Bioconductor Improvments*, *27*, 1–26.

Alman, B.A. (2015). The role of hedgehog signaling in skeletal health and disease. *Nature Reviews Rheumatology*, *11*, 552-560.

Anders, S., Pyl, P. T., & Huber, W. (2015). HTSeq-A Python framework to work with high-throughput sequencing data. *Bioinformatics*, *31*(2), 166–169. https://doi.org/10.1093/bioinformatics/btu638

Andrews, S. (2010). Fastqc. A quality control tool for high throughput sequence data. http://www.bioinformatics.babraham.ac.uk/projects/fastqc/

Arbour, J. H., & López-Fernández, H. (2014). Adaptive landscape and functional diversity of Neotropical cichlids: Implications for the ecology and evolution of

Cichlinae (Cichlidae; Cichliformes). *Journal of Evolutionary Biology*, *27*(11), 2431–2442. https://doi.org/10.1111/jeb.12486

Balshine-Earn, S., & Earn, D. J. D. (1998). On the evolutionary pathway of parental care in mouth-brooding cichlid fish. *Proceedings of the Royal Society B: Biological Sciences*, *265*(1411), 2217–2222. https://doi.org/10.1098/rspb.1998.0562

Bangs, F., & Anderson, K. V. (2017). Primary cilia and Mammalian Hedgehog signaling. *Cold Spring Harbor Perspectives in Biology*, *9*(5). https://doi.org/10.1101/cshperspect.a028175

Berbari, N. F., O'Connor, A. K., Haycraft, C. J., & Yoder, B. K. (2009). The Primary Cilium as a Complex Signaling Center. *Current Biology*, *19*(13), R526–R535. https://doi.org/10.1016/j.cub.2009.05.025

Beyer, R. E., & Fattore, J. E. (2009). The influence of age and endurance exercise on the myoglobin concentration of skeletal muscle of the rat. *Journal of Gerontology*, *39*(5), 525-530.

Bootsma, H. A., Hecky, R. E., Hesslein, R. H., & Turner, G. F. (1996). Food Partitioning Among Lake Malawi Nearshore Fishes as Revealed by Stable Isotope Analyses. *Ecology*, *77*(4), 1286–1290. https://doi.org/10.2307/2265598

Borko, Š., Trontelj, P., Seehausen, O., Moškrič, A., & Fišer, C. (2021). A subterranean adaptive radiation of amphipods in Europe. *Nature Communications*, *12*(1), 1–12. https://doi.org/10.1038/s41467-021-24023-w

Bouton, N., Witte, F., & Van Alphen, J. J. M. (2002). Experimental evidence for adaptive phenotypic plasticity in a rock-dwelling cichlid fish from Lake Victoria. *Biological Journal of the Linnean Society*, *77*(2), 185–192. https://doi.org/10.1046/j.1095-8312.2002.00093.x

Bradshaw, A.D. (1965). Evolutionary significance of phenotypic plasticity in plants. *Advances in Genetics*, *13*, 115-155.

Brunskill, E. W., Potter, A. S., Distasio, A., Dexheimer, P., Plassard, A., Aronow, B. J., & Potter, S. S. (2014). A gene expression atlas of early craniofacial development. *Developmental Biology*, *391*(2), 133–146. https://doi.org/10.1016/j.ydbio.2014.04.016

Buenrostro, J. D., Giresi, P. G., Zaba, L. C., Chang, H. Y., & Greenleaf, W. J. (2013). Transposition of native chromatin for fast and sensitive epigenomic profiling of open chromatin, DNA-binding proteins and nucleosome position. *Nature Methods*, *10*(12), 1213–1218. https://doi.org/10.1038/nmeth.2688

Burns, J. G., Di Nardo, P., & Rodd, F. H. (2009). The role of predation in variation in body shape in guppies Poecilia reticulata: A comparison of field and common garden phenotypes. *Journal of Fish Biology*, *75*(6), 1144–1157. https://doi.org/10.1111/j.1095-8649.2009.02314.x

Busch-Nentwich, E., Kettleborough, R., Dooley, C.M., Scahill, C., Sealy, I., White, R., Herd, C., Mehroke, S., Wali, N., & Carruthers, S. (2013). Sanger Institute Zebrafish Mutation Project mutant data submission. ZFIN Direct Data Submission. Available from: http://zfin.org.

Buxton, P., Davey, M. G., Paton, I. R., Morrice, D. R., Francis-West, P. H., Burt, D. W., & Tickle, C. (2004). Craniofacial development in the talpid3 chicken mutant. *Differentiation*, *72*(7), 348–362. https://doi.org/10.1111/j.1432-0436.2004.07207006.x

Callaghan, T. V., Björn, L. O., Chernov, Y., Chapin, T., Christensen, T. R., Huntley, B., … Zöckler, C. (2004). Biodiversity, distributions and adaptations of arctic species in the context of environmental change. *Ambio*, *33*(7), 404–417. https://doi.org/10.1579/0044-7447-33.7.404

Campbell, C. S., Adams, C. E., Bean, C. W., Pilakouta, N., & Parsons, K. J. (2021). Evolvability under climate change: Bone development and shape plasticity are heritable and correspond with performance in Arctic charr (Salvelinus alpinus). *Evolution and Development*, *23*(4), 333–350. https://doi.org/10.1111/ede.12379

Capecchi, G., Baldassarri, M., Ferranti, S., Guidoni, E., Cioni, M., Nürnberg, P., … Grosso, S. (2018). CKAP2L mutation confirms the diagnosis of Filippi syndrome. *Clinical Genetics*, *93*(5), 1109–1110. https://doi.org/10.1111/cge.13188

Cardoso, S. J., Roland, F., Loverde-Oliveira, S. M., & Huszar, V. L. de M. (2012). Phytoplankton abundance, biomass and diversity within and between Pantanal wetland habitats. *Limnologica*, *42*(3), 235–241. https://doi.org/10.1016/j.limno.2012.01.002

Carleton, K. L., Hárosi, F. I., & Kocher, T. D. (2000). Visual pigments of African cichlid fishes: Evidence for ultraviolet vision from microspectrophotometry and DNA sequences. *Vision Research*, *40*(8), 879–890. https://doi.org/10.1016/S0042-6989(99)00238-2

Casanovas-Vilar, I., & van Dam, J. (2013). Conservatism and Adaptability during Squirrel Radiation: What Is Mandible Shape Telling Us? *PLoS ONE*, *8*(4). https://doi.org/10.1371/journal.pone.0061298

Chang, C. C., Lin, W. C., Pai, L. M., Lee, H. S., Wu, S. C., Ding, S. T., … Sung, L. Y. (2015). Cytoophidium assembly reflects upregulation of IMPDH activity. *Journal of Cell Science*, *128*(19), 3550–3555. https://doi.org/10.1242/jcs.175265

Chatterji, R. M., Hipsley, C. A., Sherratt, E., Hutchinson, M. N., & Jones, M. E. H. (2022). Ontogenetic allometry underlies trophic diversity in sea turtles (Chelonioidea). *Evolutionary Ecology*, *36*(4), 511–540. https://doi.org/10.1007/s10682-022-10162-z

Chen, J. C., Hoey, D. A., Chua, M., Bellon, R., & Jacobs, C. R. (2016). Mechanical signals promote osteogenic fate through a primary cilia-mediated mechanism. *FASEB Journal*, *30*(4), 1504–1511. https://doi.org/10.1096/fj.15-276402

Chen, N. C., Yang, F., Capecci, L. M., Gu, Z., Schafer, A. I., Durante, W., … Wang, H. (2010). Regulation of homocysteine metabolism and methylation in human and mouse tissues. *The FASEB Journal*, *24*(8), 2804–2817. https://doi.org/10.1096/fj.09-143651

Chen, Y., Lun, A. T. L., & Smyth, G. K. (2014). Differential expression analysis of complex RNA-seq experiments using edgeR. In S. Datta & D. Nettleton (Eds.), *Statistical analysis of next generation sequencing data* (pp. 51–74). Springer International Publishing.

Choi, K., Kim, J., Müller, S. Y., Oh, M., Underwood, C., Henderson, I., & Lee, I. (2016). Regulation of microRNA-mediated developmental changes by the SWR1 chromatin remodeling complex. *Plant Physiology*, *171*(2), 1128–1143. https://doi.org/10.1104/pp.16.00332

Chutimanitsakun, Y., Nipper, R. W., Cuesta-Marcos, A., Cistué, L., Corey, A., Filichkina, T., … Hayes, P. M. (2011). Construction and application for QTL analysis of a Restriction Site Associated DNA (RAD) linkage map in barley. *BMC Genomics*, *12*, 1–13. https://doi.org/10.1186/1471-2164-12-4

Cohen, S. P., LaChappelle, A. R., Walker, B. S., & Lassiter, C. S. (2014). Modulation of estrogen causes disruption of craniofacial chondrogenesis in Danio rerio. *Aquatic Toxicology*, *152*, 113–120. https://doi.org/10.1016/j.aquatox.2014.03.028

Collyer, M. L., & Adams, D. C. (2018). RRPP: An r package for fitting linear models to high-dimensional data using residual randomization. *Methods in Ecology and Evolution*, *9*(7), 1772–1779. https://doi.org/10.1111/2041-210X.13029

Collyer, M. L., Sekora, D. J., & Adams, D. C. (2015). A method for analysis of phenotypic change for phenotypes described by high-dimensional data. *Heredity*, *115*(4), 357–365. https://doi.org/10.1038/hdy.2014.75

Conith, A. J., & Albertson, R. C. (2021). The cichlid oral and pharyngeal jaws are evolutionarily and genetically coupled. *Nature Communications*, *12*(1), 1–11. https://doi.org/10.1038/s41467-021-25755-5

Conte, M. A., Joshi, R., Moore, E. C., Nandamuri, S. P., Gammerdinger, W. J., Roberts, R. B., … Kocher, T. D. (2019). Chromosome-scale assemblies reveal the structural evolution of African cichlid genomes. *GigaScience*, *8*(4), 1–20. https://doi.org/10.1093/gigascience/giz030

Cooper, W. J., Parsons, K., McIntyre, A., Kern, B., McGee-Moore, A., & Albertson, R. C. (2010). Bentho-pelagic divergence of cichlid feeding architecture was prodigious and consistent during multiple adaptive radiations within African Rift-Lakes. *PLoS ONE*, *5*(3). https://doi.org/10.1371/journal.pone.0009551

Cooper, W. J., Wirgau, R. M., Sweet, E. M., & Albertson, R. C. (2013). Deficiency of zebrafish fgf20a results in aberrant skull remodeling that mimics both human cranial disease and evolutionarily important fish skull morphologies. *Evolution and Development*, *15*(6), 426–441. https://doi.org/10.1111/ede.12052

Corces, M. R., Trevino, A. E., Hamilton, E. G., Greenside, P. G., Sinnott-Armstrong, N. A., Vesuna, S., … Chang, H. Y. (2017). An improved ATAC-seq protocol reduces background and enables interrogation of frozen tissues. *Nature Methods*, *14*(10), 959–962. https://doi.org/10.1038/nmeth.4396

Davey, M. G., Paton, I. R., Yin, Y., Schmidt, M., Bangs, F. K., Morrice, D. R., … Burt, D. W. (2006). The chicken talpid3 gene encodes a novel protein essential for Hedgehog signaling. *Genes and Development*, *20*(10), 1365–1377. https://doi.org/10.1101/gad.369106

Day, T., & McPhail, J. D. (1996). The effect of behavioural and morphological plasticity on foraging efficiency in the threespine stickleback (Gasterosteus sp.). *Oecologia*, *108*(2), 380–388. https://doi.org/10.1007/BF00334665

DeLorenzo, L., DeBrock, V., Carmona Baez, A., Ciccotto, P. J., Peterson, E. N., Stull, C., … Powder, K. E. (2022). Morphometric and Genetic Description of Trophic Adaptations in Cichlid Fishes. *Biology*, *11*(8), 1–19. https://doi.org/10.3390/biology11081165

Deng, Q., Li, P., Che, M., Liu, J., Biswas, S., Ma, G., … Li, B. (2019). Activation of hedgehog signaling in mesenchymal stem cells induces cartilage and bone tumor formation via wnt/β - catenin. *ELife*, *8*, 1–24. https://doi.org/10.7554/eLife.50208

Ding, B., Curole, J., Husemann, M., & Danley, P. D. (2015). Habitat complexity predicts the community diversity of rock-dwelling cichlid fish in Lake Malawi, East Africa. *Hydrobiologia*, *748*(1), 133–143. https://doi.org/10.1007/s10750-014-1932-3

Diouf, I., Derivot, L., Koussevitzky, S., Carretero, Y., Bitton, F., Moreau, L., & Causse, M. (2020). Genetic basis of phenotypic plasticity and genotype × environment interactions in a multi-parental tomato population. *Journal of Experimental Botany*, *71*(18), 5365–5376. https://doi.org/10.1093/jxb/eraa265

Doenz, C. J., Krähenbühl, A. K., Walker, J., Seehausen, O., & Brodersen, J. (2019). Ecological opportunity shapes a large Arctic charr species radiation. *Proceedings of the Royal Society B: Biological Sciences*, *286*(1913). https://doi.org/10.1098/rspb.2019.1992

Doerfler, W. (1983). DNA methylation and gene activity. *Annual Reviews of Biochemistry*, *52*, 93–124.

Drost, H.-G., & Paszkowski, J. (2017). Biomartr: Genomic data retrieval with R. *Bioinformatics*, *33*, 1216–1217. https://doi.org/10.1093/bioinformatics/btw821

Du, Y., Zhang, M., Liu, X., Li, Z., Hu, M., Tian, Y., … Zhou, Y. (2021). CDC20 promotes bone formation via APC/C dependent ubiquitination and degradation of p65. *EMBO Reports*, *22*(9), 1–21. https://doi.org/10.15252/embr.202152576

Dumont, E. R., Dávalos, L. M., Goldberg, A., Santana, S. E., Rex, K., & Voigt, C. C. (2012). Morphological innovation, diversification and invasion of a new adaptive zone. *Proceedings of the Royal Society B: Biological Sciences*, *279*(1734), 1797–1805. https://doi.org/10.1098/rspb.2011.2005

Dumont, E. R., Samadevam, K., Grosse, I., Warsi, O. M., Baird, B., & Davalos, L. M. (2014). Selection for mechanical advantage underlies multiple cranial optima in new world leaf-nosed bats. *Evolution*, *68*(5), 1436–1449. https://doi.org/10.1111/evo.12358

Durinck, S., Moreau, Y., Kasprzyk, A., Davis, S., De Moor, B., Brazma, A., & Huber, W. (2005). BioMart and Bioconductor: A powerful link between biological databases and microarray data analysis. *Bioinformatics*, *21*(16), 3439–3440. https://doi.org/10.1093/bioinformatics/bti525

Durinck, S., Spellman, P. T., Birney, E., & Huber, W. (2009). Mapping identifiers for the integration of genomic datasets with the R/ Bioconductor package biomaRt. *Nature Protocols*, *4*(8), 1184–1191. https://doi.org/10.1038/nprot.2009.97

Ehrenreich, I. M., & Pfennig, D. W. (2016). Genetic assimilation: A review of its potential proximate causes and evolutionary consequences. *Annals of Botany*, *117*(5), 769–779. https://doi.org/10.1093/aob/mcv130

Elson, A., Anuj, A., Barnea-Zohar, M., & Reuven, N. (2022). The origins and formation of bone-resorbing osteoclasts. *Bone*, *164*(June), 116538. https://doi.org/10.1016/j.bone.2022.116538

Fang, X., Corrales, J., Thornton, C., Schef, B. E., & Willett, K. L. (2013). Global and gene specific DNA methylation changes during zebrafish development. *Comparative Biochemistry and Physiology , Part B*, *166*, 99–108. https://doi.org/10.1016/j.cbpb.2013.07.007

Fu, G., Xu, Z., Chen, X., Pan, H., Wang, Y., & Jin, B. (2020). CDCA5 functions as a tumor promoter in bladder cancer by dysregulating mitochondria-mediated apoptosis, cell cycle regulation and PI3k/AKT/mTOR pathway activation. *Journal of Cancer*, *11*(9), 2408–2420. https://doi.org/10.7150/jca.35372

Fu, L., Patel, M. S., Bradley, A., Wagner, E. F., & Karsenty, G. (2005). The molecular clock mediates leptin-regulated bone formation. *Cell*, *122*(5), 803–815. https://doi.org/10.1016/j.cell.2005.06.028

Fujimura, K., & Okada, N. (2008). Bone development in the jaw of Nile tilapia Oreochromis niloticus (Pisces: Cichlidae). *Development Growth and Differentiation*, *50*(5), 339–355. https://doi.org/10.1111/j.1440-169X.2008.01032.x

Fujimura, K., & Okada, N. (2008). Shaping of the lower jaw bone during growth of Nile tilapia Oreochromis niloticus and a Lake Victoria cichlid Haplochromis chilotes: A geometric morphometric approach. *Development Growth and Differentiation*, *50*(8), 653–663. https://doi.org/10.1111/j.1440-169X.2008.01063.x

Gao, Y., Guo, C., Fu, S., Cheng, Y., Song, C. (2021). Downregulation of CDC20 suppressed cell proliferation, induced apoptosis, triggered cell cycle arrest in osteosarcoma cells, and enhances chemosensitivity to cisplatin. *Neoplasma*, *68*(2), 382–390. https://doi.org/10.4149/neo

Genner, M. J., Taylor, M. I., Cleary, D. F. R., Hawkins, S. J., Knight, M. E., & Turner, G. F. (2004). Beta diversity of rock-restricted cichlid fishes in Lake Malawi: Importance of environmental and spatial factors. *Ecography*, *27*(5), 601–610. https://doi.org/10.1111/j.0906-7590.2004.03824.x

Genner, M. J., Turner, G. F., & Hawkins, S. J. (1999). Foraging of rocky habitat cackled fishes in Lake Malawi: Coexistence through niche partitioning? *Oecologia*, *121*(2), 283–292. https://doi.org/10.1007/s004420050930

Gibbons, T. C., Metzger, D. C. H., Healy, T. M., & Schulte, P. M. (2017). Gene expression plasticity in response to salinity acclimation in threespine stickleback ecotypes from different salinity habitats. *Molecular Ecology*, *26*(10), 2711–2725. https://doi.org/10.1111/mec.14065

Gibert, J. M. (2017). The flexible stem hypothesis: evidence from genetic data. *Development Genes and Evolution*, *227*(5), 297–307. https://doi.org/10.1007/s00427-017-0589-0

Gibson, G., & Dworkin, I. (2004). Uncovering cryptic genetic variation. *Nature Reviews Genetics*, *5*(9), 681–690. https://doi.org/10.1038/nrg1426

Gilbert, M. C., Akama, A., Fernandes, C. C., & Albertson, R. C. (2020). Rapid morphological change in multiple cichlid ecotypes following the damming of a

major clearwater river in Brazil. *Evolutionary Applications*, *13*(10), 2754–2771. https://doi.org/10.1111/eva.13080

Gilbert, M. C., Tetrault, E., Packard, M., Navon, D., & Albertson, R. C. (2021). Ciliary Rootlet Coiled-Coil 2 (crocc2) Is Associated with Evolutionary Divergence and Plasticity of Cichlid Jaw Shape. *Molecular Biology and Evolution*, *38*(8), 3078–3092. https://doi.org/10.1093/molbev/msab071

Gillespie, G. J., & Fox, M. G. (2003). Morphological and life-history differentiation between littoral and pelagic forms of pumpkinseed. *Journal of Fish Biology*, *62*(5), 1099–1115. https://doi.org/10.1046/j.1095-8649.2003.00100.x

Goetz, S. C., Ocbina, P. J. R., & Anderson, K. V. (2009). The primary cilium as a Hedgehog signal transduction machine. In *Methods in cell biology* (First edition, Vol. 94). https://doi.org/10.1016/S0091-679X(08)94010-3

Goodall, C. (1991). Procrustes methods in the statistical analysis of shape. *Journal of the Royal Statistical Society*, *53*(2), 285-339.

Gordon, B. S., Rossetti, M. L., & Eroshkin, A. M. (2019). Arrdc2 and Arrdc3 elicit divergent changes in gene expression in skeletal muscle following anabolic and catabolic stimuli. *Physiological Genomics*, *51*(6), 208–217. https://doi.org/10.1152/physiolgenomics.00007.2019

Govey, P. M., Kawasawa, Y. I., & Donahue, H. J. (2015). Mapping the osteocytic cell response to fluid flow using RNA-Seq. *Journal of Biomechanics*, *48*(16), 4327–4332. https://doi.org/10.1016/j.jbiomech.2015.10.045

Gugger, S., Kesselring, H., Stöcklin, J., & Hamann, E. (2015). Lower plasticity exhibited by high- versus mid-elevation species in their phenological responses to manipulated temperature and drought. *Annals of Botany*, *116*(6), 953–962. https://doi.org/10.1093/aob/mcv155

Gunst, S. J., & Zhang, W. (2008). Actin cytoskeletal dynamics in smooth muscle: A new paradigm for the regulation of smooth muscle contraction. *American Journal of Physiology - Cell Physiology*, *295*(3), 576–587. https://doi.org/10.1152/ajpcell.00253.2008

Gunter, H. M., Fan, S., Xiong, F., Franchini, P., Fruciano, C., & Meyer, A. (2013). Shaping development through mechanical strain: The transcriptional basis of diet-induced phenotypic plasticity in a cichlid fish. *Molecular Ecology*, *22*(17), 4516–4531. https://doi.org/10.1111/mec.12417

Gunter, H. M., Schneider, R. F., Karner, I., Sturmbauer, C., & Meyer, A. (2017). Molecular investigation of genetic assimilation during the rapid adaptive radiations

of East African cichlid fishes. *Molecular Ecology*, *26*(23), 6634–6653. https://doi.org/10.1111/mec.14405

Gunz, P., & Mitteroecker, P. (2013). Semilandmarks: A method for quantifying curves and surfaces. *Hystrix*, *24*(1). https://doi.org/10.4404/hystrix-24.1-6292

Hallgrímsson, B., Katz, D. C., Aponte, J. D., Larson, J. R., Devine, J., Gonzalez, P. N., … Marcucio, R. S. (2019). Integration and the Developmental Genetics of Allometry. *Integrative and Comparative Biology*, *59*(5), 1369–1381. https://doi.org/10.1093/icb/icz105

Harrod, C., Mallela, J., & Kahilainen, K. K. (2010). Phenotype-environment correlations in a putative whitefish adaptive radiation. *Journal of Animal Ecology*, *79*(5), 1057–1068. https://doi.org/10.1111/j.1365-2656.2010.01702.x

Hawkins, M. B., Henke, K., & Harris, M. P. (2021). Latent developmental potential to form limb-like skeletal structures in zebrafish. *Cell*, *184*(4), 899-911.e13. https://doi.org/10.1016/j.cell.2021.01.003

Haycraft, C. J., Banizs, B., Aydin-Son, Y., Zhang, Q., Michaud, E. J., & Yoder, B. K. (2005). Gli2 and Gli3 Localize to Cilia and Require the Intraflagellar Transport Protein Polaris for Processing and Function. *PLoS Genetics*, *1*(4): e53. https://doi.org/10.1371/journal.pgen.0010053

Hellig, C. J., Kerschbaumer, M., Sefc, K. M., & Koblmüller, S. (2010). Allometric shape change of the lower pharyngeal jaw correlates with a dietary shift to piscivory in a cichlid fish. *Naturwissenschaften*, *97*(7), 663–672. https://doi.org/10.1007/s00114-010-0682-y

Hendrikse, J. L., Parsons, T. E., & Hallgrímsson, B. (2007). Evolvability as the proper focus of evolutionary developmental biology. *Evolution and Development*, *9*(4), 393–401. https://doi.org/10.1111/j.1525-142X.2007.00176.x

Hernandez, L. P., Bird, N. C., & Staab, K. L. (2007). Using zebrafish to investigate cypriniform evolutionary novelties: Functional development and evolutionary diversification of the kinethmoid. *Journal of Experimental Zoology Part B: Molecular and Developmental Evolution*, *308*(5), 625–641. https://doi.org/10.1002/jez.b.21166

Hohenlohe, P. A. (2014). Ecological genomics in full colour. *Molecular Ecology*, *23*(21), 5129–5131. https://doi.org/10.1111/mec.12945

Holguin, N., Brodt, M. D., & Silva, M. J. (2016). Activation of Wnt Signaling by Mechanical Loading Is Impaired in the Bone of Old Mice. *Journal of Bone and Mineral Research*, *31*(12), 2215–2226. https://doi.org/10.1002/jbmr.2900

Hu, Y., & Albertson, R. C. (2014). Hedgehog signaling mediates adaptive variation in a dynamic functional system in the cichlid feeding apparatus. *Proceedings of the National Academy of Sciences of the United States of America*, *111*(23), 8530–8534. https://doi.org/10.1073/pnas.1323154111

Hu, Y., & Albertson, R. C. (2017). Baby fish working out: An epigenetic source of adaptive variation in the cichlid jaw. *Proceedings of the Royal Society B: Biological Sciences*, *284*(1860). https://doi.org/10.1098/rspb.2017.1018

Hu, Y., Ghigliotti, L., Vacchi, M., Pisano, E., Detrich, H. W., & Albertson, R. C. (2016). Evolution in an extreme environment: Developmental biases and phenotypic integration in the adaptive radiation of antarctic notothenioids. *BMC Evolutionary Biology*, *16*(1), 1–13. https://doi.org/10.1186/s12862-016-0704-2

Hu, Y., Nelson-Maney, N., & Anderson, P. S. L. (2017). Common evolutionary trends underlie the four-bar linkage systems of sunfish and mantis shrimp. *Evolution*, *71*(5), 1397–1405. https://doi.org/10.1111/evo.13208

Hu, Y., Parsons, K. J., & Albertson, R. C. (2014). Evolvability of the cichlid jaw: New tools provide insights into the genetic basis of phenotypic integration. *Evolutionary Biology*, *41*, 145–153. https://doi.org/10.1007/s11692-013-9254-3

Huidobro, C., Toraño, E. G., Fernández, A. F., Urdinguio, R. G., Bruix, J., García-rodríguez, J. L., … Mato, J. M. (2013). A DNA methylation signature associated with the epigenetic repression of glycine N -methyltransferase in human hepatocellular carcinoma. *Journal of Molecular Medicine*, *91*, 939–950. https://doi.org/10.1007/s00109-013-1010-8

Hulsey, C. D., Meyer, A., & Streelman, J. T. (2020). Convergent Evolution of Cichlid Fish Pharyngeal Jaw Dentitions in Mollusk-Crushing Predators: Comparative X-Ray Computed Tomography of Tooth Sizes, Numbers, and Replacement. *Integrative and Comparative Biology*, *60*(3), 656–664. https://doi.org/10.1093/icb/icaa089

Huysseune, A. (1995). Phenotypic plasticity in the lower pharyngeal jaw dentition of astatoreochromis alluaudi (teleostei: cichlidae). *Archives of Oral Biology*, *40*(11), 1005–1014. https://doi.org/10.1016/0003-9969(95)00074-Y

Irisarri, I., Singh, P., Koblmüller, S., Torres-Dowdall, J., Henning, F., Franchini, P., … Meyer, A. (2018). Phylogenomics uncovers early hybridization and adaptive loci shaping the radiation of Lake Tanganyika cichlid fishes. *Nature Communications*, *9*(1):3159. https://doi.org/10.1038/s41467-018-05479-9

Ito, T., Kawamoto, Y., Hamada, Y., & Nishimura, T. D. (2015). Maxillary sinus variation in hybrid macaques: Implications for the genetic basis of craniofacial pneumatization. *Biological Journal of the Linnean Society*, *115*(2), 333–347. https://doi.org/10.1111/bij.12528

Jamniczky, H. A., Boughner, J. C., Rolian, C., Gonzalez, P. N., Powell, C. D., Schmidt, E. J., … Hallgrímsson, B. (2010). Rediscovering Waddington in the post-genomic age: Operationalising Waddington's epigenetics reveals new ways to investigate the generation and modulation of phenotypic variation. *BioEssays*, *32*(7), 553–558. https://doi.org/10.1002/bies.200900189

Karasz, D. C., Weaver, A. I., Buckley, D. H., & Wilhelm, R. C. (2022). Conditional filamentation as an adaptive trait of bacteria and its ecological significance in soils. *Environmental Microbiology*, *24*(1), 1–17. https://doi.org/10.1111/1462-2920.15871

Kawajiri, M., Yoshida, K., Fujimoto, S., Mokodongan, D. F., Ravinet, M., Kirkpatrick, M., … Kitano, J. (2014). Ontogenetic stage-specific quantitative trait loci contribute to divergence in developmental trajectories of sexually dimorphic fins between medaka populations. *Molecular Ecology*, *23*(21), 5258–5275. https://doi.org/10.1111/mec.12933

Kelly, N. H., Schimenti, J. C., Ross, F. P., & van der Meulen, M. C. H. (2016). Transcriptional profiling of cortical versus cancellous bone from mechanically-loaded murine tibiae reveals differential gene expression. *Bone*, *86*, 22–29. https://doi.org/10.1016/j.bone.2016.02.007

Kesavan, C., Mohan, S., Srivastava, A. K., Kapoor, S., Wergedal, J. E., Yu, H., & Baylink, D. J. (2006). Identification of genetic loci that regulate bone adaptive response to mechanical loading in C57BL/6J and C3H/HeJ mice intercross. *Bone*, *39*(3), 634–643. https://doi.org/10.1016/j.bone.2006.03.005

Kocher, T. D. (2004). Adaptive evolution and explosive speciation: The cichlid fish model. *Nature Reviews Genetics*, *5*(4), 288–298. https://doi.org/10.1038/nrg1316

Komarova, N. L. (2014). Spatial interactions and cooperation can change the speed of evolution of complex phenotypes. *Proceedings of the National Academy of Sciences of the United States of America*, *111*,10789–10795. https://doi.org/10.1073/pnas.1400828111

Konings, A. (2007). Malawi Cichlids in their natural habitat. Cichlid Press.

Küttner, E., Parsons, K. J., Easton, A. A., Skúlason, S., Danzmann, R. G., & Ferguson, M. M. (2014). Hidden genetic variation evolves with ecological specialization: The genetic basis of phenotypic plasticity in Arctic charr ecomorphs. *Evolution and Development*, *16*(4), 247–257. https://doi.org/10.1111/ede.12087

Lafuente, E., Duneau, D., & Beldade, P. (2018). Genetic basis of thermal plasticity variation in Drosophila melanogaster body size. *PLoS Genetics*, *14*(9), 1–24. https://doi.org/10.1371/journal.pgen.1007686

Laitinen, R. A. E., & Nikoloski, Z. (2019). Genetic basis of plasticity in plants. *Journal of Experimental Botany*, *70*(3), 795–804. https://doi.org/10.1093/jxb/ery404

Laland K, Uller T, Feldman M, Sterelny K, Müller GB, Moczek A, … Futuyma DJ. (2014). Does evolutionary theory need a rethink? *Nature*, *514*(7521), 161–164.

Landy, J. A., Oschmann, A., Munch, S. B., & Walsh, M. R. (2020). Ancestral genetic variation in phenotypic plasticity underlies rapid evolutionary changes in resurrected populations of waterfleas. *Proceedings of the National Academy of Sciences of the United States of America*, *117*(51), 32535–32544. https://doi.org/10.1073/pnas.2006581117

Langmead, B., & Salzberg, S. L. (2012). Fast gapped-read alignment with bowtie 2. *Nature Methods*, *9*, 357–359. https://doi.org/10.1038/nmeth.1923

Le Pabic, P., Dranow, D. B., Hoyle, D. J., Schilling, T. F., & Nichols, J. (2022). Zebrafish endochondral growth zones as they relate to human bone size, shape and disease. *Frontiers in Endocrinology* (*Lausanne*), *13*, 1060187. https://doi.org/10.3389/fendo.2022.1060187

Ledón-Rettig, C. C., Pfennig, D. W., & Crespi, E. J. (2010). Diet and hormonal manipulation reveal cryptic genetic variation: Implications for the evolution of novel feeding strategies. *Proceedings of the Royal Society B: Biological Sciences*, *277*(1700), 3569–3578. https://doi.org/10.1098/rspb.2010.0877

Levis, N. A., Reed, E. M. X., Pfennig, D. W., & Burford Reiskind, M. O. (2020). Identification of candidate loci for adaptive phenotypic plasticity in natural populations of spadefoot toads. *Ecology and Evolution*, *10*(16), 8976–8988. https://doi.org/10.1002/ece3.6602

Li, H., Handsaker, B., Wysoker, A., Fennell, T., Ruan, J., Homer, N., … Sam, T. (2009). *The Sequence Alignment / Map format and SAMtools*. *25*(16), 2078–2079. https://doi.org/10.1093/bioinformatics/btp352

Liem, K.F. (1979). Modulatory multiplicity in the feeding mechanism in cichlid fishes, as exemplified by the invertebrate pickers of Lake Tanganyika. *Journal of Zoology*, *189*(1), 93-125.

Liem, K. F. (1980). Adaptive significance of intra- and interspecific differences in the feeding repertoires of cichlid fishes. *Integrative and Comparative Biology*, *20*(1), 295–314. https://doi.org/10.1093/icb/20.1.295

Liem, K.F. (1991). A Functional Approach to the Development of the Head of Teleosts: Implications on Constructional Morphology and Constraints. In: Schmidt-Kittler, N., Vogel, K. (eds) Constructional Morphology and Evolution. Springer, Berlin, Heidelberg. https://doi.org/10.1007/978-3-642-76156-0_16

Livak, K. J., & Schmittgen, T. D. (2001). Analysis of relative gene expression data using real-time quantitative PCR and the 2-ΔΔCT method. *Methods*, *25*(4), 402–408. https://doi.org/10.1006/meth.2001.1262

Lloyd, E., Chhouk, B., Conith, A. J., Keene, A. C., & Albertson, R. C. (2021). Diversity in rest-activity patterns among Lake Malawi cichlid fishes suggests a novel axis of habitat partitioning. *Journal of Experimental Biology*, *224*(7). https://doi.org/10.1242/jeb.242186

Long, F. (2012). Building strong bones: Molecular regulation of the osteoblast lineage. *Nature Reviews Molecular Cell Biology*, *13*(1), 27–38. https://doi.org/10.1038/nrm3254

López-Fernández, H., Arbour, J., Willis, S., Watkins, C., Honeycutt, R. L., & Winemiller, K. O. (2014). *Morphology and Efficiency of a Specialized Foraging Behavior , Sediment Sifting , in Neotropical Cichlid Fishes*. *9*(3), e89832. https://doi.org/10.1371/journal.pone.0089832

Luka, Z., Mudd, S. H., & Wagner, C. (2010). Glycine N -Methyltransferase and Regulation of S -Adenosylmethionine Levels. *Journal of Biological Chemistry*, *284*(34), 22507–22511. https://doi.org/10.1074/jbc.R109.019273

Maan, M. E., Hofker, K. D., van Alphen, J. J. M., & Seehausen, O. (2006). Sensory drive in cichlid speciation. *The American Naturalist*, *167*(6), 947–954. https://doi.org/10.1086/503532

Machado-Schiaffino, G., Henning, F., & Meyer, A. (2014). Species-specific differences in adaptive phenotypic plasticity in an ecologically relevant trophic trait: Hypertrophic lips in midas cichlid fishes. *Evolution*, *68*(7), 2086–2091. https://doi.org/10.1111/evo.12367

Maldonado, E., Hubert, N., Sagnes, P., & De Mérona, B. (2009). Morphology – diet relationships in four killifishes (Teleostei , Cyprinodontidae , Orestias) from Lake Titicaca. *Journal of Fish Biology*, *74*, 502–520. https://doi.org/10.1111/j.1095-8649.2008.02140.x

Malinsky, M., Svardal, H., Tyers, A. M., Miska, E. A., Genner, M. J., Turner, G. F., & Durbin, R. (2018). Whole-genome sequences of Malawi cichlids reveal multiple radiations interconnected by gene flow. *Nature Ecology and Evolution*, *2*(12), 1940–1955. https://doi.org/10.1038/s41559-018-0717-x

Mantila Roosa, S. M., Liu, Y., & Turner, C. H. (2011). Gene expression patterns in bone following mechanical loading. *Journal of Bone and Mineral Research*, *26*(1), 100–112. https://doi.org/10.1002/jbmr.193

Marconi, A., Yang, C. Z., Mckay, S., & Santos, M. E. (2023). Morphological and temporal variation in early embryogenesis contributes to species divergence in Malawi cichlid fishes. *Evolution and Development*, *25*, 170–193. https://doi.org/10.1111/ede.12429

Margres, M. J., Wray, K. P., Seavy, M., & Mcgivern, J. J. (2015). Phenotypic integration in the feeding system of the eastern diamondback rattlesnake (Crotalus adamanteus). *Molecular Ecology*, *24*, 3405–3420. https://doi.org/10.1111/mec.13240

Martin, M. (2011). Cutadapt removes adapter sequences from high-throughput sequence reads. *EMBnet.Journal*, *17*(1), 10–12.

Martin, P., Granina, L., Martens, K., & Goddeeris, B. (1998). Oxygen concentration profiles in sediments of two ancient lakes : Lake Baikal (Siberia, Russia) and Lake Malawi (East Africa). *Hydrobiologia*, *367*, 163–174.

Marugán-Lobón, J., Nebreda, S. M., Navalón, G., & Benson, R. B. J. (2022). Beyond the beak: Brain size and allometry in avian craniofacial evolution. *Journal of Anatomy*, *240*(2), 197–209. https://doi.org/10.1111/joa.13555

Mason, J. M., Schmitz, M. A., Müller, K. M., & Arndt, K. M. (2006). Semirational design of Jun-Fos coiled coils with increased affinity: Universal implications for leucine zipper prediction and design. *Proceedings of the National Academy of Sciences of the United States of America*, *103*(24), 8989–8994. https://doi.org/10.1073/pnas.0509880103

Matthews, B., Marchinko, K. B., Bolnick, D. I., & Mazumder, A. (2010). Specialization of trophic position and habitat use by sticklebacks in an adaptive radiation. *Ecology*, *91*(4), 1025–1034. https://doi.org/10.1890/09-0235.1

Mattocks, D. A. L., Mentch, S. J., Shneyder, J., Ables, G. P., Sun, D., Richie, J. P., … Nichenametla, S. N. (2017). Short term methionine restriction increases hepatic global DNA methylation in adult but not young male C57BL / 6J mice. *Experimental Gerontology*, *88*, 1–8. https://doi.org/10.1016/j.exger.2016.12.003

Mayr, E. (1993). What was the evolutionary synthesis? *Trends in Ecological Evolution*, *8*(1), 31-33.

Mccairns, R. J. S., & Bernatchez, L. (2012). Plasticity and heritability of morphological variation within and between parapatric stickleback demes. *Journal of Evolutionary Biology*, *25*(6), 1097–1112. https://doi.org/10.1111/j.1420-9101.2012.02496.x

McGee, M. D., Schluter, D., & Wainwright, P. C. (2013). Functional basis of ecological divergence in sympatric stickleback. *BMC Evolutionary Biology*, *13*, 277.

McGirr, J. A., & Martin, C. H. (2021). Few Fixed Variants between Trophic Specialist Pupfish Species Reveal Candidate Cis-Regulatory Alleles Underlying Rapid Craniofacial Divergence. *Molecular Biology and Evolution*, *38*(2), 405–423. https://doi.org/10.1093/molbev/msaa218

Mcguigan, K., Nishimura, N., Currey, M., Hurwit, D., & Cresko, W. A. (2011). Cryptic genetic variation and body size evolution in threespine stickleback. *Evolution*, *65*(4), 1203–1211. https://doi.org/10.1111/j.1558-5646.2010.01195.x

McKaye, K.R.; Kocher, T.; Harrison, R.; Kornfield, I. (1984). Genetic evidence for allopatric and sympatric differentiation among color morphs of a Lake Malawi cichlid fish. *Evolution*, *38*(1), 215–219.

Meuthen, D., Baldauf, S. A., Bakker, T. C. M., & Thünken, T. (2018). Neglected patterns of variation in phenotypic plasticity: Age- and sex-specific antipredator plasticity in a cichlid fish. *American Naturalist*, *191*(4), 475–490. https://doi.org/10.1086/696264

Mirvis, M., Stearns, T., & Nelson, W. J. (2018). Cilium structure, assembly, and disassembly regulated by the cytoskeleton. *Biochemical Journal*, *475*(14), 2329–2353. https://doi.org/10.1042/BCJ20170453

Mizuno, A., Amizuka, N., Irie, K., Murakami, A., Fujise, N., Kanno, T., … Ozawa, H. (1998). Severe osteoporosis in mice lacking osteoclastogenesis inhibitory factor/osteoprotegerin. *Biochemical and Biophysical Research Communications*, *247*(3), 610–615. https://doi.org/10.1006/bbrc.1998.8697

Moczek, A. P. (2008). On the origins of novelty in development and evolution. *BioEssays*, *30*(5), 432–447. https://doi.org/10.1002/bies.20754

Mohan, S., Timbers, T. A., Kennedy, J., Blacque, O. E., & Leroux, M. R. (2013). Striated rootlet and nonfilamentous forms of rootletin maintain ciliary function. *Current Biology*, *23*(20), 2016–2022. https://doi.org/10.1016/j.cub.2013.08.033

Moore, E. R., Chen, J. C., & Jacobs, C. R. (2019). Prx1-Expressing Progenitor Primary Cilia Mediate Bone Formation in response to Mechanical Loading in Mice. *Stem Cells International*, *2019*, 3094154. https://doi.org/10.1155/2019/3094154

Morgan, R., Andreassen, A. H., Åsheim, E. R., Finnøen, M. H., & Dresler, G. (2022). Reduced physiological plasticity in a fish adapted to stable conditions. *Proceedings of the National Academy of Sciences of the United States of America*, *119*(22), e2201919119. https://doi.org/10.1073/pnas.2201919119/-/DCSupplemental.Published

Mork, L., Crump, G., & Angeles, L. (2016). Zebrafish Craniofacial Development: A Window into Early Patterning. *Curr Top Dev Biol.*, *115*, 235–269. https://doi.org/10.1016/bs.ctdb.2015.07.001.Zebrafish

Muschick, M., Barluenga, M., Salzburger, W., & Meyer, A. (2011). Adaptive phenotypic plasticity in the Midas cichlid fish pharyngeal jaw and its relevance in adaptive radiation. *BMC Evolutionary Biology*, *11*(116).

Musser, G., & Clarke, J. A. (2020). An Exceptionally Preserved Specimen From the Green River Formation Elucidates Complex Phenotypic Evolution in Gruiformes and Charadriiformes. *Frontiers in Ecology and Evolution*, *8*(October), 1–18. https://doi.org/10.3389/fevo.2020.559929

Nakahama, K. I. (2010). Cellular communications in bone homeostasis and repair. *Cellular and Molecular Life Sciences*, *67*(23), 4001–4009. https://doi.org/10.1007/s00018-010-0479-3

Navalón, G., Marugán-Lobón, J., Bright, J. A., Cooney, T. ., & Rayfield, E. J. (2020). The consequences of craniofacial integration for the adaptive radiations of Darwin's finches and Hawaiian honeycreepers. *Nature Ecology and Evolution*, *4*, 270–278.

Navon, D., Hatini, P., Zogbaum, L., & Albertson, R. C. (2021). The genetic basis of coordinated plasticity across functional units in a Lake Malawi cichlid mapping population. *Evolution*, *75*(3), 672–687. https://doi.org/10.1111/evo.14157

Navon, D., Male, I., Tetrault, E. R., Aaronson, B., Karlstrom, R. O., & Craig Albertson, R. (2020). Hedgehog signaling is necessary and sufficient to mediate craniofacial plasticity in teleosts. *Proceedings of the National Academy of Sciences of the United States of America*, *117*(32), 19321–19327. https://doi.org/10.1073/pnas.1921856117

Navon, D., Olearczyk, N., & Albertson, R. . (2017). Genetic and developmental basis for fin shape variation in African cichlid fishes. *Molecular Ecology*, *26*, 291–303. https://doi.org/10.1111/mec.13905

Nei, M. (1987). *Molecular evolutionary genetics*. New York: Columbia University Press.

Nelson, C. M., Jean, R. P., Tan, J. L., Liu, W. F., Sniadecki, N. J., Spector, A. A., & Chen, C. S. (2005). Emergent patterns of growth controlled by multicellular form and mechanics. *Proceedings of the National Academy of Sciences of the United States of America*, *102*(33), 11594–11599. https://doi.org/10.1073/pnas.0502575102

Neph, S., Kuehn, M. S., Reynolds, A. P., Haugen, E., Thurman, R. E., Johnson, A. K., … Stamatoyannopoulos, J. A. (2012). BEDOPS : high-performance genomic feature operations. *Bioinformatics*, *28*(14), 1919–1920. https://doi.org/10.1093/bioinformatics/bts277

Nguyen, A. M., & Jacobs, C. R. (2013). Emerging role of primary cilia as mechanosensors in osteocytes. *Bone*, *54*(2), 196–204. https://doi.org/10.1016/j.bone.2012.11.016

Nikinmaa, M., & Rees, B. B. (2005). Oxygen-dependent gene expression in fishes. *American Journal of Physiology - Regulatory Integrative and Comparative Physiology*, *288*(5), R1079-1090. https://doi.org/10.1152/ajpregu.00626.2004.

Norberg, U.M. 1990. Vertebrate flight: mechanics, physiology, morphology, ecology, and evolution (Zoophysiology). Springer, Berlin, 291 p.

Nudds, R. L., Dyke, G. J., & Rayner, J. M. V. (2007). Avian brachial index and wing kinematics: Putting movement back into bones. *Journal of Zoology*, *272*(2), 218–226. https://doi.org/10.1111/j.1469-7998.2006.00261.x

Obata, F., Kuranaga, E., Tomioka, K., Ming, M., Takeishi, A., & Chen, C. (2014). Article Necrosis-Driven Systemic Immune Response Alters SAM Metabolism through the FOXO-GNMT Axis. *Cell Reports*, *7*(3), 821–833. https://doi.org/10.1016/j.celrep.2014.03.046

O'Connor, M. J., Thakar, T., Nicolae, C. M., & Moldovan, G. L. (2021). PARP14 regulates cyclin D1 expression to promote cell-cycle progression. *Oncogene*, *40*(30), 4872–4883. https://doi.org/10.1038/s41388-021-01881-8

Ohfuchi, E., Kato, M., Sasaki, M., Sugimoto, K., Oma, Y., & Harata, M. (2006). Vertebrate Arp6, a novel nuclear actin-related protein, interacts with heterochromatin protein 1. *European Journal of Cell Biology*, *85*(5), 411–421. https://doi.org/10.1016/j.ejcb.2005.12.006

Olsen, A. M., & Westneat, M. W. (2015). StereoMorph: An R package for the collection of 3D landmarks and curves using a stereo camera set-up. *Methods in Ecology and Evolution*, *6*(3), 351–356. https://doi.org/10.1111/2041-210X.12326

Ouattara, A., Cooke, D., Gopalakrishnan, R., Huang, T., & Ables, G. P. (2016). Bone Reports Methionine restriction alters bone morphology and affects osteoblast differentiation. *Bone Reports*, *5*, 33–42. https://doi.org/10.1016/j.bonr.2016.02.002

Packard, M. C., Gilbert, M. C., Tetrault, E., & Albertson, R. C. (2023). Zebrafish crocc2 mutants exhibit divergent craniofacial shape, misregulated variability, and aberrant cartilage morphogenesis. *Developmental Dynamics*, (March), 1–20. https://doi.org/10.1002/dvdy.591

Pagano, M., Pepperkok, R., Verde, F., Ansorge, W., & Draetta, G. (1992). Cyclin A is required at two points in the human cell cycle. *EMBO Journal*, *11*(3), 961–971. https://doi.org/10.1002/j.1460-2075.1992.tb05135.x

Pallares, L. F., Harr, B., Turner, L. M., & Tautz, D. (2014). Use of a natural hybrid zone for genomewide association mapping of craniofacial traits in the house mouse. *Molecular Ecology*, *23*(23), 5756–5770. https://doi.org/10.1111/mec.12968

Pan, A., Chang, L., Nguyen, A., & James, A. W. (2013). A review of hedgehog signaling in cranial bone development. *Frontiers in Physiology*, *4 APR*. https://doi.org/10.3389/fphys.2013.00061

Papachroni, K. K., Karatzas, D. N., Papavassiliou, K. A., Basdra, E. K., & Papavassiliou, A. G. (2009). Mechanotransduction in osteoblast regulation and bone disease. *Trends in Molecular Medicine*, *15*(5), 208–216. https://doi.org/10.1016/j.molmed.2009.03.001

Parnell, N. F., Hulsey, C. D., & Streelman, J. T. (2012). The genetic basis of a complex functional system. *Evolution*, *66*(11), 3352–3366. https://doi.org/10.1111/j.1558-5646.2012.01688.x

Parnell, N. F., & Streelman, J. T. (2011). The macroecology of rapid evolutionary radiation. *Proceedings of the Royal Society B: Biological Sciences*, *278*, 2486–2494. https://doi.org/10.1098/rspb.2010.1950

Parsons, K. J., Concannon, M., Navon, D., Wang, J., Ea, I., Groveas, K., … Albertson, R. C. (2016). Foraging environment determines the genetic architecture and evolutionary potential of trophic morphology in cichlid fishes. *Molecular Ecology*, *25*(24), 6012–6023. https://doi.org/10.1111/mec.13801

Parsons, K. J., Ma, E., & Albertson, R. C. (2012). Constraint and opportunity : The genetic basis and evolution of modularity in the cichlid mandible. *The American Naturalist*, *179*(1), 64–78. https://doi.org/10.1086/663200

Parsons, K. J., & Robinson, B. W. (2006). Replicated evolution of integrated plastic responses during early adaptive divergence. *Evolution*, *60*(4), 801-813. https://doi.org/10.1554/05-213.1

Parsons, K. J., & Robinson, B. W. (2007). Foraging performance of diet-induced morphotypes in pumpkinseed sunfish (Lepomis gibbosus) favours resource polymorphism. *Journal of Evolutionary Biology*, *20*(2), 673–684. https://doi.org/10.1111/j.1420-9101.2006.01249.x

Parsons, K. J., Trent Taylor, A., Powder, K. E., & Albertson, R. C. (2014a). Wnt signalling underlies the evolution of new phenotypes and craniofacial variability in Lake Malawi cichlids. *Nature Communications*, *5*, 1–11. https://doi.org/10.1038/ncomms4629

Parsons, K. J., Wang, J., Anderson, G., & Craig Albertson, R. (2015). Nested levels of adaptive divergence: The genetic basis of craniofacial divergence and ecological sexual dimorphism. *G3: Genes, Genomes, Genetics*, *5*(8), 1613–1624. https://doi.org/10.1534/g3.115.018226

Parsons, T. E., Weinberg, S. M., Khaksarfard, K., Howie, R. N., Elsalanty, M., Yu, J. C., & Cray, J. J. (2014b). Craniofacial shape variation in Twist1+/- mutant mice. *Anatomical Record*, *297*(5), 826–833. https://doi.org/10.1002/ar.22899

Patek, S. N., Nowroozi, B. N., Baio, J. E., Caldwell, R. L., & Summers, A. P. (2007). Linkage mechanics and power amplification of the mantis shrimp's strike. *Journal of Experimental Biology*, *210*(20), 3677–3688. https://doi.org/10.1242/jeb.006486

Patterson, M., Wolfe, A. K., Fleming, P. A., Bateman, P. W., Martin, M. L., Sherratt, E., & Warburton, N. M. (2022). Ontogenetic shift in diet of a large elapid snake is facilitated by allometric change in skull morphology. *Evolutionary Ecology*, *36*(4), 489–509. https://doi.org/10.1007/s10682-022-10164-x

Percival, C. J., Marangoni, P., Tapaltsyan, V., Klein, O., & Hallgrímsson, B. (2017). The interaction of genetic background and mutational effects in regulation of mouse craniofacial shape. *G3: Genes, Genomes, Genetics*, *7*(5), 1439–1450. https://doi.org/10.1534/g3.117.040659

Pfennig, D. W., Wund, M. A., Snell-Rood, E. C., Cruickshank, T., Schlichting, C. D., & Moczek, A. P. (2010). Phenotypic plasticity's impacts on diversification and speciation. *Trends in Ecology and Evolution*, *25*(8), 459–467. https://doi.org/10.1016/j.tree.2010.05.006

Pigliucci, M. (2005). Evolution of phenotypic plasticity: Where are we going now? *Trends in Ecology and Evolution*, *20*(9), 481–486. https://doi.org/10.1016/j.tree.2005.06.001

Pigliucci, M. (2007). Do we need an extended evolutionary synthesis? *Evolution*, *61*(12), 2743–2749. https://doi.org/10.1111/j.1558-5646.2007.00246.x

Pigliucci, M. (2008). Is evolvability evolvable? *Nature Reviews Genetics*, *9*(1), 75-82.

Pigliucci, M. (2009). An extended synthesis for evolutionary biology. *Annals of the New York Academy of Sciences*, *1168*, 218–228. https://doi.org/10.1111/j.1749-6632.2009.04578.x

Pigliucci, M., Murren, C. J., & Schlichting, C. D. (2006). Phenotypic plasticity and evolution by genetic assimilation. *Journal of Experimental Biology*, *209*(12), 2362–2367. https://doi.org/10.1242/jeb.02070

Plaisant, M., Fontaine, C., Cousin, W., Rochet, N., Dani, C., & Peraldi, P. (2009). Activation of Hedgehog Signaling Inhibits Osteoblast Differentiation of Human Mesenchymal Stem Cells. *Stem Cells*, *27*(3), 703–713. https://doi.org/10.1634/stemcells.2008-0888

Plaisant, M., Giorgetti-Peraldi, S., Gabrielson, M., Loubat, A., Dani, C., & Peraldi, P. (2011). Inhibition of hedgehog signaling decreases proliferation and clonogenicity of human mesenchymal stem cells. *PLoS ONE*, *6*(2). https://doi.org/10.1371/journal.pone.0016798

Plummer, J., Park, M., Perodin, F., Horowitz, M. C., & Hens, J. R. (2017). Methionine-Restricted Diet Increases miRNAs That Can Target RUNX2 Expression and Alters Bone Structure in Young Mice. *Journal of Cellular Biochemistry*, *42*(May 2016), 31–42. https://doi.org/10.1002/jcb.25604

Potthoff, T. (1984). Clearing and staining techniques. *Ontogeny and systematics of fishes*, *1*, 35-37.

Powder, K. E., & Albertson, R. C. (2016). Cichlid fishes as a model to understand normal and clinical craniofacial variation. *Developmental Biology*, *415*(2), 338–346. https://doi.org/10.1016/j.ydbio.2015.12.018

Powder, K. E., Cousin, H., McLinden, G. P., & Craig Albertson, R. (2014). A nonsynonymous mutation in the transcriptional regulator lbh is associated with cichlid craniofacial adaptation and neural crest cell development. *Molecular Biology and Evolution*, *31*(12), 3113–3124. https://doi.org/10.1093/molbev/msu267

Præbel, K., Knudsen, R., Siwertsson, A., Karhunen, M., Kahilainen, K. K., Ovaskainen, O., … Amundsen, P. A. (2013). Ecological speciation in postglacial European whitefish: Rapid adaptive radiations into the littoral, pelagic, and profundal lake habitats. *Ecology and Evolution*, *3*(15), 4970–4986. https://doi.org/10.1002/ece3.867

Price, T. D., Qvarnström, A., & Irwin, D. E. (2003). The role of phenotypic plasticity in driving genetic evolution. *Proceedings of the Royal Society B: Biological Sciences*, *270*(1523), 1433–1440. https://doi.org/10.1098/rspb.2003.2372

Qiu, N., Xiao, Z., Cao, L., Buechel, M. M., David, V., Roan, E., & Quarles, L. D. (2012). Disruption of Kif3a in osteoblasts results in defective bone formation and osteopenia. *Journal of Cell Science*, *125*(8), 1945–1957. https://doi.org/10.1242/jcs.095893

Quinlan, A. R., & Hall, I. M. (2010). BEDTools: a flexible suite of utilities for comparing genomic features. *Bioinformatics*, *26*(6), 841–842. https://doi.org/10.1093/bioinformatics/btq033

R Core Team. (2018). *R: A language and environment for statistical computing.* Vienna, Austria.

R Core Team. (2021). *R: A language and environment for statistical computing*. R Foundation for Statistical Computing.

Raab-Cullen, D. M., Thiede, M. A., Petersen, D. N., Kimmel, D. B., & Recker, R. R. (1994). Mechanical Loading stimulates rapid changes in periosteal gene expression. *Calcified Tissue International*, *55*, 473–478.

Rankin, S., Ayad, N. G., & Kirschner, M. W. (2005). Sororin, a substrate of the anaphase- promoting complex, is required for sister chromatid cohesion in vertebrates. *Molecular Cell*, *18*(2), 185–200. https://doi.org/10.1016/j.molcel.2005.03.017

Ribbink, B. J., Marsh, A. J., Marsh, B. A., Ribbink, A., & Sharp, A. (1983). A preliminary survey of the cichlid fishes of rocky habitats in Lake Malawi: results-The Mbuna-Pseudotropheus. *African Zoology*, *18*(3), 157–200.

Ribeiro, E., Davis, A. M., Rivero-Vega, R. A., Guillermo, O., & Betancur-r, R. (2018). Post-Cretaceous bursts of evolution along the benthic-pelagic axis in marine fishes. *Proceedings of the Royal Society B: Biological Sciences*, *285*, 20182010.

Roberts, R. B., Hu, Y., Albertson, R. C., & Kocher, T. D. (2011). Craniofacial divergence and ongoing adaptation via the hedgehog pathway. *Proceedings of the National Academy of Sciences of the United States of America*, *108*(32), 13194–13199. https://doi.org/10.1073/pnas.1018456108

Roberts, R. B., Moore, E., & Kocher, T. D. (2017). An allelic series at pax7a is associated with colour polymorphism diversity in Lake Malawi cichlid fish. *Molecular Ecology*, *26*, 2625–2639. https://doi.org/10.1111/mec.13975

Robinson, M. D., Mccarthy, D. J., & Smyth, G. K. (2010). edgeR : a Bioconductor package for differential expression analysis of digital gene expression data. *Bioinformatics*, *26*(1), 139–140. https://doi.org/10.1093/bioinformatics/btp616

Rodriguez, A. C., Vahrenkamp, J. M., Berrett, K. C., Kathleen, A., Guillen, K. P., Scherer, S. D., … Gertz, J. (2020). ETV4 is necessary for estrogen signaling and growth in endometrial cancer cells. *Cancer Research*, *80*(6), 1234–1245. https://doi.org/10.1158/0008-5472.CAN-19-1382.ETV4

Rohatgi, R., Milenkovic, L., & Scott, M. (2007). Patched1 regulates hedgehog signaling at the primary cilium. *Science*, *317*(5836), 372–376. https://doi.org/10.2307/j.ctv9zcj2n.53

Rohlf, F. J., & Slice, D. (1990). Extensions of the procrustes method for the optimal superimposition of landmarks. *Systematic Zoology*, *39*(1), 40–59. https://doi.org/10.2307/2992207

Roosenboom, J., Hens, G., Mattern, B. C., Shriver, M. D., & Claes, P. (2016). Exploring the underlying genetics of craniofacial morphology through various sources of

knowledge. *BioMed Research International*, *2016*. https://doi.org/10.1155/2016/3054578

Rowling, M. J., Mcmullen, M. H., Chipman, D. C., & Schalinske, K. L. (2002). Hepatic glycine N -methyltransferase is up-regulated by excess dietary methionine in rats. *The Journal of Nutrition*, *132*(9), 2545–2550.

Sakamoto, M. (2010). Jaw biomechanics and the evolution of biting performance in theropod dinosaurs. *Proceedings of the Royal Society B: Biological Sciences*, *277*(1698), 3327–3333. https://doi.org/10.1098/rspb.2010.0794

Salzburger, W. (2009). The interaction of sexually and naturally selected traits in the adaptive radiations of cichlid fishes. *Molecular Ecology*, *18*, 169–185. https://doi.org/10.1111/j.1365-294X.2008.03981.x

Sanchez-Roman, I., Gomez, A., Gomez, J., Suarez, H., Sanchez, C., Pamplona, R., & Barja, G. (2011). Forty percent methionine restriction lowers DNA methylation, complex I ROS generation, and oxidative damage to mtDNA and mitochondrial proteins in rat heart. *Journal of Bioenergetics and Biomembranes*, *43*, 699–708. https://doi.org/10.1007/s10863-011-9389-9

Schaefer, K., Mitteroecker, P., Gunz, P., Bernhard, M., & Bookstein, F. L. (2004). Craniofacial sexual dimorphism patterns and allometry among extant hominids. *Annals of Anatomy*, *186*(5–6), 471–478. https://doi.org/10.1016/S0940-9602(04)80086-4

Scheiner, S. M. (1993). Genetics and evolution of phenotypic plasticity. *Annual Review of Ecology and Systematics*, *24*, 35–68. https://doi.org/10.1146/annurev.es.24.110193.000343

Schindler, D. E., & Scheuerell, M. D. (2002). Habitat coupling in lake ecosystems. *Oikos*, *98*(2), 177–189. https://doi.org/10.1034/j.1600-0706.2002.980201.x

Schlichting, C.D., & Pigliucci, M. (1998). *Phenotypic evolution. A reaction norm perspective.* Sunderland: Sinauer Associates.

Schluter, D. (2000). *The ecology of adaptive radiation*. Oxford University Press.

Schmitz, J., Watrin, E., Lénárt, P., Mechtler, K., & Peters, J. M. (2007). Sororin Is Required for Stable Binding of Cohesin to Chromatin and for Sister Chromatid Cohesion in Interphase. *Current Biology*, *17*(7), 630–636. https://doi.org/10.1016/j.cub.2007.02.029

Schneider, R. F., Li, Y., Meyer, A., & Gunter, H. M. (2014). Regulatory gene networks that shape the development of adaptive phenotypic plasticity in a cichlid fish. *Molecular Ecology*, *23*(18), 4511–4526. https://doi.org/10.1111/mec.12851

Schneider, R. F., & Meyer, A. (2017). How plasticity, genetic assimilation and cryptic genetic variation may contribute to adaptive radiations. *Molecular Ecology*, *26*(1), 330–350. https://doi.org/10.1111/mec.13880

Schock, E. N., Chang, C., Youngworth, I. A., Davey, M. G., Delany, M. E., & Brugmann, S. A. (2016). Utilizing the chicken as an animal model for human craniofacial ciliopathies. *Developmental Biology*, *415*(2), 326–337. https://doi.org/10.1016/j.ydbio.2015.10.024

Schulte, P. M. (2007). *Responses to environmental stressors in an estuarine fish : Interacting stressors and the impacts of local adaptation*. *32*, 152–161. https://doi.org/10.1016/j.jtherbio.2007.01.012

Schwander, T., Libbrecht, R., & Keller, L. (2014). Supergenes and complex phenotypes. *Current Biology*, *24*(7), R288–R294. https://doi.org/10.1016/j.cub.2014.01.056

Seehausen, O. (2006). African cichlid fish: A model system in adaptive radiation research. *Proceedings of the Royal Society B: Biological Sciences*, *273*(1597), 1987–1998. https://doi.org/10.1098/rspb.2006.3539

Seehausen, O., Mayhew, P. J., & Van Alphen, J. J. M. (1999). Evolution of colour patterns in East African cichlid fish. *Journal of Evolutionary Biology*, *12*(3), 514–534. https://doi.org/10.1046/j.1420-9101.1999.00055.x

Sfakianakis, D. G., Leris, I., Laggis, A., & Kentouri, M. (2011). The effect of rearing temperature on body shape and meristic characters in zebrafish (Danio rerio) juveniles. *Environmental Biology of Fishes*, *92*(2), 197–205. https://doi.org/10.1007/s10641-011-9833-z

Shekhar, R., Priyanka, P., Kumar, P., Ghosh, T., Khan, M., Nagarajan, P., & Saxena, S. (2019). The microRNAs miR-449a and miR-424 suppress osteosarcoma by targeting cyclin A2 expression. *Journal of Biological Chemistry*, *294*(12), 4381–4400. https://doi.org/10.1074/jbc.RA118.005778

Siepielski, A. M., Morrissey, M. B., Buoro, M., Carlson, S. M., Caruso, C. M., Clegg, S. M., … Maccoll, A. D. C. (2017). Precipitation drives global variation in natural selection. *Science*, *355*, 959–962.

Sih, A., Ferrari, M. C. O., & Harris, D. J. (2011). Evolution and behavioural responses to human-induced rapid environmental change. *Evolutionary Applications*, *4*(2), 367–387. https://doi.org/10.1111/j.1752-4571.2010.00166.x

Singh, P., Bo, C., More, H., & Sturmbauer, C. (2017). The role of alternative splicing and differential gene expression in cichlid adaptive radiation. *Genome Biology and Evolution*, *9*, 2764–2781. https://doi.org/10.1093/gbe/evx204

Snapper, S. B., & Rosen, F. S. (1999). THE WISKOTT-ALDRICH SYNDROME PROTEIN (WASP): Roles in signaling and cytoskeletal organization. *Annual Review in Immunology*, *17*, 905–929.

Staab, K. L., & Hernandez, L. P. (2010). Development of the cypriniform protrusible jaw complex in danio rerio: Constructional insights for evolution. *Journal of Morphology*, *271*(7), 814–825. https://doi.org/10.1002/jmor.10836

Stark, R., & Brown, G. (2011). DiffBind: Differential binding analysis of ChIP-seq data. R package version 3.0.15.

St-Jacques, B., Hammerschmidt, M., & Mcmahon, A. P. (1999). Indian hedgehog signaling regulates proliferation and differentiation of chondrocytes and is essential for bone formation. *Development*, *13*, 2072–2086. Retrieved from www.genesdev.org

Sturmbauer, C., & Meyer, A. (1992). Genetic divergence, speciation and morphological stasis in a lineage of African cichlid fishes. *Nature*, *358*(6387), 578–581. https://doi.org/10.1038/358578a0

Styczynska-Soczka, K., & Jarman, A. P. (2015). The Drosophila homologue of Rootletin is required for mechanosensory function and ciliary rootlet formation in chordotonal sensory neurons. *Cilia*, *4*, 9. https://doi.org/10.1186/s13630-015-0018-9

Sun, J., & Deng, W. M. (2007). Hindsight Mediates the Role of Notch in Suppressing Hedgehog Signaling and Cell Proliferation. *Developmental Cell*, *12*(3), 431–442. https://doi.org/10.1016/j.devcel.2007.02.003

Szabo-Rogers, H. L., Smithers, L. E., Yakob, W., & Liu, K. J. (2010). New directions in craniofacial morphogenesis. *Developmental Biology*, *341*(1), 84–94. https://doi.org/10.1016/j.ydbio.2009.11.021

Tamagnini, D., Meloro, C., & Cardini, A. (2017). Anyone with a Long-Face? Craniofacial Evolutionary Allometry (CREA) in a Family of Short-Faced Mammals, the Felidae. *Evolutionary Biology*, *44*(4), 476–495. https://doi.org/10.1007/s11692-017-9421-z

Tange, O. (2018). Gnu Parallel 2018 (Zenodo).

Taylor, W.R., & Van Dyke, G.C. (1985). Revised procedures for staining and clearing small fishes and other vertebrates for bone and cartilage study. *Cybium*, *9*, 107-119.

Temiyasathit, S., Tang, W. J., Leucht, P., Anderson, C. T., Monica, S. D., Castillo, A. B., … Jacobs, C. R. (2012). Mechanosensing by the primary cilium: Deletion of Kif3a reduces bone formation due to loading. *PLoS ONE*, *7*(3):e33368. https://doi.org/10.1371/journal.pone.0033368

Terai, K., Takano-Yamamoto, T., Ohba, Y., Hiura, K., Sugimoto, M., Sato, M., … Nomura, S. (1999). Role of osteopontin in bone remodeling caused by mechanical stress. *Journal of Bone and Mineral Research*, *14*(6), 839–849. https://doi.org/10.1359/jbmr.1999.14.6.839

Tetrault, E., Swenson, J., Aaronson, B., Marcho, C., & Albertson, C. (2022). The transcriptional state and chromatin landscape of cichlid jaw shape variation across species and environments. *Molecular Ecology*, *00*, 1–20. https://doi.org/10.1111/mec.16975

Tiet, T. D., Hopyan, S., Nadesan, P., Gokgoz, N., Poon, R., Lin, A. C., … Wunder, J. S. (2006). Constitutive Hedgehog signaling in chondrosarcoma up-regulates tumor cell proliferation. *American Journal of Pathology*, *168*(1), 321–330. https://doi.org/10.2353/ajpath.2006.050001

Tremolizzo, L., Carboni, G., Ruzicka, W. B., Mitchell, C. P., Sugaya, I., Tueting, P., … Guidotti, A. (2002). An epigenetic mouse model for molecular and behavioral neuropathologies related to schizophrenia vulnerability. *Proceedings of the National Academy of Sciences of the United States of America*, *99*(26), 17095–17100. https://doi.org/10.1073/pnas.262658999

Tu, X., Rhee, Y., Condon, K. W., Bivi, N., Allen, M. R., Dwyer, D., … Bellido, T. (2012). Sost downregulation and local Wnt signaling are required for the osteogenic response to mechanical loading. *Bone*, *50*(1), 209–217. https://doi.org/10.1016/j.bone.2011.10.025

van Heerwaarden, B., & Sgrò, C. M. (2017). The quantitative genetic basis of clinal divergence in phenotypic plasticity. *Evolution*, *71*(11), 2618–2633. https://doi.org/10.1111/evo.13342

van Snick Gray, E., & Stauffer, J. (2004). Phenotypic plasticity : its role in trophic radiation and explosive speciation in cichlids (Teleostei : Cichlidae). *Animal Biology*, *54*(2), 137–158.

Via, S., Gomulkiewicz, R., De Jong, G., Scheiner, S. M., Schlichting, C. D., & Van Tienderen, P. H. (1995). Adaptive phenotypic plasticity: consensus and controversy. *Trends in Ecology and Evolution*, *10*, 212–217.

Vijayan, V., Khandelwal, M., Manglani, K., Gupta, S., & Surolia, A. (2014). Methionine down-regulates TLR4 / MyD88 / NF- κ B signalling in osteoclast precursors to

reduce bone loss during osteoporosis. *British Journal of Pharmacology*, *171*, 107–121. https://doi.org/10.1111/bph.12434

Visintin, R., Prinz, S., & Amon, A. (1997). CDC20 and CDH1: A family of substrate-specific activators of APC- dependent proteolysis. *Science*, *278*(5337), 460–463. https://doi.org/10.1126/science.278.5337.460

Waddington, C. H. (1953). Genetic assimilation of an acquired character author. *JSTOR Evolution*, *7*(2), 118–126.

Waddington, C. H. (1959). Canalization of development and genetic assimilation of acquired characters. *Nature*, *183*(4676), 1654–1655. https://doi.org/10.1038/1831654a0

Wainwright, P. C., McGee, M. D., Longo, S. J., & Patricia Hernandez, L. (2015). Origins, Innovations, and Diversification of Suction Feeding in Vertebrates. *Integrative and Comparative Biology*, *55*(1), 134–145. https://doi.org/10.1093/icb/icv026

Wang, Y., Chen, Y., Lin, Y., Liu, S., & Chiang, E. I. (2011). GNMT expression increases hepatic folate contents and folate-dependent methionine synthase-mediated homocysteine remethylation. *Molecular Medicine*, *17*, 486–494. https://doi.org/10.2119/molmed.2010.00243

Warnes, G. R., Bolker, B., Bonebakker, L., Gentleman, R., Huber, W., Liaw, A., Lumley, T., Maechler, M., Magnusson, A., Moeller, S., Schwartz, M., & Venables, B. (2015). Gplots: Various R programming tools for plotting data. R Package Version 2.17.0. Retrieved from http:// CRAN.R-project.org/package=gplots

Welch, K. D., Panter, K. E., Lee, S. T., Gardner, D. R., Stegelmeier, B. L., & Cook, D. (2009). Cyclopamine-induced synophthalmia in sheep: Defining a critical window and toxicokinetic evaluation. *Journal of Applied Toxicology*, *29*(5), 414–421. https://doi.org/10.1002/jat.1427

Westbrook, L., Manuvakhova, M., Kern, F. G., Estes, N. R., Ramanathan, H. N., & Thottassery, J. V. (2007). Cks1 regulates cdk1 expression: A novel role during mitotic entry in breast cancer cells. *Cancer Research*, *67*(23), 11393–11401. https://doi.org/10.1158/0008-5472.CAN-06-4173

West-Eberhard, M. J. (1989). Phenotypic plasticity and the origins of diversity. *Annual Review of Ecology and Systematics*, *20*, 249–278. https://doi.org/10.1146/annurev.es.20.110189.001341

West-Eberhard, M. J. (1998). Evolution in the light of developmental and cell biology, and vice versa. *Proceedings of the National Academy of Sciences of the United States of America*, *95*(15), 8417–8419. https://doi.org/10.1073/pnas.95.15.8417

West-Eberhard, M.J. (2003). *Developmental plasticity and evolution*. New York: Oxford University Press.

West-Eberhard, M. J. (2005). Developmental plasticity and the origin of species differences. *Proceedings of the National Academy of Sciences of the United States of America*, *102*, 6543–6549. https://doi.org/10.1073/pnas.0501844102

Westneat, M.W. (1990). Feeding mechanics of teleost fishes (Labridae; Perciformes): a test of four-bar linkage models. *Journal of Morphology*, *205*(3), 269-295.

Westneat, M. W. (1991). Linkage Biomechanics and Evolution of the Unique Feeding Mechanism of Epibulus Insidiator (Labridae: Teleostei). *Journal of Experimental Biology*, *159*(1), 165–184. https://doi.org/10.1242/jeb.159.1.165

Westneat, M. W. (2004). Evolution of levers and linkages in the feeding mechanisms of fishes. *Integrative and Comparative Biology*, *44*(5), 378–389. https://doi.org/10.1093/icb/44.5.378

Willhoft, O., & Wigley, D. B. (2020). INO80 and SWR1 complexes: the non-identical twins of chromatin remodelling. *Current Opinion in Structural Biology*, *61*, 50–58. https://doi.org/10.1016/j.sbi.2019.09.002

Willis, C. G., Ruhfel, B., Primack, R. B., Miller-Rushing, A. J., & Davis, C. C. (2008). Phylogenetic patterns of species loss in Thoreau's woods are driven by climate change. *Proceedings of the National Academy of Sciences of the United States of America*, *105*(44), 17029–17033. https://doi.org/10.1073/pnas.0806446105

Wilson, L. A. B., Colombo, M., Hanel, R., & Salzburger, W. (2013). Ecomorphological disparity in an adaptive radiation : opercular bone shape and stable isotopes in Antarctic icefishes. *Ecology and Evolution*, *3*(9), 3166–3182. https://doi.org/10.1002/ece3.708

Wimberger, P. H. (1991). Plasticity of jaw and skull morphology in the neotropical cichlids Geophagus Brasiliensis and G. Steindachneri. *Evolution. International Journal of Organic Evolution*, *45*(7), 1545–1563.

Wollenick, K., Hu, J., Kristiansen, G., Schraml, P., Rehrauer, H., Berchner-pfannschmidt, U., … Stiehl, D. P. (2012). Synthetic transactivation screening reveals ETV4 as broad coactivator of hypoxia-inducible factor signaling. *Nucleic Acids Research*, *40*(5), 1928–1943. https://doi.org/10.1093/nar/gkr978

Woolfson, D. N. (2005). The design of coiled-coil structures and assemblies. *Advances in Protein Chemistry*, *70*(04), 79–112. https://doi.org/10.1016/S0065-3233(05)70004-8

Wu, Y., Liu, J., Guo, H., Luo, Q., Yu, Z., Liao, E., & Zu, X. (2013). Establishment of OPG transgenic mice and the effect of OPG on bone microarchitecture. *International Journal of Endocrinology, 2013*. https://doi.org/10.1155/2013/125932

Wu, X., Walker, J., Zhang, J., Ding, S., & Schultz, P. G. (2004). Purmorphamine induces osteogenesis by activation of the hedgehog signaling pathway. *Chemistry & Biology, 11*, 1229–1238. https://doi.org/10.1016/j

Wund, M. A., Baker, J. A., Clancy, B., Golub, J. L., & Foster, S. A. (2008). A test of the "flexible stem" model of evolution: Ancestral plasticity, genetic accommodation, and morphological divergence in the threespine stickleback radiation. *American Naturalist, 172*(4), 449–462. https://doi.org/10.1086/590966

Xiao, Z., Zhang, S., Mahlios, J., Zhou, G., Magenheimer, B. S., Guo, D., … Quarles, L. D. (2006). Cilia-like structures and polycystin-1 in osteoblasts/osteocytes and associated abnormalities in skeletogenesis and Runx2 expression. *Journal of Biological Chemistry, 281*(41), 30884–30895. https://doi.org/10.1074/jbc.M604772200

Yang, J., Gao, J., Adamian, M., Wen, X.-H., Pawlyk, B., Zhang, L., … Li, T. (2005). The Ciliary Rootlet Maintains Long-Term Stability of Sensory Cilia. *Molecular and Cellular Biology, 25*(10), 4129–4137. https://doi.org/10.1128/mcb.25.10.4129-4137.2005

Yang, J., Liu, X., Yue, G., Adamian, M., Bulgakov, O., & Li, T. (2002). Rootletin, a novel coiled-coil protein, is a structural component of the ciliary rootlet. *Journal of Cell Biology, 159*(3), 431–440. https://doi.org/10.1083/jcb.200207153

Yasuda, H., Shima, N., Nakagawa, N., Yamaguchi, K., Kinosaki, M., Goto, M., … Higashio, K. (1999). A novel molecular mechanism modulating osteoclast differentiation and function. *Bone, 25*(1), 109–113. https://doi.org/10.1016/S8756-3282(99)00121-0

Yates, A. D., Achuthan, P., Akanni, W., Allen, J., Allen, J., Alvarez-Jarreta, J., Amode, M. R., Armean, I. M., Azov, A. G., Bennett, R., Bhai, J., Billis, K., Boddu, S., Marugán, J. C., Cummins, C., Davidson, C., Dodiya, K., Fatima, R., Gall, A., ... Flicek, P. (2020). Ensembl 2020. Nucleic Acids Research, 48(D1), D682–D688. https://doi.org/10.1093/nar/gkz966

Yin, Y., Bangs, F., Paton, I. R., Prescott, A., James, J., Davey, M. G., … Tickle, C. (2009). The Talpid3 gene (KIAA0586) encodes a centrosomal protein that is essential for primary cilia formation. *Development, 136*(4), 655–664. https://doi.org/10.1242/dev.028464

Yoshida, T., Shimada, K., Oma, Y., Kalck, V., Akimura, K., Taddei, A., … Harata, M. (2010). Actin-related protein Arp6 influences H2A.Z-dependent and -independent

gene expression and links ribosomal protein genes to nuclear pores. *PLoS Genetics*, *6*(4), 10–17. https://doi.org/10.1371/journal.pgen.1000910

Yoshioka, M., Boivin, A., Ye, P., Labrie, F., & St-Amand, J. (2006). Effects of dihydrotestosterone on skeletal muscle transcriptome in mice measured by serial analysis of gene expression. *Journal of Molecular Endocrinology*, *36*(2), 247–259. https://doi.org/10.1677/jme.1.01964

Young, K. A., Snoeks, J., & Seehausen, O. (2009). Morphological Diversity and the Roles of Contingency , Chance and Determinism in African Cichlid Radiations. *PLoS ONE*, *4*(3), e4740. https://doi.org/10.1371/journal.pone.0004740

Yu, H. (2002). Regulation of APC – Cdc20 by the spindle checkpoint. *Current Opinion in Cell Biology*, *14*(6), 706–714.

Yuan, X., Serra, R. A., & Yang, S. (2015). Function and regulation of primary cilia and intraflagellar transport proteins in the skeleton. *Annals of the New York Academy of Sciences*, *1335*(1), 78–99. https://doi.org/10.1111/nyas.12463

Zaman, F., Zhao, Y., Celvin, B., Mehta, H. H., Wan, J., Chrysis, D., … Sävendahl, L. (2019). Humanin is a novel regulator of Hedgehog signaling and prevents glucocorticoid-induced bone growth impairment. *FASEB Journal*, *33*(4), 4962–4974. https://doi.org/10.1096/fj.201801741R

Zhang, Q., Guo, R., Lu, Y., Zhao, L., Zhou, Q., Schwarz, E. M., … Xing, L. (2008). VEGF-C, a lymphatic growth factor, is a RANKL target gene in osteoclasts that enhances osteoclastic bone resorption through an autocrine mechanism. *Journal of Biological Chemistry*, *283*(19), 13491–13499. https://doi.org/10.1074/jbc.M708055200

Zhang, N. (2018). Role of methionine on epigenetic modi fi cation of DNA methylation and gene expression in animals. *Animal Nutrition*, *4*(1), 11–16. https://doi.org/10.1016/j.aninu.2017.08.009

Zhao, L. J., Liu, X. G., Liu, Y. Z., Liu, Y. J., Papasian, C. J., Sha, B. Y., … Deng, H. W. (2010). Genome-wide association study for femoral neck bone geometry. *Journal of Bone and Mineral Research*, *25*(2), 320–329. https://doi.org/10.1359/jbmr.090726

Zogbaum, L., Friend, P. G., & Albertson, R. C. (2021). Plasticity and genetic basis of cichlid gill arch anatomy reveal novel roles for Hedgehog signaling. *Molecular Ecology*, *30*(3), 761–774. https://doi.org/10.1111/mec.15766